

รายงานวิจัยฉบับสมบูรณ์

โครงการ การปรับปรุงเซลล์เม็ดเลือดขาว macrophage ที่ฝังในเนื้อเยื่อมะเร็งให้เสริม ฤทธิ์ทำลายเซลล์มะเร็งของเซลล์เม็ดเลือดขาวประเภท cytokine-induced killer cell

โดย รศ. นพ.อดิศักดิ์ วงศ์ขจรศิลป์ และคณะ

30 กันยายน 2556

รายงานวิจัยฉบับสมบูรณ์

โครงการ การปรับปรุงเซลล์เม็ดเลือดขาว macrophage ที่ฝังในเนื้อเยื่อมะเร็งให้เสริม ฤทธิ์ทำลายเซลล์มะเร็งของเซลล์เม็ดเลือดขาวประเภท cytokine-induced killer cell

> รศ. นพ.อดิศักดิ์ วงศ์ขจรศิลป์ ภาควิชาเภสัชวิทยา คณะแพทยศาสตร์ศิริราชพยาบาล มหาวิทยาลัยมหิดล

สหับสนุนโดยสำนักงานกองทุนสนับสนุนการวิจัย

ACKNOWLEDGEMENTS

We would like to express our gratitude toward Thailand Research Fund for providing us this crucial research grant. We are indebted to the Faculty of Medicine Siriraj Hospital, Mahidol University for providing key equipments and research facilities. I am also grateful to the Chalermprakiat Fund from the Faculty of Medicine Siriraj Hospital, Mahidol University. We thank K. Patanapanyasat at the Division of Instruments for Research, Office of Research and Development, Faculty of Medicine Siriraj, Hospital, Mahidol University for providing flow cytometry facility. Lastly, I thank all colleagues for their precious collective efforts.

Adisak Wongkajornsilp, M.D., Ph.D. September 30, 2013

บทคัดย่อภาษาไทย

รหัสโครงการ: RSA5280023

ชื่อโครงการ: การปรับปรุงเซลล์เม็ดเลือดขาว macrophage ที่ ฝั่งในเนื้อเยื่อมะเร็งให้เสริมฤทธิ์

ทำลายเซลล์์มะเร็งของเซลล์เม็ดเลือดขาวประเภท cytokine-induced killer cell

ชื่อนักวิจัย : รศ. นพ.อดิศักดิ์ วงศ์ขจรศิลป์ E-mail Address: adisak.won@mahidol.ac.th

ระยะเวลาโครงการ: 3 ปี

การบำบัดมะเร็งด้วยระบบภูมิคุ้มกันต้องอาศัยความสามารถในการทำลายเซลล์มะเร็งโดยตรง ร่วมกับการต่อต้านภาวะกดภูมิคุ้มกันเฉพาะที่ ภาวะกดภูมิคุ้มกันรอบ ๆก้อนมะเร็งเกิดขึ้นได้โดยอาศัย ทั้งตัวเซลล์มะเร็งโดยตรงและจากเม็ดเลือดขาวชนิดแมคโครฟาจที่ฝั่งตัวรอบเซลล์มะเร็ง เซลล์เม็ดเลือด ขาวชนิด CIK ได้ถูกนำมาใช้ในการทดลองรักษาโรคมะเร็งหลายชนิดโดยที่ความสามารถในการทำลาย มะเร็งถูกกระตุ้นได้โดยเม็ดเลือดขาวชนิดเต็นไดรติกที่เลี้ยงร่วมกัน คณะผู้วิจัยพบว่าความสามารถ ทำลายมะเร็งของเซลล์ CIK จะสูงเพิ่มขึ้นมากถ้าเลี้ยงร่วมกับเซลล์เต็นไดรติกที่ได้สัมผัสกับยา sunitinib การที่เซลล์ CIK สัมผัสกับ sunitinib โดยตรงไม่สามารถทำให้ความสามารถในการทำลายมะเร็งสูงขึ้น ซึ่ง บ่งบอกว่าการกระตุ้นด้วย sunitinib ต้องเกิดขึ้นผ่านเซลล์เด็นไดรติกอีกทอดหนึ่ง การกระตุ้นเซลล์เด็น ไดรติกด้วย sunitinib ส่งเสริมให้เกิดการผลิต cytokine ในกลุ่ม Th1 เช่น IL-12, IFN-γ และ IL-6 จาก เซลล์เด็นไดรติกโดยที่ลดการผลิต cytokine ทั้งในกลุ่ม Th2 คือ IL-13 และในกลุ่มยับยั้งภูมิคุ้มกันคือ PD-L1 และ IDO ผลโดยรวมจึงกระตุ้นเซลล์กลุ่มย่อยของเซลล์ CIK ชนิด CD3⁺CD56⁺ มีการแสดงออก ของ Th1 phenotypic markers คือ IFN-γ และ T-bet เพิ่มขึ้น ในขณะที่ทั้ง Th2 signature คือ GATA-3 และ Th17 marker คือ RORC มีการแสดงออกลดลง โดยสรุปแล้ว การที่เซลล์เด็นไดรติกสัมผัสกับ sunitinib จะเหนียวนำให้เซลล์กลุ่มย่อยของเซลล์ CIK ชนิด CD3⁺CD56⁺ เปลี่ยนการแสดงออกไปเป็น แบบ Th1 ซึ่งเพิ่มความสามารถในการทำลายเซลล์มะเร็ง

Keywords: CIK, dendritic cell, macrophage, anti-tumor cytotoxicity, sunitinib

Abstract

Project Code: RSA5280023

Project Title: The modulation of tumor-associated macrophage to enhance anti-tumor

cytolytic activity of the co-culturing cytokine-induced killer cell

Investigator: Adisak Wongkajornsilp, M.D., Ph.D.

E-mail Address: adisak.won@mahidol.ac.th

Project Period: 3 years

Successful tumor immunotherapy requires not only potent anti-tumor cytotoxicity, but also overcoming the local immunosuppression. The immunosuppression in the tumor microenvironment has been attributed to either the tumor itself or the tumor-associated macrophages (TAM). Cytokine-induced killer (CIK) cells have reached clinical trials for leukemia and solid tumors. Their anti-tumor cytotoxicity had earlier been shown to be intensified after the co-culture with dendritic cells (DCs). We observed markedly enhanced anti-tumor cytotoxicity activity of CIK cells after the co-culture with sunitinib-pretreated DCs over that of untreated DCs. This cytotoxicity was reliant upon DC modulation by sunitinib because the direct exposure of CIK cells to sunitinib had no significant effect. Sunitinib promoted Th1-inducing and pro-inflammatory phenotypes (IL-12, IFN-γ and IL-6) in DCs at the expense of Th2 inducing phenotype (IL-13) and regulatory phenotype (PD-L1, IDO). Sunitinib-treated DCs subsequently induced the upregulation of Th1 phenotypic markers (IFN-γ and T-bet) and the downregulation of the Th2 signature (GATA-3) and the Th17 marker (RORC) on the CD3+CD56+ subset of CIK cells. It concluded that sunitinib-pretreated DCs drove the CD3+CD56+ subset toward Th1 phenotype with increased anti-tumor cytotoxicity.

Keywords: CIK, dendritic cell, macrophage, anti-tumor cytotoxicity, sunitinib

CONTENTS

	Page
ACKNOWLEDGMENTS	ii
ABSTRACT (THAI)	iii
ABSTRACT (ENGLISH)	iv
LIST OF TABLE	vi
LIST OF FIGURES	vii
CHAPTER I INTRODUCTION	1
CHAPTER II MATERIALS AND METHODS	6
CHAPTER III RESULTS	11
CHAPTER IV DISCUSSION AND CONCLUSION	17
REFERENCES	19
OUTPUT FROM PROJECT	25
APPENDICES	27
APPENDIX I REPRINTS	
APPENDIX II MANUSCRIPT	

LIST OF TABLE

Table		Page
1	The primer pairs for real-time RT-PCR	9

LIST OF FIGURES

Figure		Page
1	The cytotoxic activity against HubCCA1 cell line after the priming with	12
	sunitinib-pretreated DCs.	
2	The real-time RT-PCR analysis in macrophages (Φ), iDC and mDC after	13
	sunitinib exposure.	
3	The FACS analysis for the maturity of macrophages, iDCs, and mDCs after $$	14
	sunitinib exposure.	
4	The FACS analysis for the alteration in the proportion of subpopulations in	14
	CIK cells.	
5	The real-time RT-PCR analysis for the polarization of CD3 ⁺ CD56 ⁺ subset	15
	after different treatments.	
6	The cytotoxic activity of all conditions of CD3 ⁺ CD56 ⁺ cells could be	16
	neutralized with α IFN- γ treatment.	

CHAPTER I

INTRODUCTION

Tumor-associated immunosuppression has been documented in several cancer models(1). Immunological cells in tumor microenvironment have been proposed to promote tumor growth and progression(2). Tumor-associated macrophages (TAM), a major leukocyte population present in tumors, have been shown to take part in this pro-tumoral role(3). TAM have poor antigen presenting capacity, suppress T cell activation and proliferation(4). Certain cytokines and chemokines assist tumor evasion of immunological destruction. TAM is associated with poor prognosis in many tumors(5). Yet TAM also have contradictory polarization toward promoting tumor cytotoxicity(6) that demonstrated their plasticity. Macrophages are categorized as M1 and M2 cells(6). Classically activated M1 macrophages are inducible by IFN-V, LPS, TNF- α and GM-CSF, but are suppressed by IL-4 and IL-13. The alternatively activated M2 macrophages involved in tuning inflammatory responses and adaptive immunity, scavenge debris, promote angiogenesis(4), tissue remodeling, and repair. macrophages were further subdivided as M2a, M2b and M2c. M2a were generated after the exposure to IL-4 or IL-13. M2b were generated after the exposure to immune complexes in combination with IL-1 β or LPS. M2c were generated after the exposure to IL-10, TGF- β or M1 have an IL-12^{high}, IL-23^{high}, IL-10^{low} phenotype and exhibit potent alucocorticoids. microbicidal properties and promote strong IL-12-mediated Th1 responses (i.e., produce reactive oxygen and nitrogen intermediates, IL-1 β , TNF- α , IL-6). M2 have an IL-12^{low}, IL-23^{low}, IL-10^{high} phenotype and support Th2-associated effector functions, resolution of inflammation similar to the functions of TAM in terms of cytotoxicity and the expression of inflammatory cytokines (e.g., poor producers of reactive oxygen intermediates (ROIs)(7), IL-12, IL-10, TNF-Q, and IL-6(4)).

The M1/M2 paradigm is likely to be responsible for TAM-induced immunoregulation. The tumor microenvironment polarized the recruited macrophage toward M2 protumoral function(4) through the local cytokines including IL-10, and TGF- β secreted from both ovarian cancer cells and TAM. IDO metabolites and prostaglandins, also have been proposed TAM-derived suppressive mediators(8). IL-10 promotes the differentiation of monocytes to mature macrophages, blocks their differentiation to dendritic cells (DC)(9), induces TAM-derived CCL18 that in turn attracts naïve T cells and subsequently leads to anergy(10). The gradient of tumor-derived IL-10 accounted for differentiation along the DC versus the macrophage pathway in different microanatomical localizations in a tumor(11). TAM could not trigger Th1 immune

response due to the defective IL-12 production in response to IFN- γ and LPS(12), but instead induce regulatory T (Treg) cells. The responsible intracellular signals in tumor-infiltrating immune cells that inhibited the production of several proinflammatory cytokines and chemokines but enhanced the release of factors that suppress DC maturation are the constitutively activated Stat3(13) and IKK β (14, 15). The inhibition of Stat3 led to the trigger of intrinsic immune-surveillance system that inhibits tumor growth and metastasis. TAM display defective NF-KB activation in response to LPS, TNF- α , IL-1 β (15), IRF-3/STAT-1, and galectin-1. The high level of IRF-3/STAT-1 activation can promote TAM-mediated T cell deletion(16).

TAM were attracted to the tumor through tumor-derived chemotactic factor (TDCF)(17) or CCL2/MCP-1(18), CCL7, CCL8, vascular endothelial growth factor (VEGF), macrophage colony stimulating factor (M-CSF), and placenta-derived growth factor (PIGF)(19). CCL2 might bias the immunity toward Th2 direction through the stimulation of IL-10 production from TAM(20). The production of IL-10, TGF- β , and PGE₂ by cancer cells and TAM contributes to a general suppression of antitumor activities(4). TAM promoted tumor cell proliferation, dissolution of connective tissues, and tumor neovascularization through VEGF(4) and angiogenic factor thymidine phosporylase (TP)(21), EGF, PDGF, TGF- β , VEGF, and chemokines. TAM accumulated in hypoxic regions of tumors and hypoxia triggers a proangiogenic program in these cells.

In certain conditions, TAM can express antitumor reactivity. The re-education of TAM from M2 to M1 is a novel strategy for the reversal of tumor-associated immunosuppression. The functional targets for re-education include their activation, recruitment, angiogenic activity, survival, matrix remodeling and immunosuppression. The signaling targets of TAM include the restoration of the defective NF-KB activation. Prior strategies include the combination of CpG plus an anti-IL-10 receptor antibody (22); suppression of signal transducer and activator of transcription 6 (STAT6) (23) or STAT3; restoration of SHIP1 phosphatase(24); suppression of both inducible nitric oxide synthase (NOS2) and arginase (Arg1)(25); suppression of MCP-1/CCL2(26); suppression of CSF-1(27); suppression of HIF-1/CXCR4 pathway(28) that disrupts HIF-1-inducible VEGF, suppression of matrix-metalloproteases (e.g., MMP2, MMP9) using the biphosphonate zoledronic acid(29); suppression of NF-KB in cancer cells using IL-1 and TNF- Ω (30); suppression of toll-like receptors (TLR)(31); and suppression of galectin-1(32) that was regulated by TGF- Ω 1 and hypoxia. Other proposed models include the suppression of IL-13, PGE2, CXCL12/SDF1or CCL12/MDC, IDO, VEGF, VEGF-R1/FLT1, c-kit and BTK.

The mechanisms of tumor immune evasion involve several biological molecules including indoleamine 2, 3-dioxygenase (IDO), PD-L1, GATA and interferon (IFN). IDO, a cytosolic protein that catalyzes the rate-limiting step of tryptophan (Trp) metabolism, stimulates immune tolerance in human cancer(33). IDO generates immunosuppressive dendritic cells (DCs)(34). Trp metabolites mediate cytotoxic effects on CD8⁺ tumor-infiltrating lymphocytes and CD4⁺Th1 cells(35-37). PD-L1 can have an inhibitory function that primarily acts to inhibit the priming and activation of immune responses and T cell-mediated killing of cancer cells in particular in the tumor beds (38). The zinc finger DNA binding GATA factors coordinate cellular maturation with proliferation arrest and cell survival(39). Alteration of GATA factors was shown to be causatively involved in various cancers in human patients(39). GATA-3 primarily induces Th2 differentiation(40) and therefore causes Th2 immune deviation that leads to the expansion of fibrocytes with immunosuppressive properties observed in patients with cancer(41). This may be the mechanism that GATA-3 contributes to tumor progression via immune evasion. The above data suggested the requirement of therapeutic overriding of tumor immune evasion by boosting cytotoxic effects of responsible effector cells.

Cytokine-induced killer (CIK) cells have been deployed against a number of solid tumors with *in vitro* and *in vivo* evidences. The major effector of CIK cells is the CD3⁺CD56⁺ subset(42, 43). The anti-tumor action of CIK cells could be augmented after being co-cultured with dendritic cells (DCs)(44-47). The depletion of regulatory T cell (Treg) subset in CIK cells after the co-culture with DCs was proposed as the responsible mechanism(45). We previously observed similar enhancement of the anti-tumor action of the isolated CD3⁺CD56⁺ subset against cholangiocarcinoma(48) and osteosarcoma(49) after being co-cultured with DCs. This observation implied that the activity of CD3⁺CD56⁺ subset was not invariably naturally active, but inducible. The *ex vivo* optimization for the anti-tumor activity of the CD3⁺CD56⁺ subset as well as the dissection for the involved signal transduction has posed as a challenge for CIK cell-based immunotherapy. We approached this challenge through the treatment of CIK cells, co-cultured DCs with a promising molecule, sunitinib.

Sunitinib, a protein kinase inhibitor (PKI), is conventionally intended for direct treatment of lung cancer and renal cell carcinoma. It indirectly affects the tumors through the host components of immune response(50). The pharmacological concentrations of sunitinib had no effect toward PI3K and ERK phosphorylation in NK cells and did not exert any toxicity toward peripheral blood mononuclear (PBMCs)(51). Not all tyrosine kinase inhibitors provide the beneficial effects toward immune cells(50). Only sunitinib could enhance the maturation and the expansion of DCs. Sorafenib, but not sunitinib, mediated its immunosuppressive effect at

pharmacological concentrations through the induction of human NK cell-derived cytotoxic activity, IFN- γ release(51), and suppressed mouse DCs and antigen-specific T cells functions(52).

Sunitinib might exert its immunostimulatory activity through the modulation of the ratio of immunostimulatory versus immunoregulatory cells. Recently sunitinib was shown to reverse the immune suppression of tumor microenvironment (TME) by suppressing the development of regulatory T cells (Treg)(53). Both Treg and myeloid-derived suppressor cells (MDSC) are the major immunosuppressive cellular components in TME(54, 55). The presence of Treg subset compromised the overall anti-tumor activity of CIK cells(48, 49, 56). The fraction of peripheral blood MDSC(57, 58) and Treg(57, 59, 60) were dramatically decreased in subjects treated with sunitinib. In contrast, the fraction of DCs was significantly increased after sunitinib treatment and this correlated with tumor regression in patients with renal cell carcinoma(58). combination of sunitinib treatment with DC vaccination acted synergistically in suppressing the implanted melanoma in mice(61). The responders with tumor regression after sunitinib treatment were associated with the reduction in MDSC and Treg in the TME in concomitant with the rising of CD8⁺ T cells. Sunitinib shifted tumor-infiltrating lymphocytes (TILs) in mice from releasing Th2 cytokines (IL-10, TGF- β) to Th1 cytokines (IFN- γ). The expression of coinhibitory molecules (CTLA-4 and PD-1) and Foxp3 in these TILs was also suppressed. This reversal of immunosuppression was proposed to be mediated through the inhibition of c-kit in MDSCs(62). The MDSC suppressive activity of sunitinib might be counteracted by locally high level of GM-CSF(63). The immunomodulation might be mediated through anti-VEGFR and NF-KB-suppressive actions of sunitinib. The heightened proliferation and antigen-specific T-cell activity of CD8⁺ T cells was attributed to the suppression of STAT3(64). However, other investigators reported the absence of favorable immunological action of sunitinib. Sunitinib was unable to reverse VEGF / tumor supernatant-induced suppression of DC maturation(65). Some renal cell carcinoma subjects treated with sunitinib for 4 weeks carried lower Th1/Th2 ratio in peripheral blood(66), as opposed to those found in the earlier studies(59).

Improving the density as well as the activity of CD3⁺CD56⁺ subset, while suppressing those of Treg subset, would be desirable for CIK cell-based immunotherapy. We investigated whether the introduction of sunitinib to the DC-CIK co-culture system could improve anti-tumor effects. We examined the proportion of each subset in CIK cells that represented the quantitative changes in the density of CIK cell subsets. For qualitative change, we measured the alteration in the maturation status or immunological markers of both DCs and CIK cells. In DCs, the markers studied included Th1 promoting genes (IL-12, IFN- γ); Th2 promoting gene

(IL-13); Th17 promoting genes (IL-23, IL-6); and Treg promoting genes (PD-L1, IDO, IL-10). In CIK cells, the markers assessed included Th1 genes (IFN- γ , T-bet); Th2 genes (IL-4, GATA-3); Th17 genes (RORC, IL-17, STAT3); and Treg (IDO, IL-10).

There has not been any report on the interactions between CIK cells and TAM. Since TAM have a niche in the tumor micro-environment that can impede the anti-tumor efficacy of CIK cells. The actions of TAM to modulate the activities of CIK cells toward selected solid tumors (e.g., osteosarcoma, glioma, lung cancer, and cholangiocarcinoma) will be studied. Mechanisms that can provide immunosuppression will be explored (e.g, IDO, IL-10, Treg, etc) using several methods including inhibitors, real-time RT-PCR, siRNA, and flow cytometry. An emphasis will be put on the immunosuppressive enzyme IDO and the involvement of PD-1/PD-L1 interactions. This study will provide a crucial background for the immunotherapy using CIK cells that can home to the tumor tissue and unavoidably exposed to TAM's and tumor's microenvironment.

CHAPTER II

MATERIALS AND METHODS

Generation of CIK cells and DCs from peripheral blood mononuclear cells

CIK cells and DCs were generated from PBMCs of 6 consented healthy volunteers as described previously(48). PBMCs were isolated from whole blood by Ficoll gradient centrifugation (IsoPrep, Robbins Scientific, Sunnyvale, CA). The cells were allowed to adhere over the 6-well plate at a density of 1.2×10^6 cells/mL/well for 1 h at 37°C in RPMI 1640, 10% FBS, 100 U/mL penicillin, and 100 μ g/mL streptomycin. The adherent cells (5.0 \times 10⁴ cells/well) were used to generate DCs.

To generate CIK cells, non-adherent PBMCs were resuspended in RPMI 1640 (Invitrogen, Carlsbad, CA), 10% FBS, 25 mM Hepes, 100 U/mL penicillin and 100 μ g/mL streptomycin. Human interferon γ (IFN- γ , 1,000 U/mL (*Amoytop* Biotech, Xiamen, China) was added and incubated at 37°C, 5% CO₂ for 24 h. After 24-h incubation, 50 ng/mL monoclonal antibody against CD3 (*eBioscience*, San Diego, CA) and 300 IU/mL IL-2 (*Amoytop* Biotech) were added. CIK cells were maintained at a density of \leq 6 × 10⁶ cells/mL in RPMI 1640, 10% FBS, 300 IU/mL IL-2, 25 mM Hepes, 2 mM L-glutamine, 100 U/mL penicillin, and 100 μ g/mL streptomycin with medium replacement every 5 days. Cells were harvested on day 14 with apparent viability above 90%.

To generate DCs, the adherent cells were maintained in 2 mL RPMI 1640, 10% FBS, 400 U/mL granulocyte-macrophage colony-stimulating factor (GM-CSF, *Amoytop* Biotech), 500 U/mL IL-4 (*Amoytop* Biotech) for 14 d. DC maturation could be achieved by adding 1,000 U/mL tumor necrosis factor α (TNF- α ; *Amoytop* Biotech) in the final 24 h. Some designated wells were treated with 1 μ M sunitinib (Sigma, St. Louis, MO) for 48 h. The viability of mature DCs was above 95%.

Preparation of CD3⁺CD56⁺ cells

An aliquot of CIK cells (1.0×10^8 cells) on day 14 was purified for CD3⁺CD56⁺ subset using CD3 Microbeads kit and CD56 Microbeads kit (Miltenyi Biotec, Germany) according to the manufacturer instruction. This usually yielded $0.8 - 2.0 \times 10^7$ purified CD3⁺CD56⁺ cells.

Co-culture of CIK cells and DCs

On day 14 after CIK and DCs generation, CIK cells or the purified CD3⁺CD56⁺ cells were seeded on DCs of different conditions at the stimulators (DCs): responders (CIK cells)(S: R) ratio of 1: 20. The co-cultured cells were maintained in RPMI 1640, 10% FBS, 25 mM

Hepes, 2 mM L-glutamine, 100 U/mL penicillin, and 100 μg/mL streptomycin, 300 IU/mL IL-2 for 5 days prior to *in vitro* cytotoxicity assay.

Primary cultured cholangiocarcinoma cells isolated from sediments of biliary fluid

A human cholangiocarcinoma cell line prepared from intrahepatic biliary fluid, HubCCA1(48), was propagated in growth medium (DMEM, 15% FBS, 1 mM sodium pyruvate, 1 mg/mL insulin, 0.66 mg/mL transferrin, 0.67 μg/mL sodium selenite, 0.1 mM non-essential amino acid solution, 2 mM L-glutamine, 50 unit/mL penicillin, and 50 μg/mL streptomycin) at 37°C with 5% CO₂.

Fluorescence-activated cell sorting (FACS) analysis

Either DCs or CIK cells were washed twice in PBS containing 5% FBS (PBS/FBS) and resuspended in 100 μL PBS/FBS. The cell pellet was incubated with 2 μL of the corresponding primary monoclonal antibodies (1 mg/mL) for 30 min at 25°C, washed twice and resuspended in 200 μL of PBS/FBS. For the staining of intracellular immunogens, cells were fixed and permeabilized prior to the intracellular staining in accordance with the manufacturers. Flow cytometry analysis on 10,000 cells was performed using a FACSCalibur (Becton Dickinson, San Jose, CA). The employed primary mouse monoclonal antibodies raised against human immunogens included anti-FOXP3-Alexa Fluor 488, anti-CD4-PE-Cy5, anti-CD25-PE from Biolegend, anti-IL-10-Alexa Fluor 647, anti-CD3-FITC, anti-CD56-PE, anti-CD80-FITC, anti-CD83-PE, anti-CD86-PE-Cy5, anti-CD40-APC from eBiosceince, anti-RORC-PerCP, anti-IL-17-APC from R&D Systems. Data were analyzed using FlowJo version 10.0.5.

Cytotoxic Assay

Propidium iodide (PI)-based cytotoxic assay was used to estimate the anti-tumor cytotoxic activity of CIK cells. The tumor cells (5×10³ cells/well) were seeded as target cells on the 96-well plate for 24 h at 37°C, 5% CO₂. The target cells were washed with serum-free RPMI and co-cultured with the effector cells at the designated ratio in 80 μL RPMI/well for 4 h at 37°C, 5% CO₂. For IFN-γ neutralization, 0.02 μg/mL anti-IFN-γ (clone 25718, R&D Systems) was added to the effector cells 2 h prior to the co-culture. PI (20 μL of 10 μg/mL in PBS) was added to and incubated with the cell mixture for additional 30 min. The mixture was measured for fluorescence with an excitation wavelength of 482 nm and an emission wavelength of 630 nm using the SpectraMax M5 microplate reader (Molecular Devices, Sunnyvale, CA). The background wells were those with the corresponding numbers of effector cells, but without target cells. The 100% lysis came from wells containing target in RPMI cells

plus 20 μ L isopropanol. The 0% lysis came from wells containing only the target cells. The % cytotoxicity was calculated using the following expression:

$$\% \text{ cytotoxicity} = \frac{Fl_x - Fl_0}{Fl_{100} - Fl_0} \times 100$$

 Fl_0 represents the fluorescence of the well containing the target cells without the exposure to any effector cells. Fl_{100} represents the fluorescence of from the well containing the target cells in RPMI plus 20% isopropanol. Fl_x represents the fluorescence of the well containing the target cells after the exposure to the indicated numbers of effector cells.

RNA preparation and quantitative real-time PCR analysis

Total RNA was extracted from different conditions of CD3 $^+$ CD56 $^+$ cells, macrophages, iDCs and mDCs. Cells were homogenized in 350 µL of RA1 buffer and 3.5 µL of β -mercaptoethanol (illustra $^{\text{TM}}$ RNAspin Mini RNA Isolation Kit, GE Healthcare, UK) to isolate total RNA. Reverse transcription was performed with 1 µg of total RNA. First-strand cDNA synthesis was performed with the ImProm-II Reverse Transcription System (Promega, Madison, WI). The gene-specific primers pairs (Table 1) were designed using Primer Express 3.0 (*ABI*, Foster City, *CA*) and ordered from 1st BASE (Singapore). They were amplified using FastStart SYBR $^\oplus$ Green Master (*Roche Diagnostics*, Mannheim, Germany) and *StepOnePlus Real-Time PCR system* (*ABI*). Real-time PCR was performed using 1.5 µL of 200 ng/µL cDNA in 15 µL reaction mixture with the following conditions: 95°C for 10 min, followed by 40 cycles of amplification at 95°C for 15 sec, 60°C for 40 sec, and 72°C for 40 sec. The obtained Ct's were subtracted with the Ct of GAPDH of the same condition to obtain Δ Ct. The Δ Ct's of the treated cells were subtracted with Δ Ct's of the untreated cells of the same period to obtain Δ Ct. The fold-changes could be obtained from the expression of $2^{-\Delta\Delta Ct}$.

Table 1 The primer pairs for real-time RT-PCR

Genes	Oligonucleotides (5' →3')	Size (bp)	Annealing (°C)
GAPDH	Forward: GAAATCCCATCACCATCTTCC	124	60
	Reverse: AAATGAGCCCCAGCCTTCTC		
PD-L1	Forward: TCAATGCCCCATACAACAAA	120	60
	Reverse: TGCTTGTCCAGATGACTTCG		
IDO	Forward: AGTCCGTGAGTTTGTCCTTTCAA	68	60
	Reverse: TTTCACACAGGCGTCATAAGCT		
GATA-3	Forward: ACTACGGAAACTCGGTCAGG	100	60
	Reverse: CAGGGTAGGGATCCATGAAG		
IFN-γ	Forward: GTGTGGAGACCATCAAGGAAGAC	80	60
	Reverse: CAGCTTTTCGAAGTCATCTCGTTT		
IL-4	Forward: AACAGCCTCACAGAGCAGAAGAC	101	60
	Reverse: GCCCTGCAGAAGGTTTCCTT		
IL-6	Forward: GCTGCAGGCACAGAACCA	68	60
	Reverse: ACTCCTTAAAGCTGCGCAGAA		
IL-10	Forward: CTGGGTTGCCAAGCCTTGT	100	60
	Reverse: AGTTCACATGCGCCTTGATG		
IL-12	Forward: GCAAAACCCTGACCATCCAA	100	60
	Reverse: TGAAGCAGCAGGAGCGAAT		
IL-13	Forward: GAGTGTGTTTGTCACCGTTG	253	60
	Reverse: TACTCGTTGGTCGAGAGCTG		
IL-23	Forward: GCTTACAAACTCGGTGAACAACTG	80	60
	Reverse: TCCACTTGCTTTGAGCCTGAT		
RORC	Forward: CCACAGAGACATCACCGAGCC	114	60
	Reverse: GTGGATCCCAGATGACTTGTCC		
STAT3	Forward: ACCAAGCGAGGACTGAGCAT	90	58
	Reverse: TGTGATCTGACACCCTGAATAATTC		
тgғ-β	Forward: GCGTGCTAATGGTGGAAACC	100	60
	Reverse: GCTTCTCGGAGCTCTGATGTGT		
T-bet	Forward: AGGATTCCGGGAGAACTTTGA	123	60
	Reverse: TACTGGTTGGGTAGGAGAGAGTA		

Statistical analysis

The results are shown as mean \pm standard error of the mean (SEM) of triplicate determinants. Data were plotted using GraphPad Prism version 5.03. Two-way ANOVA was used to determine the significance of difference between means of cytotoxic experiments. Student's t-test was used for real-time PCR analysis. A p value of less than 0.05 was considered significant.

CHAPTER III

RESULTS

The cytotoxic activity of CIK cells after the priming with sunitinib-treated DCs toward cholangiocarcinoma cell line

Among all investigated conditions of effector cells, the untreated CIK cells provided the lowest cytotoxicity toward the HubCCA-1 (Fig. 1A). The cytotoxicity was improved after the co-culture with mDC. The highest anti-tumor cytotoxic activity came from CIK cells that had been co-cultured with either sunitinib-treated iDCs or sunitinib-treated mDCs. This enhancement could not be obtained from CIK cells co-cultured with sunitinib-treated macrophages. The direct exposure of CIK cells to sunitinib could not confer any significant improvement in the anti-tumor cytotoxicity over that of the untreated CIK cells until the E:T ratio reached 12:1, and therefore demonstrated little enhancement. Isolated CD3⁺CD56⁺ subset contained anti-tumor cytotoxic activity (Fig. 1B). Likewise, the direct exposure of CD3⁺CD56⁺ subset to sunitinib could not confer further significant improvement. The co-culture of CD3⁺CD56⁺ subset with sunitinib-treated mDCs provided the optimal improvement.

The alteration in the polarization of macrophages, iDCs and mDCs after the exposure to sunitinib

Macrophages, iDCs and mDCs were studied for their polarization using real-time RT-PCR analysis for a number of markers (Table 1). The untreated macrophages contained lower IL-12 expression (Fig. 2A) than those in iDCs and mDCs. After sunitinib treatment, the level of IL-12 expression was enhanced in macrophages and mDCs, but not in iDCs. Both iDCs and mDCs carried higher IFN-γ expression than did macrophages. Only in mDCs was the expression of IFN-γ (Fig. 2B) significantly increased after sunitinib treatment. The expression level of IL-6 (Fig. 2C) was rising in mDCs after sunitinib treatment, but was reciprocally suppressed in macrophages. The expression of IL-13 in macrophages and iDCs, but not mDCs, was undetectable. The IL-13 expression in mDCs was suppressed after sunitinib treatment (Fig. 2D). The untreated macrophages and iDCs contained higher IL-10 expression (Fig. 2E) than did mDCs. Upon sunitinib treatment, the expression of IL-10 was decreased in macrophages, but not significantly altered in iDCs nor mDCs. Sunitinib treatment suppressed the expression of PD-L1 (Fig. 2F) in mDCs. The IDO expression (Fig. 2G) was suppressed in iDCs and mDCs after sunitinib treatment. Sunitinib enhanced the expression of IL-23 (Fig. 2H) in macrophages and mDCs, but not in iDCs.

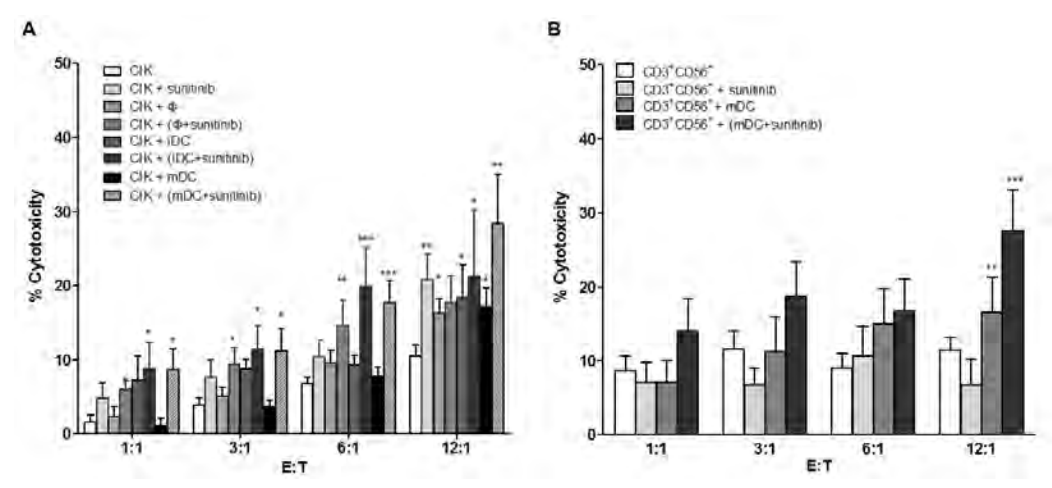


Figure 1. The cytotoxic activity against HubCCA1 cell line after the priming with sunitinibpretreated DCs. The CIK cells (A) at 1.0×10⁵ cells/well from each condition were
inoculated with the attached HubCCA1 cells (5,000 cells/well) for 4 h before the PI
assay. The CIK cell preparations comprised untreated condition, direct sunitinib
treatment, macrophage pre-inoculation, sunitinib-treated macrophage pre-inoculation,
iDC pre-inoculation, and sunitinib-treated iDC pre-inoculation, mDC pre-inoculation,
and sunitinib-treated mDC pre-inoculation. The isolated CD3⁺CD56⁺ cells (B) were
studied in similar fashion. These included untreated CD3⁺CD56⁺ cells, direct sunitinib
treatment, mDC pre-inoculation, and sunitinib-treated mDC pre-inoculation. * and **
designate data with significant different from those of the untreated CIK cells at the
same E:T ratio with p < 0.05 and <0.01 respectively.

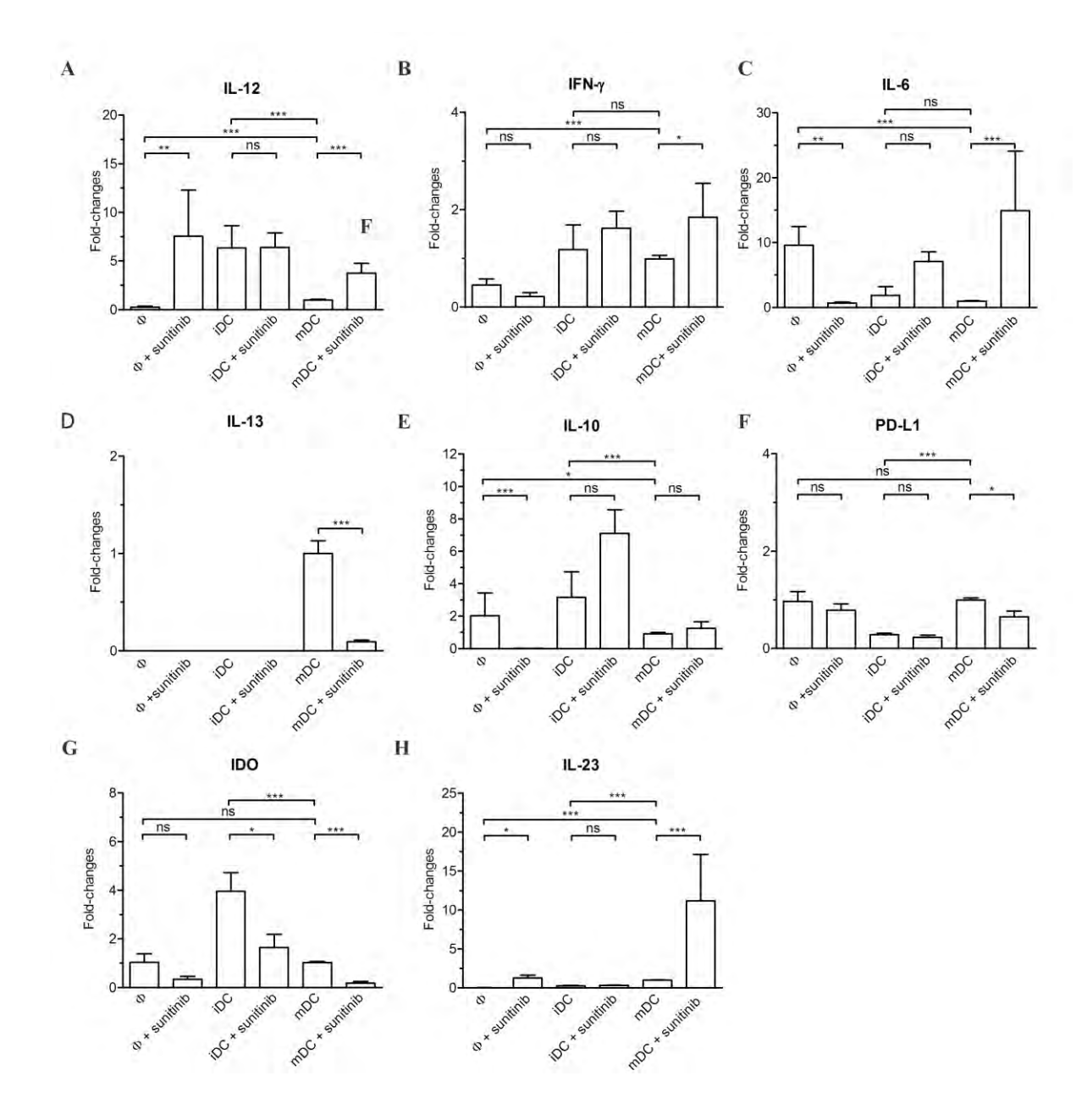


Figure 2. The real-time RT-PCR analysis in macrophages (Φ), iDC and mDC after sunitinib exposure. These cells were evaluated for the expression of IL-12 (A), IFN-γ (B), IL-6 (C), IL-13 (D), IL-10 (E), PD-L1 (F), IDO (G), and IL-23 (H). The expression levels of these genes were normalized with those of their respective untreated mDCs.

The alteration in the maturity of macrophages, iDCs, and mDCs after sunitinib treatment

The flow cytometry analysis of iDCs, and mDCs did not promote their maturation based on the staining of CD80, CD83 and CD86 (Fig. 3A). In contrast, the sunitinib treatment to macrophages resulted in not only less DC maturation markers (CD80, CD83, CD86 and CD40), but also macrophage markers (CD14 and CD40, Fig. 3B). There was no alteration in IL-10,

and IDO (Fig. 3C) in both iDCs and mDCs, but there was less IDO in macrophages after sunitinib treatment.

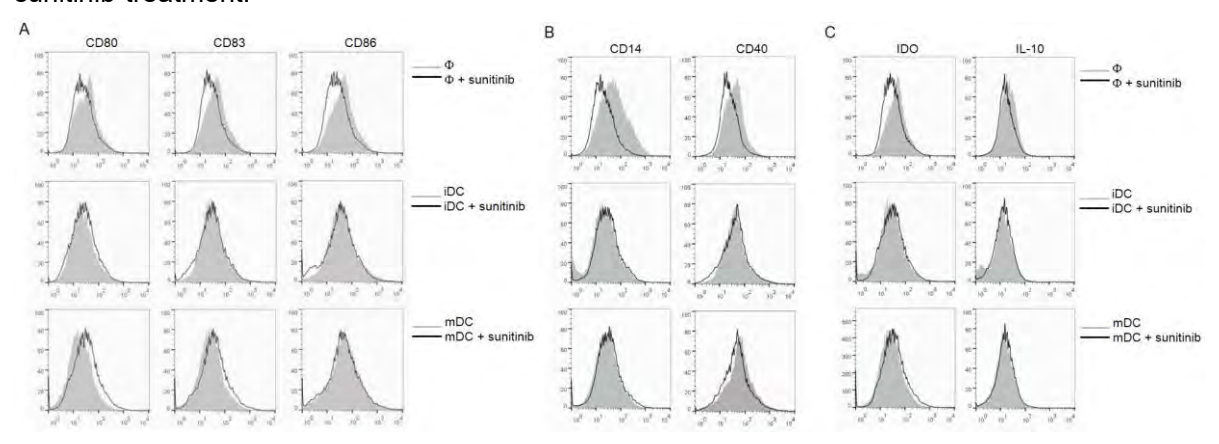


Figure 3. The FACS analysis for the maturity of macrophages, iDCs, and mDCs after sunitinib exposure. The markers for the maturity of DCs (A) are CD80, CD83 and CD86. The macrophage markers (B) are CD14 and CD40. The selected immunosuppressive molecules (C) are IDO and IL-10.

The examination for the alteration of the ratios of CD3⁺CD56⁺, Treg, and Th17 subsets in the whole CIK cell population after the priming with sunitinib-treated DCs

CIK that had been either directly treated with sunitinib, primed with mDCs or primed with sunitinib-pretreated mDCs did not significantly alter the proportions of the CD3⁺CD56⁺ subset (Fig. 4A), the Th17 subset (Fig. 4B), nor the Treg (CD4⁺CD25⁺Foxp3⁺) subset (Fig. 4C).

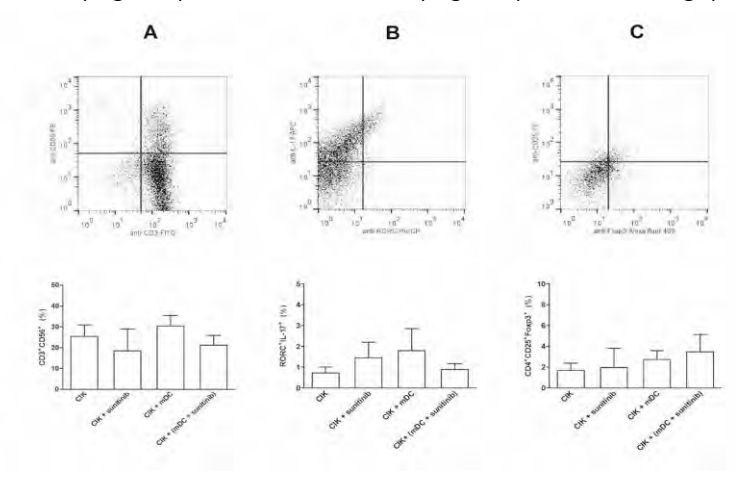


Figure 4. The FACS analysis for the alteration in the proportion of subpopulations in CIK cells. The studied subpopulations included CD3⁺CD56⁺(A), Th17 (RORC⁺IL-17⁺, B) and Treg (CD4⁺CD25⁺Foxp3⁺, C) subsets. The corresponding dot plot analysis demonstrated the gating of each subset. The CIK cells were either exposed to sunitinib directly, primed with mDCs or primed with sunitinib-pretreated DCs.

The analysis for the polarization of CD3⁺CD56⁺ cells after the priming with either sunitinibtreated mDCs or untreated mDCs

The co-culture of CD3⁺CD56⁺ cells with untreated mDCs raised the expression of IDO, and Th1 markers (IFN- γ and T-bet) (Fig. 5). In contrast, the expression of Th2 markers (GATA-3) and Th17 (RORC, STAT3) markers was reduced. The co-culture of CD3⁺CD56⁺ cells with sunitinib-pretreated mDCs maintained the rising IDO, IFN- γ , T-bet; the lessening of GATA-3 and RORC.

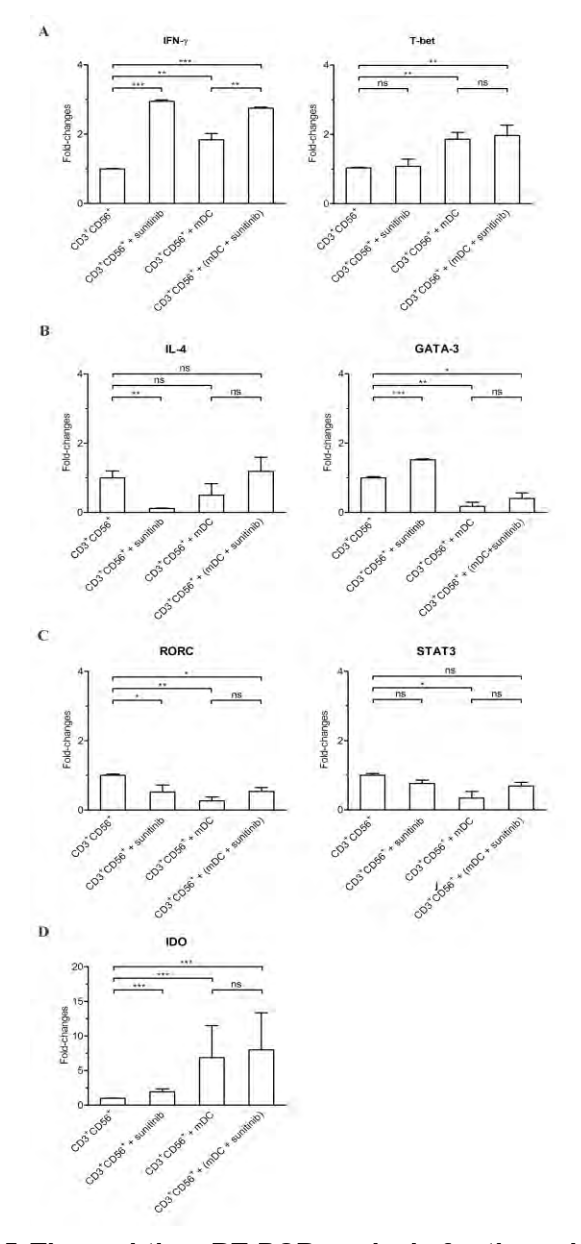


Figure 5. The real-time RT-PCR analysis for the polarization of CD3⁺CD56⁺ subset after different treatments. The CD3⁺CD56⁺ subset that had been directly exposed to sunitinib or co-cultured with sunitinib-pretreated mDCs were analyzed for the expression of IFN-γ, T-bet, IL-4, GATA-3, RORC, STAT3, and IDO.

The cytotoxic activity of all treatment conditions of CD3⁺CD56⁺ cells required IFN-γ

The CD3⁺CD56⁺ subset that had been exposed to mDC or sunitinib treated mDCs were examined whether they mediated their anti-tumor cytotoxic action through IFN- γ . The isolated CD3⁺CD56⁺ subset from each condition was pretreated with the neutralizing monoclonal anti-IFN- γ (α IFN- γ) prior to the exposure to the target HubCCA1 target cells. All studied conditions of CD3⁺CD56⁺ subset were susceptible to the suppressive effect of anti-IFN- γ (Fig. 6).

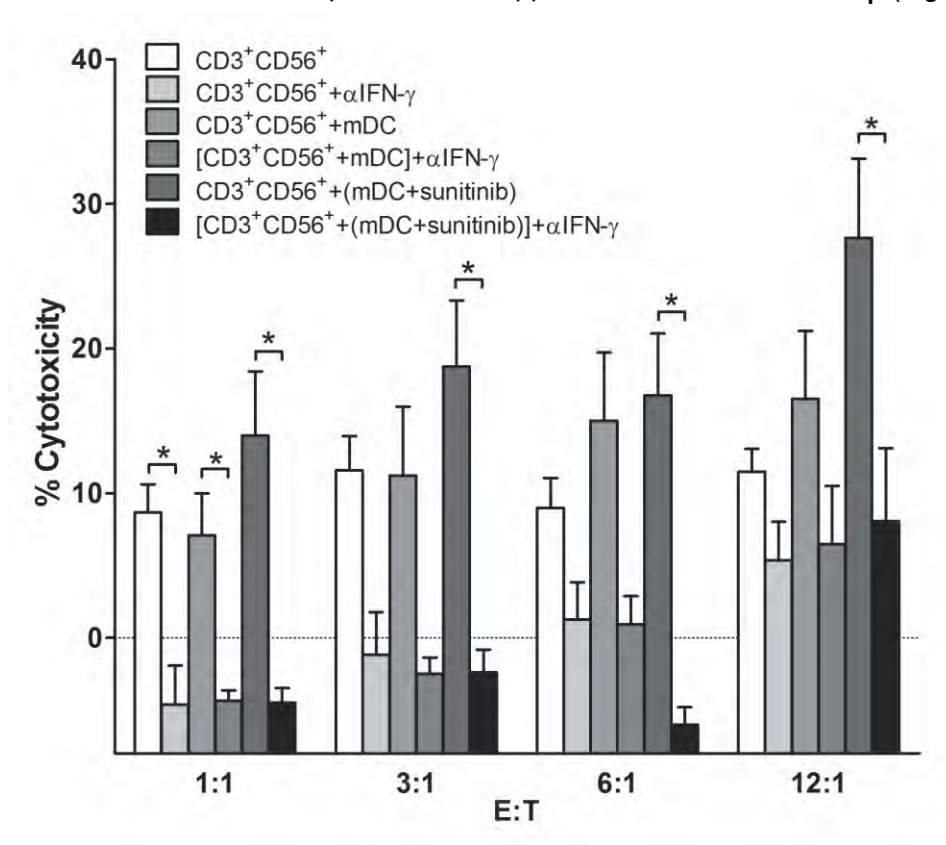


Figure 6. The cytotoxic activity of all conditions of CD3⁺CD56⁺ cells could be neutralized

with αIFN-γ treatment. The CD3⁺CD56⁺ cells from each condition were inoculated with the attached HubCCA1 cells (5,000 cells/well) for 4 h before the PI assay. These conditions included the untreated CD3⁺CD56⁺ cells, αIFN-γ treatment to CD3⁺CD56⁺ cells, CD3⁺CD56⁺ cells primed with mDC, αIFN-γ treatment to CD3⁺CD56⁺ cells primed with sunitinib-pretreated mDC, and αIFN-γ treatment to CD3⁺CD56⁺ cells primed with sunitinib-pretreated mDC. * designates conditions that provided statistically difference after αIFN-γ treatment at the same E:T ratio with p < 0.05.

CHAPTER IV

DISCUSSION AND CONCLUSION

To our knowledge, the present finding provided the first notion that the CD3⁺CD56⁺ subset of CIK cells was not invariably naturally active. The CD3⁺CD56⁺ subset could be polarized toward either Th1 or Th2 phenotype that in turn shapes its anti-tumor activity. The resting CD3⁺CD56⁺ subset predominantly expressed Th2 phenotypes, but shifted to Th1 phenotypes upon the exposure to sunitinib-pretreated DCs. The induction of Th1 immune response was first observed in T cells isolated from subjects administered with sunitinib(59). We investigated further whether the Th1-promoting action of sunitinib was derived directly from CIK cells or indirectly from mDCs. Our data revealed the sequential phenotypic changes in DCs after exposure to sunitinib. Our observation confirmed and expanded the previous report that CD3⁺CD56⁺ cells could have their anti-tumor activity expanded after the exposure to mDCs(48) and sunitinib-pretreated mDCs further enhanced this activity. This enhancement could not be

simply introduced through the direct exposure of CD3⁺CD56⁺ cells to sunitinib.

Modulation of DCs and macrophages by sunitinib

Since the improvement in anti-tumor cytotoxicity of CIK cells resulted mainly from the exposure to sunitinib-pretreated mDCs, we hypothesized that the phenotypic alterations in DCs from sunitinib might be one of the underlying mechanisms. It was possible that sunitinib could induce DC maturation that led to the corresponding enhancement of the anti-tumor cytotoxicity of CIK cells. Using the staining for the DC maturation markers (CD80, CD83 and CD86), apparently there was no significant change in DC maturation in agreement with an earlier study(65). The expression of Th1-polarizing cytokines (IL-12, IFN-γ and IL-6) was enhanced, whereas the expression of Th2-polarizing cytokine (IL-13) and the regulatory phenotype (PD-L1, IDO) were suppressed in sunitinib-treated mDCs. The increasing IL-23 expression in sunitinib-treated mDCs should foster the conversion of the nearby Treg toward Th17 cells. The sunitinib-treated monocyte-derived macrophages carried lessen DC maturation markers as well as lessen M1 differentiation markers (CD14 and CD40). The M2 differentiation was also suppressed as evidenced by the lowering IL-10 expression that might favor anti-tumor action. Taken together, sunitinib shifted mDCs toward Th1-polarizing phenotype and away from both Th2-polarizing and regulatory phenotypes.

Sunitinib-pretreated DCs drove CD3⁺CD56⁺ cells toward Th1 polarization

Following the phenotypic change in sunitinib-treated mDCs, we investigated whether there were subsequent alterations in the proportion or the phenotypes of the co-culturing CIK subsets. There was no significant alteration in the proportion of any subset with any treatment. As opposed to the earlier study(45), we could not observe the lessening of Treg subset following the co-culture with DCs. The quantitative change was evaluated through the alteration in the proportion of CD3⁺CD56⁺ subset within the whole CIK cell population. The CD3⁺CD56⁺ subset proportion was not significantly altered after the exposure to sunitinib-pre-treated mDCs. The functional change was observed through the monitoring for alterations in Th1/Th2/Th17 The polarization toward Th1 differentiation of the CD3⁺CD56⁺ subset was phenotypes. evidenced by the heightening expression of IFN-V and T-bet. The Th2 differentiation were lessened as evidenced by decreasing GATA-3 expression. The alteration in Th1/Th2 phenotypes was in agreement with the observations in DCs. The Th17 differentiation in CD3⁺CD56⁺ subset disagreed with the observation in DCs since RORC expression was decreased while STAT3 expression was not significantly altered. This observation was not unexpected, since the Treg subset, not the CD3⁺CD56⁺ subset, was envisaged to undergo Th17 differentiation(67). The heightening antitumor activity in all conditions of CD3⁺CD56⁺ subset relied heavily on IFN-V secretion as this anti-tumor action could be reverse with the neutralizing anti-IFN-γ mAb.

Earlier sunitinib study involving mDCs reported the increasing frequency of mDCs in subjects receiving systemic sunitinib treatment(58) with no deleterious effect toward their immunostimulatory function. We have characterized the changes in sunitinib-pretreated mDCs as well as the co-culturing CIK cells regarding to the Th1/Th2/Treg balance. Our *ex vivo* observation implied the immunostimulatory action of sunitinib in addition to the elimination of immunoregulatory cells as reported by others(50, 52, 53). Although our studied sunitinib concentration (1 μM) was beyond pharmaceutical concentration, we did not observe any deleterious effect toward mDCs in agreement with the earlier study(52). The employed concentration was well above the recommended trough plasma concentration (Cmin) at 94 nM(68) and the observed maximal plasma concentration (Cmax) at 188 nM(69), signified the application of *ex vivo* approach to circumvent systemic adverse reactions(70) in clinical trials. The future direction for CIK cell-based immunotherapy may aim to raise the Th1 phenotype of its effectors in addition to neutralizing the immunosuppressive activity in its Treg subset or in TME.

REFERENCES

- 1. Zou W. Immunosuppressive networks in the tumour environment and their therapeutic relevance. Nat Rev Cancer. 2005;5(4):263-74.
- 2. Nardin A, Abastado JP. Macrophages and cancer. Front Biosci. 2008;13:3494-505.
- 3. Marigo I, Dolcetti L, Serafini P, Zanovello P, Bronte V. Tumor-induced tolerance and immune suppression by myeloid derived suppressor cells. Immunol Rev. 2008;222:162-79.
- Mantovani A, Sozzani S, Locati M, Allavena P, Sica A. Macrophage polarization: tumorassociated macrophages as a paradigm for polarized M2 mononuclear phagocytes. Trends Immunol. 2002;23(11):549-55.
- 5. Saji H, Koike M, Yamori T, Saji S, Seiki M, Matsushima K, et al. Significant correlation of monocyte chemoattractant protein-1 expression with neovascularization and progression of breast carcinoma. Cancer. 2001;92(5):1085-91.
- 6. Martinez FO, Sica A, Mantovani A, Locati M. Macrophage activation and polarization. Front Biosci. 2008;13:453-61.
- 7. Klimp AH, Hollema H, Kempinga C, van der Zee AG, de Vries EG, Daemen T. Expression of cyclooxygenase-2 and inducible nitric oxide synthase in human ovarian tumors and tumor-associated macrophages. Cancer Res. 2001;61(19):7305-9.
- 8. Mantovani A, Allavena P, Sozzani S, Vecchi A, Locati M, Sica A. Chemokines in the recruitment and shaping of the leukocyte infiltrate of tumors. Semin Cancer Biol. 2004;14(3):155-60.
- 9. Allavena P, Sica A, Vecchi A, Locati M, Sozzani S, Mantovani A. The chemokine receptor switch paradigm and dendritic cell migration: its significance in tumor tissues. Immunol Rev. 2000;177:141-9.
- Adema GJ, Hartgers F, Verstraten R, de Vries E, Marland G, Menon S, et al. A dendriticcell-derived C-C chemokine that preferentially attracts naive T cells. Nature. 1997;387(6634):713-7.
- 11. Scarpino S, Stoppacciaro A, Ballerini F, Marchesi M, Prat M, Stella MC, et al. Papillary carcinoma of the thyroid: hepatocyte growth factor (HGF) stimulates tumor cells to release chemokines active in recruiting dendritic cells. Am J Pathol. 2000;156(3):831-7.
- 12. Sica A, Saccani A, Bottazzi B, Polentarutti N, Vecchi A, van Damme J, et al. Autocrine production of IL-10 mediates defective IL-12 production and NF-kappa B activation in tumorassociated macrophages. J Immunol. 2000;164(2):762-7.

- 13. Kortylewski M, Kujawski M, Wang T, Wei S, Zhang S, Pilon-Thomas S, et al. Inhibiting Stat3 signaling in the hematopoietic system elicits multicomponent antitumor immunity. Nat Med. 2005;11(12):1314-21.
- Hagemann T, Lawrence T, McNeish I, Charles KA, Kulbe H, Thompson RG, et al. "Re-educating" tumor-associated macrophages by targeting NF-kappaB. J Exp Med. 2008;205(6):1261-8.
- 15. Fong CH, Bebien M, Didierlaurent A, Nebauer R, Hussell T, Broide D, et al. An antiinflammatory role for IKKbeta through the inhibition of "classical" macrophage activation. J Exp Med. 2008;205(6):1269-76.
- Kusmartsev S, Gabrilovich DI. STAT1 signaling regulates tumor-associated macrophagemediated T cell deletion. J Immunol. 2005;174(8):4880-91.
- 17. Bottazzi B, Polentarutti N, Acero R, Balsari A, Boraschi D, Ghezzi P, et al. Regulation of the macrophage content of neoplasms by chemoattractants. Science. 1983;220(4593):210-2.
- 18. Ueno T, Toi M, Saji H, Muta M, Bando H, Kuroi K, et al. Significance of macrophage chemoattractant protein-1 in macrophage recruitment, angiogenesis, and survival in human breast cancer. Clin Cancer Res. 2000;6(8):3282-9.
- 19. Porta C, Subhra Kumar B, Larghi P, Rubino L, Mancino A, Sica A. Tumor promotion by tumor-associated macrophages. Adv Exp Med Biol. 2007;604:67-86.
- 20. Gu L, Tseng S, Horner RM, Tam C, Loda M, Rollins BJ. Control of TH2 polarization by the chemokine monocyte chemoattractant protein-1. Nature. 2000;404(6776):407-11.
- 21. Hotchkiss KA, Ashton AW, Klein RS, Lenzi ML, Zhu GH, Schwartz EL. Mechanisms by which tumor cells and monocytes expressing the angiogenic factor thymidine phosphorylase mediate human endothelial cell migration. Cancer Res. 2003;63(2):527-33.
- 22. Guiducci C, Vicari AP, Sangaletti S, Trinchieri G, Colombo MP. Redirecting in vivo elicited tumor infiltrating macrophages and dendritic cells towards tumor rejection. Cancer Res. 2005;65(8):3437-46.
- 23. Sinha P, Clements VK, Ostrand-Rosenberg S. Reduction of myeloid-derived suppressor cells and induction of M1 macrophages facilitate the rejection of established metastatic disease. J Immunol. 2005;174(2):636-45.
- 24. Rauh MJ, Sly LM, Kalesnikoff J, Hughes MR, Cao LP, Lam V, et al. The role of SHIP1 in macrophage programming and activation. Biochem Soc Trans. 2004;32(Pt 5):785-8.
- 25. Bronte V, Zanovello P. Regulation of immune responses by L-arginine metabolism. Nat Rev Immunol. 2005;5(8):641-54.

- 26. Conti I, Rollins BJ. CCL2 (monocyte chemoattractant protein-1) and cancer. Semin Cancer Biol. 2004;14(3):149-54.
- 27. Pollard JW. Tumour-educated macrophages promote tumour progression and metastasis. Nat Rev Cancer. 2004;4(1):71-8.
- 28. Phillips RJ, Mestas J, Gharaee-Kermani M, Burdick MD, Sica A, Belperio JA, et al. Epidermal growth factor and hypoxia-induced expression of CXC chemokine receptor 4 on non-small cell lung cancer cells is regulated by the phosphatidylinositol 3kinase/PTEN/AKT/mammalian target of rapamycin signaling pathway and activation of hypoxia inducible factor-1alpha. J Biol Chem. 2005;280(23):22473-81.
- 29. Giraudo E, Inoue M, Hanahan D. An amino-bisphosphonate targets MMP-9-expressing macrophages and angiogenesis to impair cervical carcinogenesis. J Clin Invest. 2004;114(5):623-33.
- 30. Balkwill F, Charles KA, Mantovani A. Smoldering and polarized inflammation in the initiation and promotion of malignant disease. Cancer Cell. 2005;7(3):211-7.
- 31. Mantovani A, Garlanda C. Inflammation and multiple myeloma: the Toll connection. Leukemia. 2006;20(6):937-8.
- 32. Rubinstein N, Alvarez M, Zwirner NW, Toscano MA, Ilarregui JM, Bravo A, et al. Targeted inhibition of galectin-1 gene expression in tumor cells results in heightened T cell-mediated rejection; A potential mechanism of tumor-immune privilege. Cancer Cell. 2004;5(3):241-51.
- 33. Friberg M, Jennings R, Alsarraj M, Dessureault S, Cantor A, Extermann M, et al. Indoleamine 2,3-dioxygenase contributes to tumor cell evasion of T cell-mediated rejection. Int J Cancer. 2002;101(2):151-5.
- 34. Brenk M, Scheler M, Koch S, Neumann J, Takikawa O, Hacker G, et al. Tryptophan deprivation induces inhibitory receptors ILT3 and ILT4 on dendritic cells favoring the induction of human CD4+CD25+ Foxp3+ T regulatory cells. J Immunol. 2009;183(1):145-54.
- 35. Frumento G, Piazza T, Di Carlo E, Ferrini S. Targeting tumor-related immunosuppression for cancer immunotherapy. Endocrine, metabolic & immune disorders drug targets. 2006;6(3):233-7.
- 36. Frumento G, Rotondo R, Tonetti M, Damonte G, Benatti U, Ferrara GB. Tryptophanderived catabolites are responsible for inhibition of T and natural killer cell proliferation induced by indoleamine 2,3-dioxygenase. J Exp Med. 2002;196(4):459-68.

- 37. Terness P, Bauer TM, Rose L, Dufter C, Watzlik A, Simon H, et al. Inhibition of allogeneic T cell proliferation by indoleamine 2,3-dioxygenase-expressing dendritic cells: mediation of suppression by tryptophan metabolites. J Exp Med. 2002;196(4):447-57.
- 38. Chen DS, Mellman I. Oncology meets immunology: the cancer-immunity cycle. Immunity. 2013;39(1):1-10.
- 39. Zheng R, Blobel GA. GATA Transcription Factors and Cancer. Genes & cancer. 2010;1(12):1178-88.
- 40. Amsen D, Spilianakis CG, Flavell RA. How are T(H)1 and T(H)2 effector cells made? Current opinion in immunology. 2009;21(2):153-60.
- 41. Zhang H, Maric I, Diprima MJ, Khan J, Orentas RJ, Kaplan RN, et al. Fibrocytes represent a novel MDSC subset circulating in patients with metastatic cancer. Blood. 2013.
- 42. Lu PH, Negrin RS. A novel population of expanded human CD3+CD56+ cells derived from T cells with potent in vivo antitumor activity in mice with severe combined immunodeficiency. J Immunol. 1994;153(4):1687-96.
- 43. Schmidt-Wolf GD, Negrin RS, Schmidt-Wolf IG. Activated T cells and cytokine-induced CD3+CD56+ killer cells. Annals of hematology. 1997;74(2):51-6.
- 44. Marten A, Ziske C, Schottker B, Renoth S, Weineck S, Buttgereit P, et al. Interactions between dendritic cells and cytokine-induced killer cells lead to an activation of both populations. J Immunother. 2001;24(6):502-10.
- 45. Schmidt J, Eisold S, Buchler MW, Marten A. Dendritic cells reduce number and function of CD4+CD25+ cells in cytokine-induced killer cells derived from patients with pancreatic carcinoma. Cancer Immunol Immunother. 2004;53(11):1018-26.
- 46. Erhardt M, Schmidt-Wolf IG, Sievers E, Frank S, Strehl J, von Lilienfeld-Toal M, et al. Antitumoral capabilities of effector cells after IFN-alpha or CpG-motif treatment of cocultured dendritic cells. Archivum immunologiae et therapiae experimentalis. 2006;54(6):403-9.
- 47. Li H, Wang C, Yu J, Cao S, Wei F, Zhang W, et al. Dendritic cell-activated cytokine-induced killer cells enhance the anti-tumor effect of chemotherapy on non-small cell lung cancer in patients after surgery. Cytotherapy. 2009;11(8):1076-83.
- 48. Wongkajornsilp A, Somchitprasert T, Butraporn R, Wamanuttajinda V, Kasetsinsombat K, Huabprasert S, et al. Human cytokine-induced killer cells specifically infiltrated and retarded the growth of the inoculated human cholangiocarcinoma cells in SCID mice. Cancer Invest. 2009;27(2):140-8.

- 49. Wongkajornsilp A, Sangsuriyong S, Hongeng S, Waikakul S, Asavamongkolkul A, Huabprasert S. Effective osteosarcoma cytolysis using cytokine-induced killer cells pre-inoculated with tumor RNA-pulsed dendritic cells. J Orthop Res. 2005;23(6):1460-6.
- 50. Nishioka Y, Aono Y, Sone S. Role of tyrosine kinase inhibitors in tumor immunology. Immunotherapy. 2011;3(1):107-16.
- 51. Krusch M, Salih J, Schlicke M, Baessler T, Kampa KM, Mayer F, et al. The kinase inhibitors sunitinib and sorafenib differentially affect NK cell antitumor reactivity in vitro. J Immunol. 2009;183(12):8286-94.
- 52. Hipp MM, Hilf N, Walter S, Werth D, Brauer KM, Radsak MP, et al. Sorafenib, but not sunitinib, affects function of dendritic cells and induction of primary immune responses. Blood. 2008;111(12):5610-20.
- 53. Ozao-Choy J, Ma G, Kao J, Wang GX, Meseck M, Sung M, et al. The novel role of tyrosine kinase inhibitor in the reversal of immune suppression and modulation of tumor microenvironment for immune-based cancer therapies. Cancer Res. 2009;69(6):2514-22.
- 54. Lindau D, Gielen P, Kroesen M, Wesseling P, Adema GJ. The immunosuppressive tumour network: myeloid-derived suppressor cells, regulatory T cells and natural killer T cells. Immunology. 2013;138(2):105-15.
- Morse MA, Hall JR, Plate JM. Countering tumor-induced immunosuppression during immunotherapy for pancreatic cancer. Expert opinion on biological therapy. 2009;9(3):331-9.
- 56. Li H, Yu JP, Cao S, Wei F, Zhang P, An XM, et al. CD4 +CD25 + regulatory T cells decreased the antitumor activity of cytokine-induced killer (CIK) cells of lung cancer patients. Journal of clinical immunology. 2007;27(3):317-26.
- 57. Ko JS, Zea AH, Rini BI, Ireland JL, Elson P, Cohen P, et al. Sunitinib mediates reversal of myeloid-derived suppressor cell accumulation in renal cell carcinoma patients. Clin Cancer Res. 2009;15(6):2148-57.
- 58. van Cruijsen H, van der Veldt AA, Vroling L, Oosterhoff D, Broxterman HJ, Scheper RJ, et al. Sunitinib-induced myeloid lineage redistribution in renal cell cancer patients: CD1c+dendritic cell frequency predicts progression-free survival. Clin Cancer Res. 2008;14(18):5884-92.
- 59. Finke JH, Rini B, Ireland J, Rayman P, Richmond A, Golshayan A, et al. Sunitinib reverses type-1 immune suppression and decreases T-regulatory cells in renal cell carcinoma patients. Clin Cancer Res. 2008;14(20):6674-82.

- 60. Adotevi O, Pere H, Ravel P, Haicheur N, Badoual C, Merillon N, et al. A decrease of regulatory T cells correlates with overall survival after sunitinib-based antiangiogenic therapy in metastatic renal cancer patients. Journal of immunotherapy. 2010;33(9):991-8.
- 61. Bose A, Taylor JL, Alber S, Watkins SC, Garcia JA, Rini BI, et al. Sunitinib facilitates the activation and recruitment of therapeutic anti-tumor immunity in concert with specific vaccination. Int J Cancer. 2011;129(9):2158-70.
- 62. Kao J, Ko EC, Eisenstein S, Sikora AG, Fu S, Chen SH. Targeting immune suppressing myeloid-derived suppressor cells in oncology. Crit Rev Oncol Hematol. 2011;77(1):12-9.
- 63. Ko JS, Rayman P, Ireland J, Swaidani S, Li G, Bunting KD, et al. Direct and differential suppression of myeloid-derived suppressor cell subsets by sunitinib is compartmentally constrained. Cancer Res. 2010;70(9):3526-36.
- 64. Kujawski M, Zhang C, Herrmann A, Reckamp K, Scuto A, Jensen M, et al. Targeting STAT3 in adoptively transferred T cells promotes their in vivo expansion and antitumor effects. Cancer Res. 2010;70(23):9599-610.
- 65. Alfaro C, Suarez N, Gonzalez A, Solano S, Erro L, Dubrot J, et al. Influence of bevacizumab, sunitinib and sorafenib as single agents or in combination on the inhibitory effects of VEGF on human dendritic cell differentiation from monocytes. Br J Cancer. 2009;100(7):1111-9.
- 66. Kobayashi M, Kubo T, Komatsu K, Fujisaki A, Terauchi F, Natsui S, et al. Changes in peripheral blood immune cells: their prognostic significance in metastatic renal cell carcinoma patients treated with molecular targeted therapy. Medical oncology. 2013;30(2):556.
- 67. Barbi J, Pardoll D, Pan F. Metabolic control of the Treg/Th17 axis. Immunological reviews. 2013;252(1):52-77.
- 68. Mendel DB, Laird AD, Xin X, Louie SG, Christensen JG, Li G, et al. In vivo antitumor activity of SU11248, a novel tyrosine kinase inhibitor targeting vascular endothelial growth factor and platelet-derived growth factor receptors: determination of a pharmacokinetic/pharmacodynamic relationship. Clin Cancer Res. 2003;9(1):327-37.
- 69. Houk BE, Bello CL, Kang D, Amantea M. A population pharmacokinetic meta-analysis of sunitinib malate (SU11248) and its primary metabolite (SU12662) in healthy volunteers and oncology patients. Clin Cancer Res. 2009;15(7):2497-506.
- Heine A, Held SA, Bringmann A, Holderried TA, Brossart P. Immunomodulatory effects of anti-angiogenic drugs. Leukemia: official journal of the Leukemia Society of America, Leukemia Research Fund, UK. 2011;25(6):899-905.

Output จากโครงการวิจัยที่ได้รับทุนจาก สกว.

- 1. ผลงานตีพิมพ์ในวารสารวิชาการนานาชาติ (ระบุชื่อผู้แต่ง ชื่อเรื่อง ชื่อวารสาร ปี เล่มที่ เลขที่ และ หน้า)
 - -<u>Wongkajornsilp A</u>, Wamanuttajinda V, Kasetsinsombat K, Duangsa-ard S, Sangiamsuntorn K, Hongeng S, Maneechotesuwan K. Sunitinib indirectly enhanced antitumor cytotoxicity of cytokine-induced killer cells and CD3⁺CD56⁺ subset through the coculturing dendritic cells. PLoS One (galley prove, accepted for publication)
 - -<u>Wongkajornsilp A</u>, Sa-Ngiamsuntorn K, Hongeng S. Development of immortalized hepatocyte-like cells from hMSCs. Methods in molecular biology. 2012;826: 73-87.
 - -Sa-ngiamsuntorn K, Wongkajornsilp A, Kasetsinsombat K, Duangsa-ard S, Nuntakarn L, Borwornpinyo S, et al. Upregulation of CYP 450s expression of immortalized hepatocyte-like cells derived from mesenchymal stem cells by enzyme inducers. BMC biotechnology. 2011;11: 89. (corresponding author)

2. การนำผลงานวิจัยไปใช้ประโยชน์

- เชิงวิชาการ (มีการพัฒนาการเรียนการสอน/สร้างนักวิจัยใหม่)
- 3. อื่นๆ (เช่น ผลงานตีพิมพ์ในวารสารวิชาการในประเทศ การเสนอผลงานในที่ประชุมวิชาการ หนังสือ การจดสิทธิบัตร)
 - Wongkajornsilp A, Wamanuttajinda V, Kasetsinsombat K, Duangsa-ard S, Hongeng S.
 Direct addition of picibanil to cytokine-induced killer cells improved the anti-cholangiocarcinoma cytotoxic activity. Keystone Symposia on Molecular and Cellular Biology February 7-12, 2010, Keystone Resort, Keystone, Colorado, USA.
 - Wongkajornsilp A, Wamanuttajinda V, Kasetsinsombat K, Duangsa-ard S, Maneechotesuwan K. Suppression of CD274 expression in both mature and immature dendritic cells rendered greater anti-cholangiocarcinoma activity of the co-culturing cytokine-induced killer cells. Abstract book: Keystone Symposia on Molecular and Cellular Biology: Cancer control by tumor suppressors and immune effectors, February 12 17, 2011, Santa Fe, NM, p. 206.
 - Kasetsinsombat K, Wamanuttajinda V, Duangsa-ard S, Ariyaboonsiri B, Waikakul S, Maneechotesuwan K, Wongkajornsilp A. Addition of 1-methyl tryptophan to the co-culture of cytokine-induced killer cells with macrophages improved the anti-osteosarcoma cytolysis over those co-cultured with dendritic cells. Abstract book:

- Keystone Symposia on Molecular and Cellular Biology: Cancer control by tumor suppressors and immune effectors, February 12 17, 2011, Santa Fe, NM, p. 189.
- Duangsa-ard S, Kasetsinsombat K, Wamanuttajinda V, Maneechotewuwan K, Wongkajornsilp A. Inhibition of indolamine 2,3-dioxygenase in dendritic cells improved anti-cholangiocarcinoma activity of cytokine-induced killer cells. Abstract book: Keystone Symposia on Molecular and Cellular Biology: Cancer control by tumor suppressors and immune effectors, February 12 17, 2011, Santa Fe, NM, p. 182.
- Sa-ngiamsuntorn K, Wamanuttajinda V, Duangsa-ard S, Kasetsinsombat K,
 Maneechotesuwan K, Wongkajornsilp A. Treatment of CIK cells using Poly-G3 improved the anti-cholangiocarcinoma cytotoxicity. Abstract book: Keystone Symposia on Molecular and Cellular Biology: Cancer control by tumor suppressors and immune effectors, February 12 17, 2011, Santa Fe, NM, p. 199.
- Sa-ngiamsuntorn, K., Kasetsinsombat K, Wamanuttajinda V, Duangsa-ard S,
 Ariyaboonsiri B, Waikakul S, Maneechotesuwan K, Wongkajornsilp A. Addition of 1-methyl tryptophan to the co-culture of cytokine-induced killer cells with macrophages improved the anti-osteosarcoma cytolysis over those co-cultured with dendritic cells.
 Abstract book: The 7th Princess Chulabhorn International Science Congress (CRI): Cancer: From basic research to cure, November 29 December 3, 2012, Bangkok Thailand, p.316
- Wongkajornsilp A, Wamanuttajinda V, Kasetsinsombat K, Duangsa-ard S,
 Maneechotesuwan K, Hongeng S. Sunitinib enhanced the anti-cholangiocarcinoma action of cytokine-induced killer cells through the action on CD3⁺CD56⁺ cells. American Association for Cancer Research (AACR): Tumor Immunology: Multidisciplinary science driving basic and clinical advances, December 2-5, 2012, USA
- Wongkajornsilp A, Wamanuttajinda V, Kasetsinsombat K, Duangsa-ard S,
 Maneechotesuwan K Sunitinib-treated dendritic cells promoted Th1 phenotype in
 CD3⁺CD56⁺ subset of CIK cells. Keystone Symposia on Molecular and Cellular Biology:
 Cancer Immunology and Immunotherapy, January 27 February 1, 2013, Fairmont
 Hotel Vancouver, Vancouver, British Columbia, Canada.

APPENDIX I

Reprints

Chapter 7

Development of Immortalized Hepatocyte-Like Cells from hMSCs

Adisak Wongkajornsilp, Khanit Sa-ngiamsuntorn, and Suradej Hongeng

Abstract

Clones of hepatocyte-like cells were reproducibly generated from human mesenchymal stem cells immortalized with a combined transduction of both Bmi-1 and TERT genes. These hepatocyte-like cells contained selective markers and several functional properties of hepatocytes, yet still carried proliferative potential. These cells had cuboidal morphology and arranged themselves as cord-like structure in culture. The cloned cells deposited glycogen and actively synthesized albumin. The basal expressions of CYP450 isozymes was observed, albeit only 10–20% that of primary hepatocytes. These expressions were promptly increased upon the addition of rifampicin, a known enzyme inducer. These hepatocyte-like cells may serve as a close alternative to the use of primary hepatocytes for in vitro studies.

Key words: Hepatocyte-like cell, hMSC, Cell immortalization, Hepatocyte differentiation, CYP450, Drug metabolism, Toxicology

1. Introduction

The procurement of human hepatocyte cell lines would benefit in diverse applications, namely, allotransplant, xenobiotic biotransformation, and assessment of CYP450 activation profiles. The generation of primary hepatocyte is complicated with both ethical and technical hitches. The activity of drug metabolizing enzymes and many transporter functions were rapidly lost after being cultured (1, 2). The primary human hepatocytes maintained their functions for 3 days and barely survived up to 7 days except under special condition (3–5). The primary human hepatocyte remains a gold standard for in vitro study of drug metabolism and toxicology (4). To date, there has been only a single continuous non-cancerous

human hepatocyte cell line (Fa2N-4) with a maximal induction of CYP450 transcripts was only ten times its low basal level (6, 7). The expectation of hepatocyte cell line with functional integrity is, therefore, currently not realistic and alternative cells carrying hepatocyte-emulative functions should be acceptably substituted. One of the closest examples of such cells is the hepatocyte-like cells derived from human mesenchymal stem cells (hMSCs) (8).

hMSCs could give rise to diversely specific cell types such as chondrocytes, osteocytes, adipocytes, and hepatocytes (9–12). The potential of MSCs derived from bone marrow, adipose tissue, or umbilical cord blood to differentiate into hepatocytes has long been shown in humans (13–15), using specialized growth conditions in vitro. The multipotent stem cell derived hepatocyte-like cells could be applied for the study of hepatic biotransformation of xenobiotics and hepatotoxicity (16, 17). Since hMSCs have the ability of self-renewal, the use of hMSC-derived hepatocytes would serve as an unlimited substitution for functioning human hepatocytes.

The validity for using immortalized cell line for in vitro metabolic study relies on the maintenance of hepatocyte phenotypes as represented by a panel of specific markers. These hepatocyte-like cells contain all known drug-metabolizing enzymes, including CYP450 isozymes. The precursor hMSC had been immortalized through the transduction with two entropic lentiviral plasmids separately encoding human telomerase reverse transcriptase gene (hTERT) and Bmi-1 (18). The resulting differentiated immortalized cells contained not only hepatocyte phenotypes but also proliferative activity.

2. Materials

2.1. Isolation of Mesenchymal Stem Cell

2.2. Culture of hMSCs

- 1. IsoPrep® (Robbins Scientific, Canada).
- 2. Improved Neubauer hemocytometer.
- Minimum Essential Medium-α (α-MEM, Gibco/BRL, Cat. No. 12000-063) supplemented with 10% fetal bovine serum (FBS, Biochrom AG Berlin, Germany).
- 2. Iscove's Modified Dulbecco's Medium (IMDM) (Gibco/BRL, Cat. No. 12200-036).
- 3. Porcine trypsin, 0.25% w/v, 1 mM EDTA in PBS.
- 4. Phosphate-buffered saline (PBS) without calcium and magnesium.
- 5. Plastic wares (polypropylene centrifuge tubes 15 and 50 mL, plastic tissue culture Petri dishes 10-cm diameter, cell culture flash T-25 and T-75 (Corning Incorporated, USA), 6-cm

- diameter collagen IV-coated culture dishes (Iwaki Glass Co., Tokyo, Japan).
- 6. Penicillin G sodium (Sigma, MO, Cat. No. P7794).
- 7. Streptomycin (Sigma, MO, Cat. No. S6501).
- 8. Trypan Blue solution, 0.85% in saline (Trypan blue stain (Sigma, MO).
- 9. Trypsin 250 (Difco Laboratories, USA).

2.3. The Immortalization of hMSCs

- 1. Lentivirus plasmid vector 12245: pLOX-TERT-iresTK, plasmid 12240: pLOX-CWBmi1, plasmid 12260: psPAX2 and plasmid 12259: pMD2.G (Addgene, Inc., USA).
- Luria Broth (LB, 500 mL): 5 g tryptone, 2.5 g Yeast extract, 5 g NaCl and 500 mL H₂O. Autoclave using liquid cycle and store at 4°C.
- 3. QIAGEN Plasmid Midi Kit (Qiagen, Germany, Cat. No. 12143).
- 4. Sterile syringe filter (0.45 μM Sartorius, Germany).
- 5. Chloroquine diphosphate salt (Sigma, MO, Cat. No. C6628).
- 6. Hexadimethrine bromide or polybrene (Sigma, MO, No. H9268).
- 7. 293T human embryonic kidney cells (ATCC, Cat. No. CRL-11268).
- 8. $2\times$ HEPES-buffered saline (HBS) solution (50 mM HEPES, $1.5 \, \text{mM Na}_2\text{HPO}_4$, $280 \, \text{mM NaCl}$, $10 \, \text{mM KCl}$, $12 \, \text{mM sucrose}$) filter-sterilize or autoclave. Solution can be stored at -20°C for at least 1 year. HEPES (Sigma, MO, Cat. No. H4034).
- 9. 2 M CaCl₂ stock solution: Dissolve 14.7 g of CaCl₂ and adjust to 100 ml with H₂O and filter-sterilize and store at -20°C, stable for at least 1 year. CaCl₂ (Sigma, MO, Cat. No. C-2536).

2.4. The Hepatocyte Differentiation

- 1. Human recombinant epidermal growth factor (EGF, Chemicon Millipore, CA, Cat. No. GF144).
- 2. Human recombinant basic fibroblast growth factor (bFGF, Chemicon Millipore, CA, Cat. No. GF003-AF).
- 3. Human recombinant hepatocyte growth factor (HGF, Chemicon Millipore, CA, Cat. No. GF116).
- 4. Human recombinant oncostatin M (OSM, Chemicon Millipore, CA, Cat. No. GF016).
- 5. Nicotinamide (Sigma, MO, Cat. No. N0636).
- 6. Dexamethasone water soluble (Sigma, MO, Cat. No. D2915).
- 7. Insulin-Transferrin-Selenium-A (ITS) Supplement (100×) (Invitrogen, Cat. No. 51300-044).

2.5. RNA Extraction and Quantitative Real-Time PCR

- 1. RNA extraction RNeasy Mini kit (Qiagen, Hiden, Germany, Cat. No. 74104).
- 2. ImProm-II Reverse Transcription System (Madison, WI, Cat. No. A3800).
- 3. FastStart Universal SYBR Green Master (ROX) (Roche Diagnostics, Germany, Cat. No. 04913949001).
- 4. Primer sets for Bmi-1, hTERT, and hepatocyte-specific genes (see Note 1).

2.6. The Functional Analysis of Differentiated Cells

QuantiChrom™ Urea Assay Kit (DIUR-500, Bioxys, Belgium).

2.6.1. Urea Production Assay

2.6.2. Glycogen Storage (PAS Assay)

Periodic Acid-Schiff (PAS) Kit (395B, Sigma, MO).

2.6.3. Albumin Accumulation

- 1. Human Serum Albumin antibody (ab2406, MA).
- 2. FACS Perm (BD Bioscience, CA).
- 3. Triton X-100 (Sigma, MO).
- 4. Albumin from bovine serum (Sigma, MO).

2.6.4. Immunofluorescence

- 1. Goat anti-mouse IgG conjugated to FITC (Santa Cruz Biotechnology, CA).
- 2. Cytochrome P450 3A4 antibody (Abcam, MA).

2.7. The Induction of CYP450 Activities

- 1. Rifampicin (Sigma, MO, Cat. No. R3501).
- 2. Omeprazole (Sigma, MO, Cat. No. O104).
- 3. Phenobarbital (Sigma, MO, Cat. No. P5178).
- 4. Ethanol (Sigma, MO).
- 5. DMSO (Sigma, MO).
- P450-glo Luminescent Cytochrome P450 Assay CYP1A1, 1A2, 2C9, and 3A4 (Madison, WI, Cat. No. V8751, V8771, V8791, V9001).

3. Methods

3.1. The Isolation of hMSCs from Bone Marrow Aspirate (Fig. 1)

1. The bone marrow aspirate (5 mL) was transferred to 50-mL centrifuge tube. The bone marrow aspirate was diluted with PBS at a ratio of 1:3 to reconstitute the volume up to 20 mL.

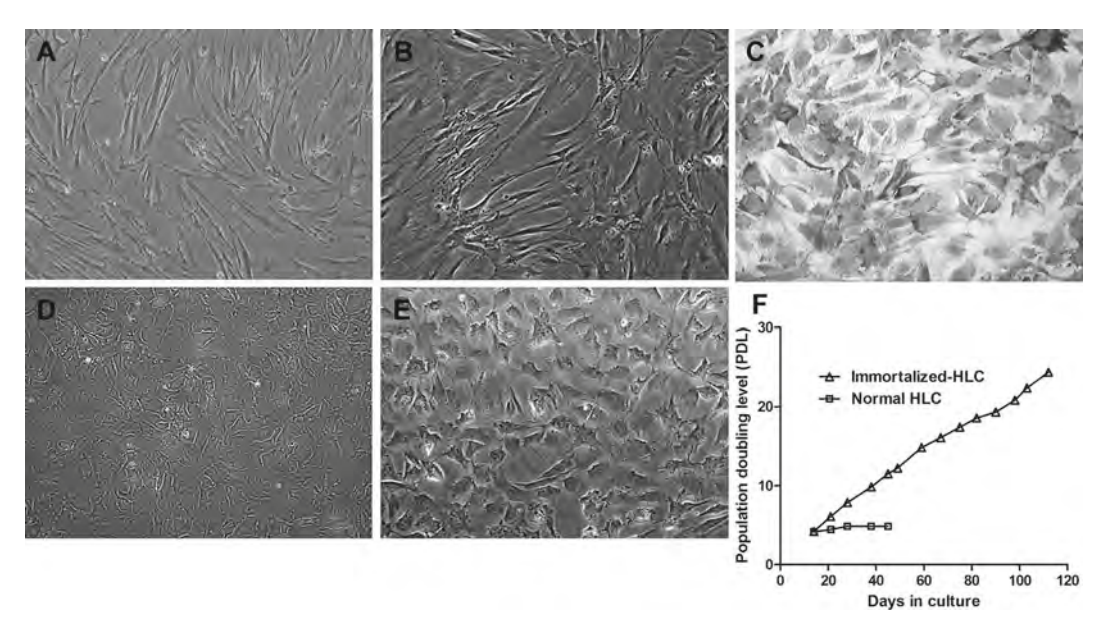


Fig. 1. The cellular morphology of hMSC and hepatocyte-like cell. The mononuclear cells from bone marrow aspirated were isolated using Ficoll gradient centrifugation (a). After reaching the 20th passage, hMSCs were immortalized (BMI/hTERT-hMSC, b). The glycogen deposit in hepatocyte-like cells in the fourth passage was demonstrated using PAS assay (c). The hepatocyte-like cells had cuboidal shape with cord-like arrangement right after the induction (d) and after being cultured in DMEM/F12 plus 10% FBS for another ten passages (e). The immortalized hepatocyte-like cell still contained proliferative property (f) as demonstrated using population doubling level (PDL).

- 2. To each of the two 15-mL polypropylene centrifuge tubes, 3 mL of Ficoll–Hypaque reagent (IsoPrep®) was added followed by the gently overlay of the 10 mL of bone marrow dilution over the Ficoll. The solvent phase junction between the bone marrow layer and the Ficoll layer should not be disrupted.
- 3. The cell suspension was centrifuged at $1,000 \times g$ for 30 min at 20° C with the break off.
- 4. After centrifugation, the mononuclear cell layer would appear as a white ring just above the interface between the diluted bone marrow layer and the Ficoll layer at the bottom. The ring could be collected using sterile Pasteur pipette and transferred to a new 50-mL centrifuge tube.
- 5. The white pellet from step 4 would be washed thrice with threefold volume of PBS and centrifuged at $1,500 \times g$ for 10 min at room temperature.
- 6. The viability of the cells could be assessed with trypan blue exclusion assay. The cell suspension (10 μ L) was mixed with 10 μ L trypan blue and laid over a hemocytometer. The cell viability should be above 80%.
- 7. The cell pellet was resuspended in 20 mL growth medium (α -MEM supplemented with 10% FBS, penicillin and streptomycin).

- 8. The cell suspension was transferred to T-75 cell culture flasks in a humidified incubator with 5% CO₂. The medium will be replaced first at day 4–5 followed by every 3–4 days thereafter.
- 9. After 7 days, the adherent cells could be assessed using an inverted microscope. Fibroblast-like colony should be presented clearly on the culture surface. The possible contamination of the culture cell with some hematopoietic cells could be eliminated through repeated passaging.

3.2. The Maintenance of hMSCs

From 3.1, hMSCs would reach 70–80% confluence by day 10–14. Upon reaching confluence, the hMSCs could be trypsinized and seeded as monolayer as followed:

- 1. The conditioned medium in T-75 culture flask will be aspirated from the adherent cells and replaced with 4 mL of trypsin/EDTA.
- 2. The T-75 cell culture flask would be brought into a 37°C incubator for 2–3 min, and inspected for the monolayer using an inverted microscope with 10× objective lens. The adherent cells should be detached from the culture surface. Additional incubation at 37°C for 5 min might be necessary if adherent cells did not detach well.
- 3. To inactivate the trypsin activity, the cell suspension was reconstituted with 4 mL of culture medium with 10% FBS, transferred to 50 mL conical centrifuge tube, and centrifuged for 10 min at 1,000×g.
- 4. The supernatant was removed from the cell pellet. The pellet was resuspended and washed with 1–2 mL of pre-warmed culture medium.
- 5. A 10 μ L aliquot of cell suspension was mixed with 10 μ L of trypan blue and count with a hemocytometer. Cell viability should be at least 80%.
- 6. Cell density per T-75 flask should stay between 2×10^6 and 5×10^6 cells and incubated in 5% CO₂ at 37°C.
- 7. The culture medium should be replaced twice a week and subculture once a week.

3.3. Preparation of Lentivirus Vectors for Immortalization

- 1. Approximately 24 h before transfection, HEK293T cells (4×10⁶ cells) in 10 mL DMEM, 10% FBS, penicillin and streptomycin were seeded over a 10-cm culture dish. The dish should be gently shaken side to side to evenly distribute the cells. After adding cells, gently mix the dish up–down and left–right. The adherent cells should reach 60–70% confluence at the time of transfection.
- 2. Lentiviruses plasmid DNA compose of psPAX2 (Addgene plasmid 12260) packaging vector and pMD2.G (Addgene plasmid 12259) vesicular stomatitis virus G envelope, and the plasmid

- encoding either hTERT (pLOX-TERT-iresTK, Addgene plasmid 12245) or Bmi-1 (pLOX-CWBmi1, Addgene plasmid 12240) were obtained by Addgene.
- 3. The lentivirus plasmid DNA was amplified using plasmid miniprep or midiprep from an overnight transformed *E. coli* culture grown in 10 mL LB medium. A 10 mL overnight LB culture should yield 5–10 μg DNA.
- 4. On the transfection date, culture medium would be gently removed from the 10-cm culture dish and replaced with 10 mL DMEM, 10% FBS, and 25 μ M chloroquine.
- 5. In a sterile 15-mL conical tube, 10 μg pLOX-TERT-iresTK or 10 μg pLOX-CWBmi1 would be mixed thoroughly with 6.5 μg psPAX2 packaging plasmid, 3.5 μg pMD2.G vesicular stomatitis virus G envelope plasmid, 290 μL 0.1× TE buffer, 160 μL sterile H₂O, and 50 μL 2M CaCl₂. 2× HBS (500 μL) would be added drop by drop while gently mixing. The mixture was left for 5 min to allow fine precipitation.
- 6. Each solution condition (1-mL) from step 5 would be layered onto the 10-cm culture dish drop by drop using a micropipette to cover all culture area.
- 7. The culture dishes were incubated in 5% CO₂ at 37°C overnight (16–18 h).
- 8. The cells will be examined under a microscope. Cells should appear healthy and be around 80–90% confluent. A fine precipitate should be visible in culture medium. The incubation was stopped by replacing the medium with 10 mL fresh DMEM, 10% FBS. The cell culture dishes were further incubated with 5% CO₂ at 37°C for 48 h. Viral particles could be harvested at 48–50 h after complete incubation period.
- 9. After 48 h, the supernatant could be collected. The supernatants were pooled into a 50-mL conical tube and filtered thought a 0.45-μm sterile syringe filter to remove cell debris. Viral stock could be concentrated by ultracentrifugation and kept frozen at -70°C until future use.
- 1. hMSCs between the third and fifth passages were seeded at a density of 2×10^6 cells/mL α -MEM, 10% FBS, antibiotic onto 6-well plate.
- 2. Before transduction, cells should reach 60–70% confluent. The Bmi-1 and hTERT lentiviral stock (1:1, 1:2, 1:4) should be diluted with culture medium to determine the suitable MOI (multiplicity of infection, see Note 1) for MSCs. Our determined optimal ratio was 1:2. Both lentiviruses were mixed together for 2-gene transduction.
- 3. The lentiviral supernatant was mixed with α -MEM, 10% FBS to reconstitute as the final transfection medium. The final

3.4. Immortalization of hMSC with Bmi-1 and hTERT Lentiviral Transduction

- transfection medium was dispensed as 1 mL/well with 6 µg/mL polybrene.
- 4. The incubation proceeded overnight (16-18 h) in 5% CO $_2$ at 37°C and was stopped by replacing the transfection medium with fresh culture medium. The infected MSCs were maintained for another 3 days to allow the expression of the transduced genes.

3.5. Cloning of Immortalized Human Mesenchymal Stem Cells

- 1. After transduction for 3–4 days, MSC should reach 80–90% confluent. The cells could be trypsinized and checked whether the viability were higher than 80%.
- 2. The cells were resuspended initially as 1×10^4 cell/mL in α -MEM medium, 10% FBS.
- 3. Five sterile conical centrifuge tubes were brought for sequential dilution. Each tube was filled with 3 mL fresh growth medium. Cell suspension (2 mL) from step 2 were transferred to tube number 1 and mixed using pipette.
- 4. A 2-mL aliquot of diluted cell suspension in tube number 1 was transferred to the tube number 2. Cell suspension was diluted and transferred to the next tube in the same manner until tube number 5. The diluted cell suspension in tube number 4 or 5 was suitable for single cell cloning.
- 5. Cell suspension (0.5 mL) from step 4 was transferred to each well of a sterile 24-well plate to achieve a single cell/well.
- 6. The 24-well plate was incubated in 5% CO₂ at 37°C for 1 week. The medium was replaced with fresh growth medium every 3–4 days. The culture was continued until the adherent cells derived from a single cell reached 70–80 confluent.
- 7. The expanded cloned cell from step 6 were trypsinized and transferred to a T-25 tissue culture flask. At least 6–8 clones were picked and screened for the highest expression of both Bmi-1 and hTERT genes.

3.6. Quantitative Real-Time PCR Analysis for Cell-Specific Markers

- 1. The adherent cells were trypsinized and washed twice with PBS by centrifugation at 1,000×g for 5 min at 4°C. The supernatant was removed while the cell pellet could be immediately used for RNA extraction or stored for a long term at -70°C. The RNA extraction was performed using RNeasy Minikit (Qiagen) following the manufacturer instruction.
- 2. The commercial ImProm-II™ Reverse Transcription system was used to synthesize single-stranded cDNA according to the manufacturer instruction. Briefly, 4 μL RNA template was mixed with 1 μL oligo (dT) in the first microcentrifuge tube. The tube was heated to 70°C for 5 min and then placed on ice for 5 min. A master mix containing 4.8 μL of 25mM MgCl₂, 4 μL of 5× reaction buffer, 3.7 μL RNase free water,

- 1 μL reverse transcriptase, 1 μL of 10 mM dNTPs, and 0.5 μL DNase inhibitor was added. The temperature was adjusted to 25°C for 5 min, 42°C for 1 h, 70°C for 15 min, and 4°C for 5 min.
- 3. The cDNA concentration was determined using the NanoDrop® spectrophotometer and diluted with double-distilled water to $10{\text -}100~\mu\text{g/mL}$ for immediate use or long-term storage at -70°C .
- 4. For real-time PCR, each reaction would contain 10 μL FastStart SYBR Green Master or equivalent, 7.5 μL double-distilled water, specific primer pairs (see Note 2), and 0.1 μg of cDNA from step 3. The temperature cycle in the real-time PCR (StepOnePlus®) consisted of 95°C for 10 min, followed by 40 cycles of 95°C for 15 s, 60°C for 40 s, and 72°C for 40 s.
- 5. For data analysis, the cycle threshold (Ct) numbers were computed for each sample using the Sequence Detection Software Version 2.01 (Applied Biosystems). To obtain accurate comparison, all hepatocyte-specific genes were normalized with the endogenous housekeeping gene, glyceraldehyde-3-phosphate dehydrogenase (GAPDH).

3.7. The Induction of Hepatogenesis

- 1. The unmanipulated hMSCs between the third and fifth passages or BMI/hTERT-transduced MSCs with a density of 1×10^4 cells/cm² were seeded for 2 days.
- For initiation step, the hMSCs were cultured in Iscove's Modified Dulbecco's Medium (IMDM), 20 ng/mL epidermal growth factor (EGF), and 10 ng/mL basic fibroblast growth factor (bFGF) for 2 days.
- 3. For differentiation step, hMSCs were maintained in IMDM, 20 ng/mL HGF, 10 ng/mL bFGF, and 0.61 g/L nicotinamide for 7 days.
- 4. For maturation step, MSCs were maintained in IMDM, 20 ng/mL oncostatin M, 1 μ M dexamethasone, and 1% (v/v) ITS for 14 days, with routine medium change every 3 days.
- 5. For CYP450 induction, a cocktail of prototypic CYPs inducers (i.e., 40 μ M rifampicin, 50 μ M dexamethasone, 1 mM omeprazole, 50 μ M phenobarbital, and 0.1% (v/v) DMSO with 2% FBS) was added to the cells and incubated for 3 days with daily medium change.

3.8. Hepatocyte Functional Analysis (Fig. 2)

3.8.1. Urea Production Assay

- 1. The cultured cells (hMSCs, hepatocyte-like cells or HepG2) in IMDM were incubated with 5 mM NH₄Cl for 48 h.
- 2. Either the classical diacetyl monoxime test or the commercial QuantiChrom Urea Assay Kit (DIUR-500) could be employed. The conditioned medium (5 μ L) from step 1 was collected and transferred in duplicate onto each well of a clear bottom

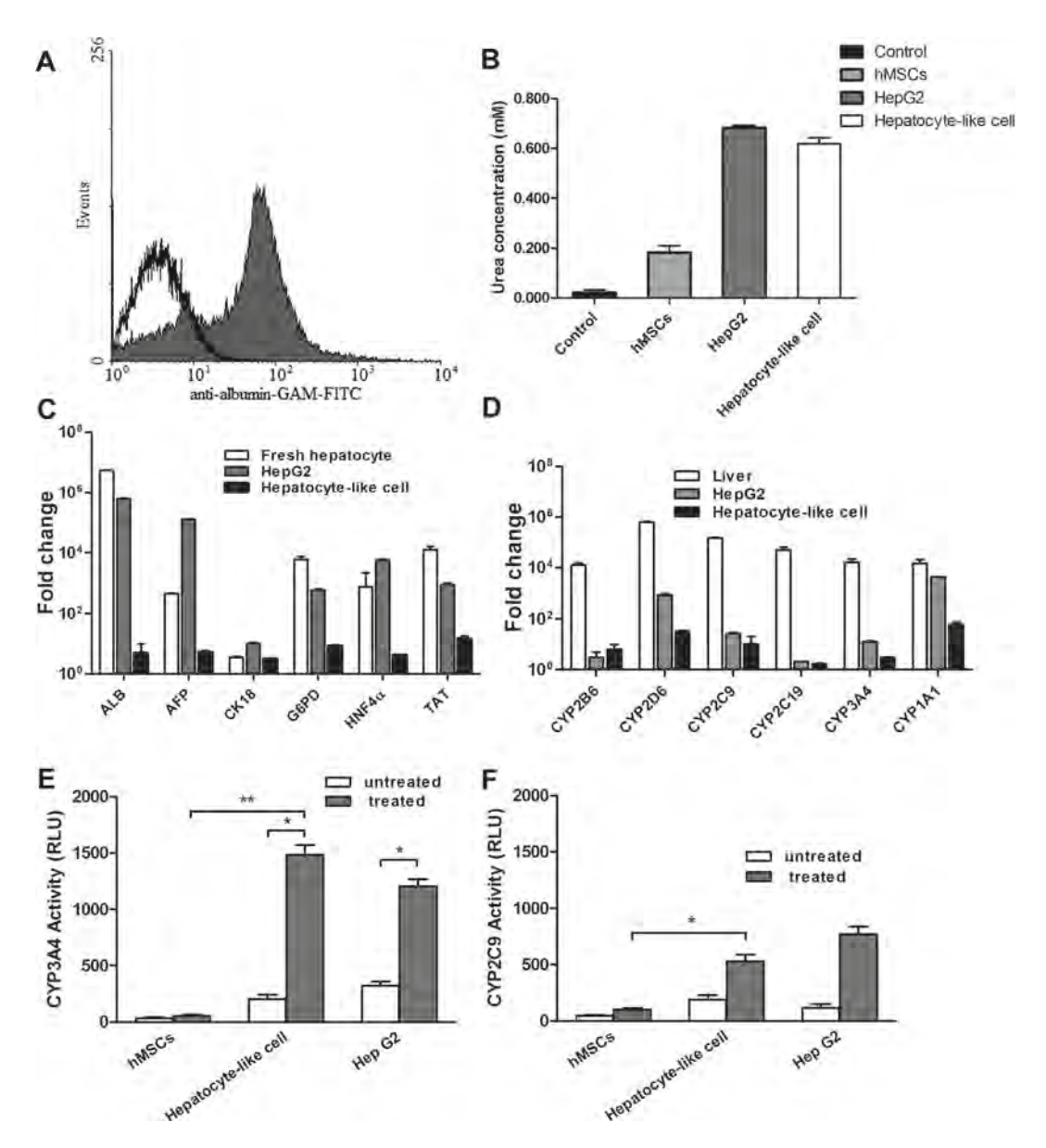


Fig. 2. The expression of hepatocyte-selective markers and functions. The hepatocyte-like cells were investigated in comparison with HepG2 for albumin synthesis using FACS (\mathbf{a}); and urea production using urea assay (\mathbf{b}). The hepatocyte-like cells were studied for the expression of hepatocyte-selective genes (\mathbf{c}) and CYP450 (\mathbf{d}) at basal stage. After the induction with 40 μ M rifampicin for 72 h, the functional activity of CYP3A4 (\mathbf{e}) and CYP2A9 (\mathbf{f}) was assayed.

96-well plate. The blank water or urea standard (50 mg/dL) was transferred in the same fashion. The 200 μL working reagent was added to each well. The solution was mixed by tapping the plate lightly. The incubation was carried out for 10–20 min at room temperature.

3. The plate was read for absorbance at 470–550 nm in a spectrophotometer. The peak absorbance is at 520 nm.

4. Urea concentration of the sample could be calculated as:

$$Urea concentration = \frac{OD_{sample} - OD_{blank}}{OD_{standard} - OD_{blank}} \times n \times 50 (mg / dL)$$

 $\mathrm{OD}_{\mathrm{sample}}$, $\mathrm{OD}_{\mathrm{blank}}$, and $\mathrm{OD}_{\mathrm{standard}}$ are OD520 nm of sample, water, and standard, respectively. n is the dilution factor. Urea at 1 mg/dL is equal to 167 $\mu\mathrm{M}$, 0.001%, or 10 ppm.

3.8.2. Glycogen Synthesis (Periodic Acid-Schiff, PAS) Assay

- 1. The trypsinized cultured cells (hMSCs, hepatocyte-like cells or HepG2) were transferred to collagen type I-coated coverslip. The cells were allowed to grow until reaching 80–90% confluent.
- 2. The coverslip was fixed with 4% paraformaldehyde for 30 min, permeabilized with 0.1% Triton X-100 for 10 min, incubated with or without diastase for 1 h at 37°C, oxidized in 1% periodic acid for 5 min, rinsed thrice with dH₂O, treated with PAS reagent for 15 min, and rinsed with water for 5–10 min.
- 3. The attached cells were counterstained with Mayer's hematoxylin for 1 min, rinsed with water, and assessed under light microscope. The resulting density of oxidized glycogen could be visualized as a color gradient starting from pink to strong red.

3.8.3. Analysis of Cellular Markers Using Flow Cytometry

- 1. The cultured cells were trypsinized and washed with PBS through centrifugation at $1,000 \times g$ for 5 min at 4°C.
- 2. The washed cells were resuspended with 0.5 mL FACS buffer depending on cell density.
- 3. The cell suspension was transferred to BD FACS tube. The primary antibody (0.5–1 μ L anti-albumin, anti-CD105, or anti-CD90, etc.) was added and mixed. The stained cells were incubated at 4°C for 30–40 min, washed, and centrifuged 2–3 times.
- 4. If any primary antibody does not conjugated with fluorochrome, secondary antibody such as GAM-FITC, GAR-PE is needed for FACS analysis.
- 5. After the staining, centrifugation, and washing thrice, the cells were suspended in 500 μ L FACS buffer in BD tube.
- 6. The suspending cells were ready for analysis using flow cytometry. Nonsingle cells and debris could be omitted based on FSC and dead cell based on SSC. At least 10,000 cells were analyzed per sample.
- 7. The FACS data could be analyzed using FlowJo version 7.63 or WinMDI version 2.9.

3.8.4. Immunofluorescence Microscopy

- 1. The trypsinized hepatocyte-like cells were transferred to collagen type I-coated coverslip. Cells were allowed to grow until reaching 80–90% confluent.
- 2. The adherent cells were washed briefly with PBS, Fix with 4% paraformaldehyde at room temperature for 30 min, followed by 100% ethanol for another 10 min.
- 3. The cells were washed thrice with PBS, blocked with 5% normal serum from the same species as the secondary antibody in 1% BSA/0.2% Triton X-100/PBS for 1 h at room temperature.
- 4. The cells were incubated with the primary antibody (anti-CYP3A4, anti-CYP2C9, or anti-CYP1A1, etc., Abcam, Cambridge, MA) for 1 h at 37°C in moist chamber.
- 5. After washing with PBS thrice, the cells were mounted with antifade mounting medium in coverslip and examined under a fluorescent microscope and photographed.

3.9. The Analysis of CYP450 Activity

- 1. The hepatocyte-like cell or HepG2 were incubated in growth medium supplement with prototypic inducers such as 40 μ M rifampicin, 50 μ M dexamethasone, 1 mM omeprazole, 50 μ M phenobarbital, 50 μ M artesunate for 72 h with daily medium change prior to the assay.
- 2. After 3-days incubation period, the cells were incubated with IMDM supplemented with 100 μM Luciferin-CEE (CYP1A1), Luciferin-H (CYP1A2), or Luciferin-ME (CYP2C9) for 3–4 h or 3 μM Luciferin-IPA (CYP3A4) for 30–60 min. A 50 μL aliquot of the incubation medium was transferred to 96-well opaque white luminometer plate. Luciferin detection reagent was added into each well.
- 3. The plate was incubated at room temperature for 20 min in dark chamber.
- 4. The luminescence was determined using a luminometer or an attached CCD camera for the measurement of luminescence unit
- 5. The relative luminescence unit (RLU) could be calculated as follows:

$$RLU = \frac{LU_{treated} - LU_{blank}}{LU_{untreated} - LU_{blank}}$$

4. Notes

1. The ratio of lentiviral supernatant to culture medium was 1:2 or 1:4 for the immortalization of hMSCs. The quantitation of living viral stocks was required to determine the exact multiplicity of infection (MOI). Freshly harvested viral stocks can be

quantitated immediately, or frozen in aliquots at -80° C for later measurement. Each freeze–thaw cycle could reduce the functional titer of the viral stock up to two- to fourfolds. The MOI is heavily relied on the cell types and measuring methods. The MOI could be determined with quantitative PCR or flow cytometry (19).

2. Primer for real-time PCR analysis

Gene	Forward primer	Reverse primer	Amplicon (bp)
ALB	TGAGAAAACG CCAGTAAGTGAC	TGCGAAATCATC CATAACAGC	265
AFP	GCTTGGTGGT GGATGAAACA	TCCTCTGTTATTT GTGGCTTTTG	157
CK18	GAGATCGAGG CTCTCAAGGA	CAAGCTGGCCT TCAGATTTC	357
G6PD	GCTGGAGTCCTG TCAGGCATTGC	TAGAGCTGAGGC GGAATGGGAG	349
HNF-4α	GCCTACCTCAAA GCCATCAT	GACCCTCCCAG CAGCATCTC	256
TAT	TGAGCAGTCTG TCCACTGCCT	ATGTGAATGAGG AGGATCTGAG	338
CYP2B6	ATGGGGCACTG AAAAAGACTGA	AGAGGCGGGGA CACTGAATGAC	283
CYP2D6	CTAAGGGAACGA CACTCATCAC	GTCACCAGGAA AGCAAAGACAC	289
CYP2C9	CCTCTGGGGCA TTATCCATC	ATATTTGCACAGT GAAACATAGGA	137
CYP2C19	TTCATGCCTTT CTCAGCAGG	ACAGATAGTGA AATTTGGAC	277
CYP2C8	ACAACAAGCACCA CTCTGAGATATG	GTCTGCCAATTACA TGATCAATCTCT	100
CYP3A4	GCCTGGTGCTC CTCTATCTA	GGCTGTTGACCA TCATAAAAGC	187
CYP1A1	TCCAGAGACAA CAGGTAAAACA	AGGAAGGGCAG AGGAATGTGAT	371
CYP1A2	ACCCCAGCTGC CCTACTTG	GCGTTGTGTC CCTTGTTGTG	101
CYP2E1	ACCTGCCCCAT GAAGCAACC	GAAACAACTCC ATGCGAGCC	246
PXR	GAAGTCGGAG GTCCCCAAA	CTCCTGAAAAA GCCCTTGCA	100
CAR	TGATCAGCTGCA AGAGGAGA	AGGCCTAGCA ACTTCGCACA	102
			(continued)

(continued)

Gene	Forward primer	Reverse primer	Amplicon (bp)
AhR	ACATCACCTA CGCCAGTCGC	TCTATGCCGCT TGGAAGGAT	101
UGT1A1	GGAGCAAAAGG CGCCATGGC	GTCCCCTCTG CTGCAGCTGC	178
LV-Bmi-1	GCTGAGGGCTA TTGAGGCGCA	ACCCCAAATCCC CAGGAGCTGT	127
hBmi-1	ACCTCCCAGCC CCGCAGAAT	AGACGCCGCTG TCAATGGGC	280
LV-hTERT	CAACCCGGCAC TGCCCTCAG	GGGGTTCCGCT GCCTGCAAA	268
hTERT	CGGAAGAGTGTC TGGAGCAAGT	GAACAGTGCCT TCACCCTCGA	258

PCR Polymerase chain reaction, ALB albumin, AFP α-fetoprotein, CK18 cytokeratin18, G6PD glucose-6-phosphate dehydrogenase, HNF-4α hepatocyte nuclear factor 4α, TAT tyrosine aminotransferase, PXR pregnane X receptor, CAR constitutive androstane receptor, AhR aryl hydrocarbon receptor, UGT1A1 uridine diphosphate glucuronyltransferase, LV-Bmi-1 lentivirus vector BMI-1, hBmi-1 human Bmi-1, LV-hTERT lentivirus vector human telomerase reverse transcriptase, hTERT human telomerase reverse transcriptase

References

- Gomez-Lechon MJ, Donato MT, Castell JV, Jover R. Human hepatocytes in primary culture: the choice to investigate drug metabolism in man. Curr Drug Metab. 2004 Oct;5(5):443–62.
- 2. Rodriguez-Antona C, Donato MT, Boobis A, Edwards RJ, Watts PS, Castell JV, et al. Cytochrome P450 expression in human hepatocytes and hepatoma cell lines: molecular mechanisms that determine lower expression in cultured cells. Xenobiotica. 2002 Jun;32(6):505–20.
- 3. Gomez-Lechon MJ, Castell JV, Donato MT. Hepatocytes--the choice to investigate drug metabolism and toxicity in man: in vitro variability as a reflection of in vivo. Chem Biol Interact. 2007 May 20;168(1):30–50.
- 4. Guguen-Guillouzo C, Corlu A, Guillouzo A. Stem cell-derived hepatocytes and their use in toxicology. Toxicology. 2010 Mar 30; 270(1):3–9.
- Khetani SR, Bhatia SN. Microscale culture of human liver cells for drug development. Nat Biotechnol. 2008 Jan;26(1):120–6.
- 6. Youdim KA, Tyman CA, Jones BC, Hyland R. Induction of cytochrome P450: assessment in an immortalized human hepatocyte cell line (Fa2N4) using a novel higher throughput cocktail assay. Drug Metab Dispos. 2007 Feb;35(2):275–82.

- Sinz M, Wallace G, Sahi J. Current industrial practices in assessing CYP450 enzyme induction: preclinical and clinical. AAPS J. 2008 Jun;10(2):391–400.
- 8. Banas A, Yamamoto Y, Teratani T, Ochiya T. Stem cell plasticity: learning from hepatogenic differentiation strategies. Dev Dyn. 2007 Dec;236(12):3228–41.
- Pittenger MF, Mackay AM, Beck SC, Jaiswal RK, Douglas R, Mosca JD, et al. Multilineage potential of adult human mesenchymal stem cells. Science. 1999 Apr 2;284(5411):143–7.
- Jaiswal RK, Jaiswal N, Bruder SP, Mbalaviele G, Marshak DR, Pittenger MF. Adult human mesenchymal stem cell differentiation to the osteogenic or adipogenic lineage is regulated by mitogen-activated protein kinase. J Biol Chem. 2000 Mar 31;275(13):9645–52.
- Nagai A, Kim WK, Lee HJ, Jeong HS, Kim KS, Hong SH, et al. Multilineage potential of stable human mesenchymal stem cell line derived from fetal marrow. PLoS One. 2007;2(12):e1272.
- 12. Ong SY, Dai H, Leong KW. Hepatic differentiation potential of commercially available human mesenchymal stem cells. Tissue Eng. 2006 Dec;12(12):3477–85.
- 13. Banas A, Teratani T, Yamamoto Y, Tokuhara M, Takeshita F, Quinn G, et al. Adipose

- tissue-derived mesenchymal stem cells as a source of human hepatocytes. Hepatology. 2007 Jul;46(1):219–28.
- 14. Zemel R, Bachmetov L, Ad-El D, Abraham A, Tur-Kaspa R. Expression of liver-specific markers in naive adipose-derived mesenchymal stem cells. Liver Int. 2009 Oct;29(9):1326–37.
- 15. Yamamoto Y, Banas A, Murata S, Ishikawa M, Lim CR, Teratani T, et al. A comparative analysis of the transcriptome and signal pathways in hepatic differentiation of human adipose mesenchymal stem cells. FEBS J. 2008 Mar;275(6):1260–73.
- 16. Kulkarni JS, Khanna A. Functional hepatocytelike cells derived from mouse embryonic stem cells: a novel in vitro hepatotoxicity model for drug screening. Toxicol In Vitro. 2006 Sep;20(6):1014–22.
- 17. Ek M, Soderdahl T, Kuppers-Munther B, Edsbagge J, Andersson TB, Bjorquist P, et al. Expression of drug metabolizing enzymes in hepatocyte-like cells derived from human embryonic stem cells. Biochem Pharmacol. 2007 Aug 1;74(3):496–503.
- 18. Unger C, Gao S, Cohen M, Jaconi M, Bergstrom R, Holm F, et al. Immortalized human skin fibroblast feeder cells support growth and maintenance of both human embryonic and induced pluripotent stem cells. Hum Reprod. 2009 Oct;24(10): 2567–81.
- Kutner RH, Zhang XY, Reiser J. Production, concentration and titration of pseudotyped HIV-1-based lentiviral vectors. Nat Protoc. 2009;4(4):495–505.



RESEARCH ARTICLE

Open Access

Upregulation of CYP 450s expression of immortalized hepatocyte-like cells derived from mesenchymal stem cells by enzyme inducers

Khanit Sa-ngiamsuntorn¹, Adisak Wongkajornsilp^{1*}, Kanda Kasetsinsombat¹, Sunisa Duangsa-ard¹, Lalana Nuntakarn⁴, Suparerk Borwornpinyo⁵, Pravit Akarasereenont¹, Somchai Limsrichamrern² and Suradei Hongeng^{3*}

Abstract

Background: The strenuous procurement of cultured human hepatocytes and their short lives have constrained the cell culture model of cytochrome P450 (CYP450) induction, xenobiotic biotransformation, and hepatotoxicity. The development of continuous non-tumorous cell line steadily containing hepatocyte phenotypes would substitute the primary hepatocytes for these studies.

Results: The hepatocyte-like cells have been developed from hTERT plus Bmi-1-immortalized human mesenchymal stem cells to substitute the primary hepatocytes. The hepatocyte-like cells had polygonal morphology and steadily produced albumin, glycogen, urea and UGT1A1 beyond 6 months while maintaining proliferative capacity. Although these hepatocyte-like cells had low basal expression of CYP450 isotypes, their expressions could be extensively up regulated to 80 folds upon the exposure to enzyme inducers. Their inducibility outperformed the classical HepG2 cells.

Conclusion: The hepatocyte-like cells contained the markers of hepatocytes including CYP450 isotypes. The high inducibility of CYP450 transcripts could serve as a sensitive model for profiling xenobiotic-induced expression of CYP450.

Keywords: hepatocyte-like cell, immortalization, CYP450, MSC

Background

Xenobiotic biotransformation has been classified into 2 phases. The majority of phase I biotransformation was implemented by cytochrome P450 (CYP450) family with 8 major isotypes in human[1]. Each isotype has overlapped spectra of substrates and catalyzes multiple reactions. Activations or suppressions of certain isotypes as a result of precipitant drugs have been associated with several clinically important drug interactions[1]. The phase II biotransformation involved several conjugation reactions (e.g., sulfonation, glucuronidation, acetylation, methylation and glutathione conjugation). These

The idealistic cell culture model to simulate *in vivo* biotransformation of xenobiotics is the use of primary human hepatocytes. However, the acquisition of normal human hepatocytes is cumbersome with ethical as well as biological considerations. The cultured cells are short lived and have to be swiftly prepared from fresh tissues [4] making them unfeasible for most studies. Alternative sources of human cells have been developed to mimic the phenotypes of hepatocytes. A viable source is the mesenchymal stem cells (MSCs) derived from bone marrow[5].

^{*} Correspondence: siawj@mahidol.ac.th; rashe@mahidol.ac.th

¹Department of Pharmacology, Faculty of Medicine Siriraj Hospital, Mahidol

University, 2 Prannok Road, Bangkoknoi, Bangkok 10700, Thailand

³Department of Pediatrics, Faculty of Medicine Ramathibodi Hospital,

Mahidol University, 270 Rama VI Road, Ratchatewi, Bangkok 10400, Thailand

Full list of author information is available at the end of the article



conjugations attach new functional groups to the xenobiotic that had gone through phase I metabolism[2]. The CYP450 isotypes in rodents are often different in gene regulation and enzymatic activity from those in human and thus cannot reliably predict the toxicity or metabolic profiles of xenobiotics in human[3].

The very first effort to generate hepatocyte-like cells was taken through the co-culture of MSCs with isolated liver cells[6]. Subsequent efforts employed fetal liverconditioned medium[7], selective cytokines and coating matrix[8]. Alternate cell sources such as adipose tissue [9-11], amniotic fluid[12] and Wharton's jelly[13-15] were employed. The major proposed application of these hepatocyte-like cells is to implement liver regeneration[13,16-19]. The xenogeneic transplants of human hepatocyte-like cells into mice after CCL₄-induced liver injury have been attempted with moderate success [5,20,21]. Several groups had characterized the phenotypes (i.e., CYP450, morphology, glycogen/urea/albumin production) in contemporary hepatocyte-like cells[22], but none has made the long-term characterization to demonstrate their stability. The long-term stability of the cells is required for the application of xenobiotic testing in new drug development.

The life span of hepatocyte-like cells from these diverse sources after differentiation induction was generally limited. Immortalizing hepatocyte-like cells or their precursors (i.e., MSCs) would be a more feasible solution, resulting in a sustainable and consistent source of hepatocytes. The polycomb group transcription factor Bmi-1[23] that could drive cancer cell proliferation[24] and normal stem cell self-renewal was selected for immortalization. The validity for using these immortalized cells for cell culture metabolic study relies on the maintenance of hepatocyte phenotypes as represented by a panel of specific markers. Hepatocyte-like cells from various MSC sources exhibited different intensities of hepatocyte specific markers [9]. We immortalized the MSC as a precursor for hepatocyte-like cells by using both human telomerase reverse transcriptase gene (hTERT) and Bmi-1 through lentiviral transduction[25], and examined whether the resulting immortalized cells after differentiation induction could maintain hepatocyte phenotypes and metabolic functions.

Results

The identification of MSCs

Cells isolated from bone marrow aspirate displayed a spindle shape upon reaching confluence (Figure 1A). The hTERT/Bmi-1-transduced MSC (BMI1/hTERT-MSC) still maintained fibroblast-like, spindle morphology at 40th passage (Figure 1B) with an exponential growth pattern (Figure 1C). The identity of the studied MSCs was confirmed by the presence of mesenchymal stem cell markers (CD90 and CD105, Figure 1D). MSCs that had gone through immortalization still contained similar levels of CD90 and CD105 (Figure 1E), but was virtually devoid of hematopoietic markers (CD34, CD45, Figure 1F) as determined by a flow cytometer.

Proliferative activity of transformed MSCs

The growth rate of MSCs was slow at the first passage, picked up and steadily increased in subsequent (2nd-7th) passages. In later (8th - 10th) passages, growth rate was again slowed down to a complete stop (Figure 1C). To bypass the replication senescence, we transformed MSCs with either hTERT plus Bmi-1 (BMI/hTERT-MSC) or hTERT alone (hTERT-MSC) from 5 independent donors. After 60 days or 20-25 population doubling level (PDL), the proliferation rate of untreated MSCs decreased to a final stop. The cellular morphology switched to epithelial-like, indicating the reduction of stem cell properties. In contrast, BMI/hTERT-MSC grew steadily for more than 8 months (75-80 PDL) and exhibited unaltered morphology (Figure 1C). In contrast, hTERT-MSCs, similar to untreated MSCs, could not bypass replication senescence. BMI/hTERT-MSC cells have been maintained for over a year, confirming their immortalization. To ensure that both Bmi-1 and hTERT were expressed in these transformed MSCs, specific primers were designed to separately quantify endogenous and exogenous expression of both Bmi-1 and hTERT using quantitative RT-PCR. The endogenous expressions of hTERT and hBmi-1 in untreated MSCs at the 4th passage were lower than those in transformed MSCs at the same passage. The ectopic expressions of both hTERT and Bmi-1 were detected at a steadily high level for over a year (120 PDL, Figure 1G). The morphology was also stable throughout the study. Our success rate for immortalization of MSC was 4 clones out of 10 clones from each donor.

The differentiation of MSCs to hepatocyte-like cells

After finishing hepatic induction, the hepatocyte-like cells carried the expansion of several basic hepatocyte genes (Figure 1H) with a corresponding polygonal morphology (Figure 2A). Immortalized hepatocyte-like cells at the first passage were loosely attached to adjacent cells (Figure 2B). Up to 70-80% of the hepatocyte-like cells deposited glycogen, especially in densely populated area (PAS assay at passage 4, Figure 2C). After switching to 10% FBS, DMEM/F12 the intercellular attachment was denser with blurring of cell boundary (Figure 2D). At confluence, duct-like structure was observed (Figure 2E). The cells could maintain cell division beyond 3 months (Figure 2F) with sustainable hepatocyte function suitable for drug screening.

Expression levels of hepatocyte-specific markers

Up to 88% of hepatocyte-like cells (Figure 3A) and immortalized hepatocyte-like cells (Figure 3B), as opposed to 5% of MSCs, contained intracellular albumin. Almost 95% of HepG2 cells contained albumin (Figure 3C). In subsequent passages, hepatocyte-like

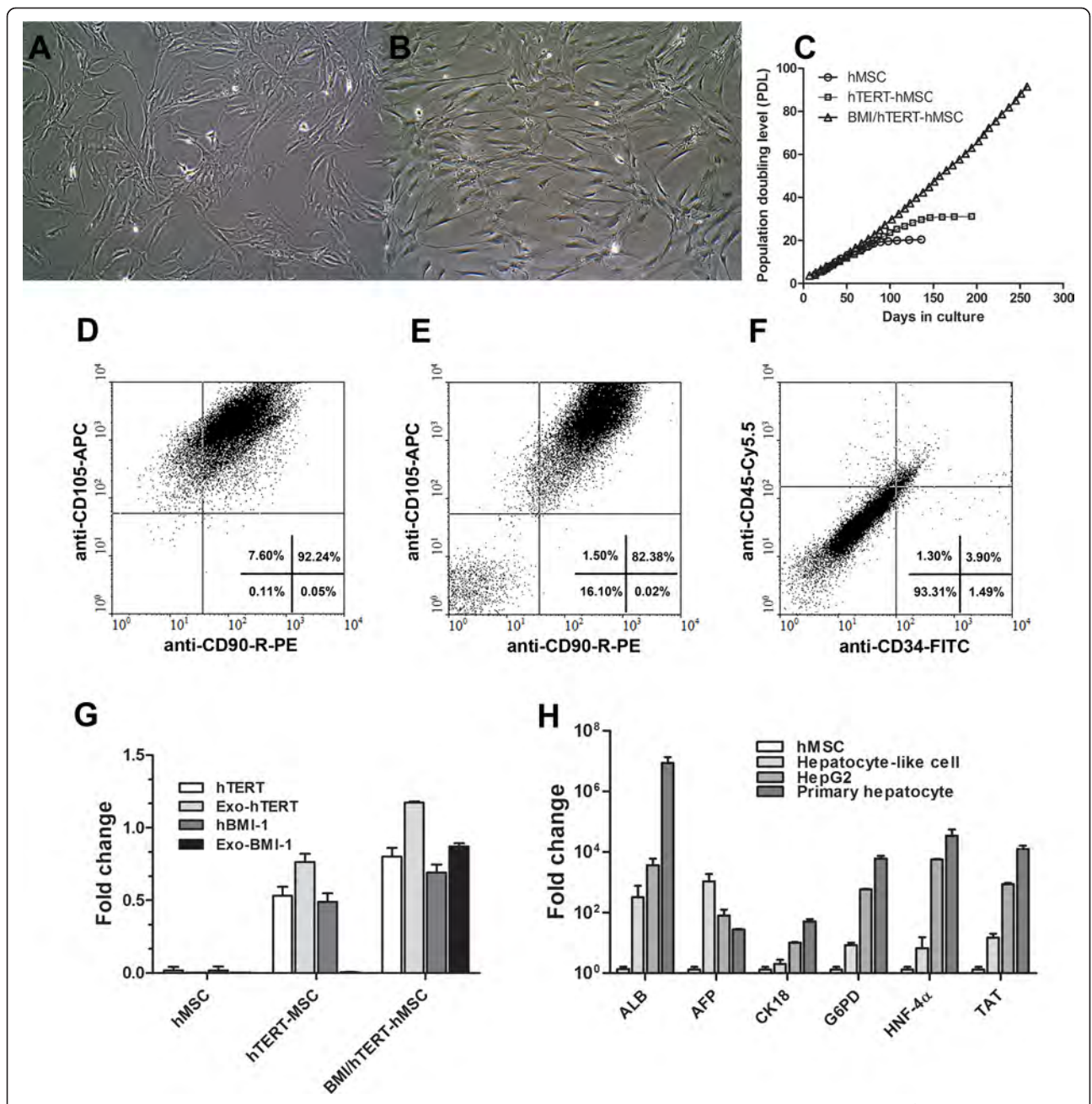


Figure 1 Characterization of immortalized MSC. MSCs and Bmi-1/hTERT-immortalized MSCs were visualized (A) after the 2^{nd} passage. The attached cells appeared fibroblast-like, spindle morphology (B) at the 40^{th} passage (12 months after isolation). The MSCs (hMSC) and the TERT-transduced MSCs (hTERT-MSC), or the double TERT/Bmi-1 transduced MSCs (BMI/hTERT-MSC) were studied for cumulative population doubling level (PDL) (C). Flow cytometry analysis confirmed the presence of CD90/CD105 in primary MSCs after isolation (D) and in BMI/hTERT-MSCs (E). All cells were depleted of CD35/CD45 hematopoietic stem cell markers (F). The endogenous and exogenous expression of Bmi-1, TERT in all cell types were studied using quantitative real-time PCR (G). The expression of hepatocyte-selective genes (i.e., albumin (ALB), α-fetoprotein (AFP), cytokeratin18 (CK18), glucose-6-phosphate dehydrogenase (G6PD), hepatocyte nuclear factor (HNF-4α), and tyrosine aminotransferase (TAT)) of BMI/hTERT-MSC after hepatic differentiation was presented as fold change over the untreated MSCs in comparison with HepG2 and the primary hepatocyte (H).

cells maintained at least 70% of albumin-containing cells (Figure 3D). The functional activity of hepatocyte-like cells at different passages was investigated using urea assay (Figure 3E). The conditioned medium of

hepatocyte-like cells contained far higher level of urea than that of MSCs, but was comparable to that of HepG2. Using mRNA levels inherent to MSCs as a reference, the relative expression levels of the

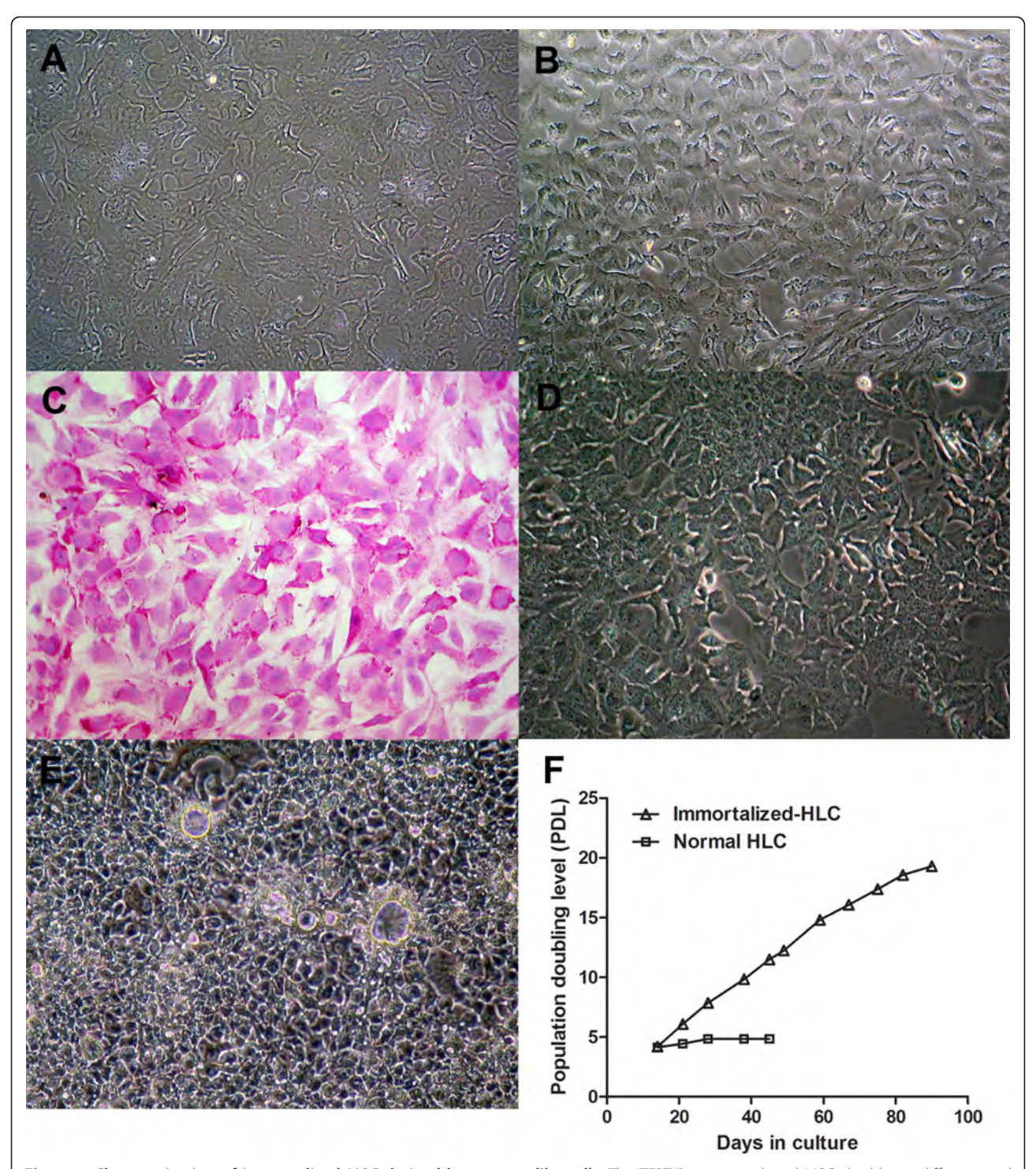


Figure 2 Characterization of immortalized MSC-derived hepatocyte-like cells. The TERT/Bmi-1-transduced MSCs had been differentiated into hepatocyte-like cells. The differentiated cell had polygonal shape, granulated cytoplasm and large nucleus (A). After the next passage, the cytoplasmic/nucleolus ratio was further decreased with loose intercellular attachment (B). The glycogen storage activity was demonstrated using Periodic Acid Schiff staining (PAS) with greater than 95% of the population were positive for glycogen (C). After the maintenance in DMEM/F12, 10% FBS in subsequent passages, cells were densely packed with closer intercellular attachment (D). After reaching confluence, cells formed duct-like structure (E). The life span of the immortalized hepatocyte-like cells was beyond 3 months (F) with active division.

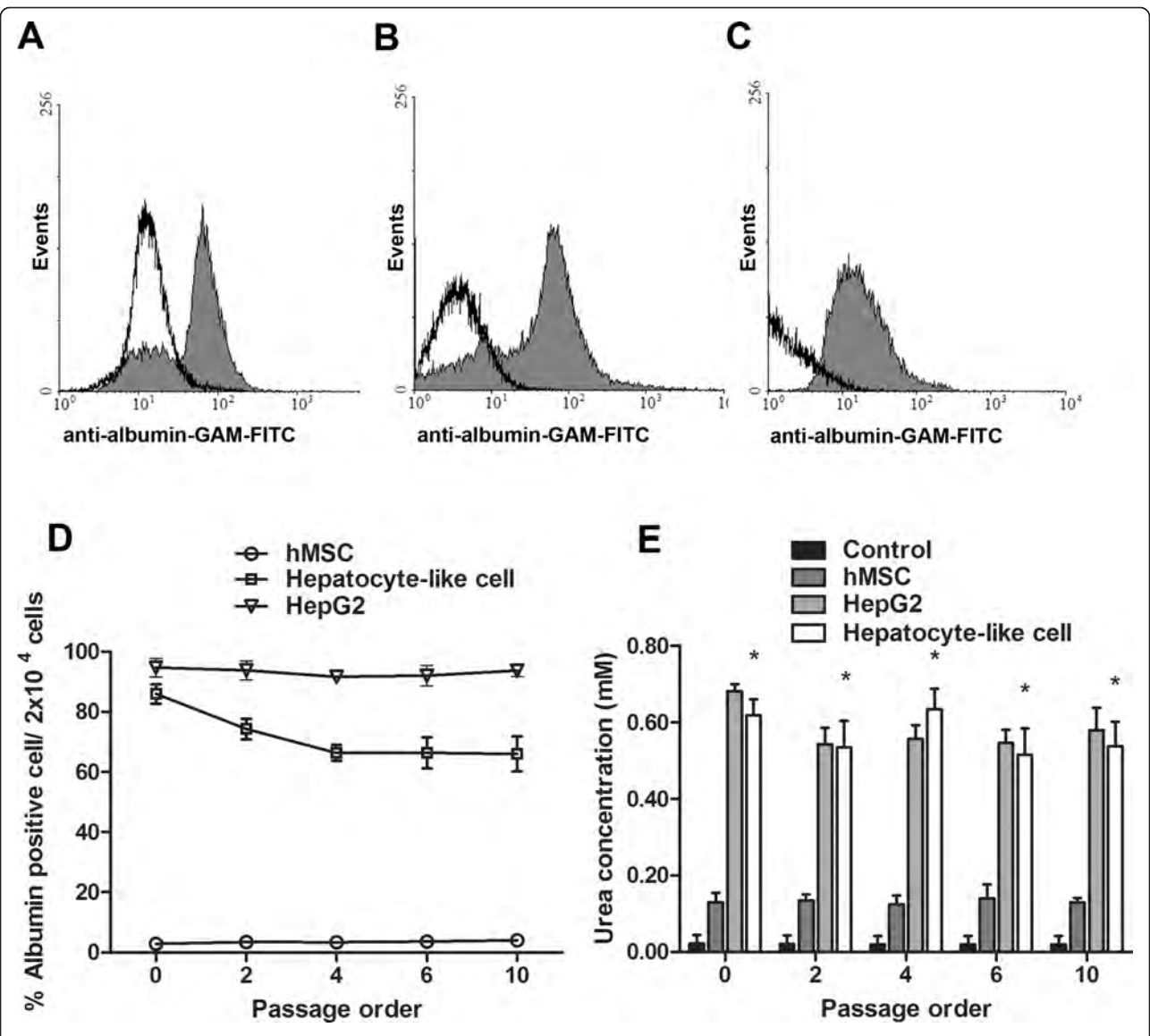


Figure 3 Functional activities of hepatocyte-like cells. The presence of albumin was analyzed using flow cytometer in the immediately differentiated cells (A), the immortalized hepatocyte-like cells (B), and in HepG2 (C). Greater than 80% of the population of hepatocyte-like cells contained albumin (D) that could be maintained at 70% beyond 10 passages. Urea production as represented by diacetyl monoxime test was demonstrated in MSCs, HepG2, and hepatocyte-like cells (E). IMDM medium supplemented with 5 mM NH₄Cl served as the control group.

corresponding genes in the hepatocyte-like cells, HepG2 cells and the primary human hepatocytes were determined using quantitative real-time PCR. The basal expression patterns for hepatocyte-specific genes at passage 5-9 (e.g., ALB, AFP, CK18, G6PD, HNF-4 α and TAT) were varied, depending on the stage of hepatocyte maturation. The AFP expression that is usually presented in hepatic progenitors was detected at higher level than those of the primary human hepatocytes and HepG2 cells (Figure 1H). The observation of cytokeratin18 expression confirmed the differentiation of MSCs into endodermal tissue. Three major hepatocyte genes

were up-regulated in hepatocyte-like cells, namely glucose-6-phosphate dehydrogenase (glucose metabolism), HNF-4 α (liver development and maturation) and tyrosine aminotransferase (amino acid metabolism). The observation of all hepatocyte specific genes confirmed that the transformed MSCs could actually differentiate into functional hepatocyte-like cells.

The basal expression of phase I and phase II enzymes in hepatocyte-like cell

After maturation induction, hepatocyte-like cell culture was continued in IMDM with 1% FBS, 2% DMSO for 2

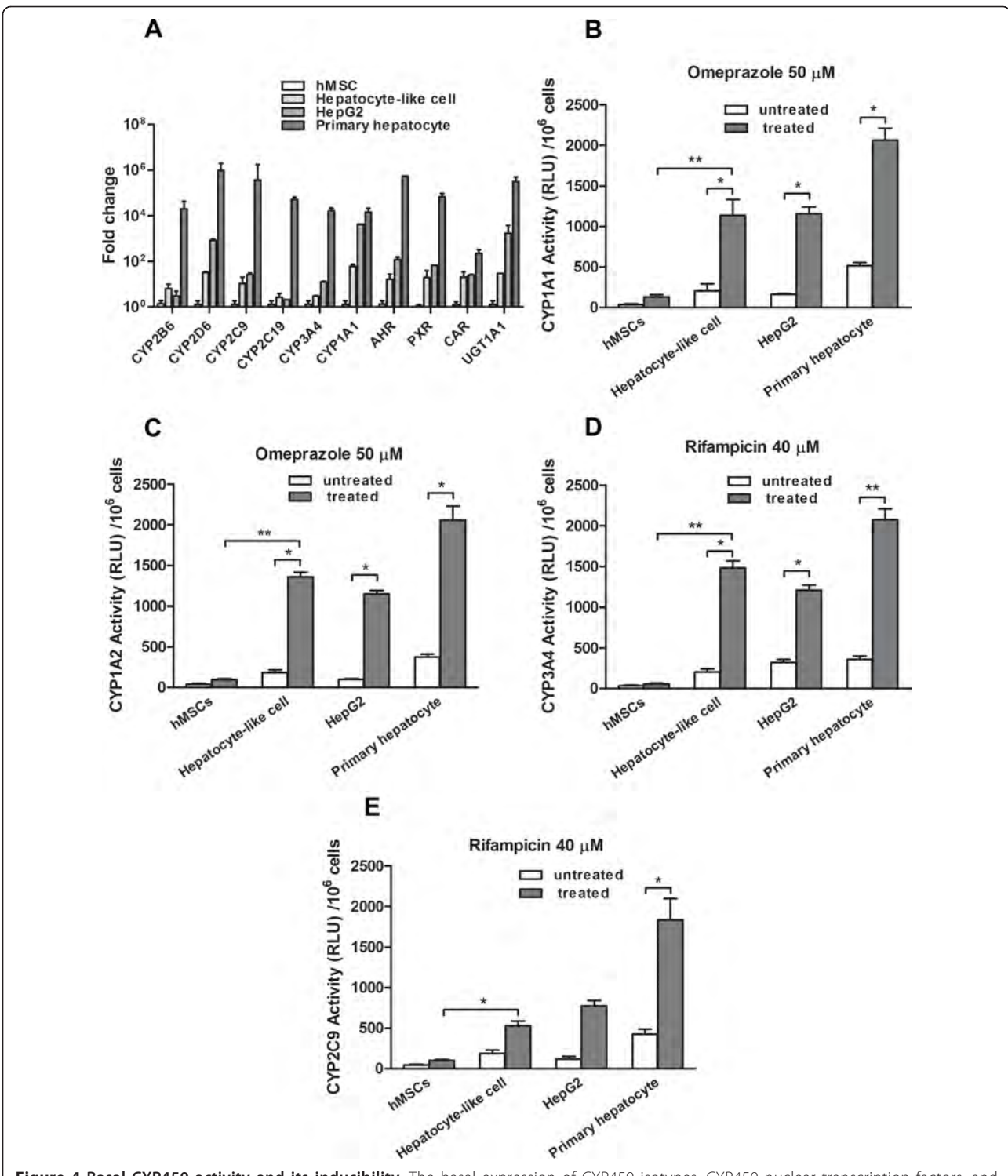


Figure 4 Basal CYP450 activity and its inducibility. The basal expression of CYP450 isotypes, CYP450 nuclear transcription factors, and UGT1A1 in MSCs, hepatocyte-like cells, HepG2 and the primary hepatocyte were analyzed using real-time qPCR (A). They were analyzed as fold-changes over that of untreated MSCs. The induction of CYP1A1 (B), CYP1A2 (C), CYP3A4 (D) or CYP2C9 (E) activities after adding the corresponding enzyme inducers for 72 h were analyzed using P450Glo™ assay kit (Promega) with different luciferin substrates. After 3-h incubation with specific substrate, luciferase activities were measured. Results are expressed as luciferase activities in relative luminescence unit (RLU) and mean ± SD of 3 independent experiments.

weeks at confluence [26]. Cells were harvested and determined for phase I and phase II enzyme expressions (Figure 4A). Specific transcription factors such as AHR, PXR and CAR in hepatocyte-like cells were increased by about 10 times those of MSCs. These genes are involved in the transcription of CYP450 isotypes [27,28]. Genes that were highly expressed in hepatocyte-like cells included one phase II enzyme UGT1A1 and 6 CYP450 isotypes (CYP2B6, CYP2D6, CYP2C9, CYP2C19, CYP3A4, and CYP1A1). In particular, the expression level of CYP2B6 in hepatocyte-like cells was even higher than that of HepG2 while other isotypes achieved comparable expression levels to those of HepG2. However, all CYP450 isotype expressions in hepatocyte-like cells were only 10-20% that of normal hepatocytes. The authenticity of the real-time RT-PCR products of hepatocyte markers and CYP450 were confirmed through the analysis for melting curve using Sequence Detection Software version 2.01 (Applied Biosystems, CA).

Enhancing phase I enzyme expression using prototypic inducers

The expressions of CYP1A1, CYP2B6, CYP2D6 and CYP2C8 in hepatocyte-like cells were significantly increased to 13, 30, 3, 12 folds respectively after the induction with dexamethasone or rifampicin (Table 1). CYP3A4 and CYP2C19 expressions were extensively up regulated by 84 and 20 folds, respectively in hepatocytelike cells. In HepG2, the expressions of CYP2B6, CYP2C8 and CYP3A4 were increased to 25, 9, 39 folds using rifampicin. In the primary hepatocyte, the expression of CYP1A1, CYP1A2, CYP2B6 were raised to 19, 13, 41 folds that were comparable to those of the hepatocyte-like cells. The induction of CYP3A4 expression in the hepatocyte-like cells (84 folds) outpaced that of the primary hepatocyte (72 folds). The expressions of most CYP450 isotypes in undifferentiated MSCs were induced by merely 2-4 folds.

Substantial induction of CYP1A1, CYP1A2, CYP2C9 and CYP3A4 isotype activities in hepatocyte-like cells

Using luminescent CYP450-specific substrates, we determined CYP1A1, CYP1A2, CYP2C9 and CYP3A4 isotype activities after the induction with either rifampicin or omeprazole in HepG2, MSC and hepatocytelike cell. We observed end-point catalytic activity after incubating substrates to the cells using a luminometer. In hepatocyte-like cell, the activity of CYP1A1, CYP1A2 and CYP3A4 was increased to approximately 6-7 folds that of the untreated cell (Figure 4B, C, D). A mild increase in CYP2C9 activity (2 folds) was observed (Figure 4E). The activity of CYP1A2 and CYP3A4 in hepatocyte-like cells was already higher than those in HepG2. The primary hepatocyte

provided the highest activities in all CYP450 isotypes. A significant increase in rifampicin-induced CYP3A4 activity was confirmed by the accumulation of CYP450 in hepatocyte-like cell as demonstrated by immunofluorescent staining (Figure 5A). The staining for AFP and hepatocyte nuclear factor 4α confirmed the identity of the hepatocyte-like cell. The corresponding staining to the primary hepatocyte served as the positive controls (Figure 5B). No significant induction was detected in untreated MSCs, but untreated HepG2 and untreated hepatocyte-like cell had low basal level of CYP1A1, CYP1A2, CYP2C9 and CYP3A4 activities.

Discussion

The hepatocyte-like cells have been developed to replace the primary hepatocytes for the studies of xenobioticinduced CYP450 isotype expression, hepatotoxicity, and xenobiotic biotransformation. Taken together, the cell morphology, cell-selective markers (i.e., gene expression profiles, flow cytometry) as well as certain specific phenotypes (urea synthesis, glycogen deposit, and CYP450 expression profiles) indicated that the putative hepatocyte-like cells were correctly driven toward hepatocyte differentiation. To our knowledge, there has not been any attempt to bring hepatocyte-like cells derived from MSC as a stable model for the study of CYP450 isotypes or new drug development. Only certain isotypes (CYP1A1, CYP1A2, CYP2B6, CYP7A1 and CYP2E1) have been studied immediately after differentiation [18,29,30]. The expression of various transcription factors that regulate CYP450 isotypes[31] including hepatocyte nuclear factor (HNF- 4α) [32] during hepatogenic differentiation has been reported. PXR, AHR and CAR are considered to be the most important regulators of xenobiotic-induced regulation of many CYP450 isotypes [28]. We observed increasing expression of PXR, CAR and HNF- 4α in correlation with the degree of hepatocyte-like cell maturation.

Several investigators had developed hepatocyte-like cells from different stem cell sources and various differentiation protocols[33]. The MSC sources were bone marrow, adipose tissue and Wharton's jelly[10,29,34,35]. The differentiation phenotypes were generally lost after a few days in all studies including one employing embryonic stem cells as precursors[36]. The senescence of the precursor MSCs led to decreasing both proliferation and plasticity [37-39]. Our MSCs also reached senescence after 20-24 population doublings, similar to others [40-42]. The generation of hepatocyte-like cells from MSCs has been plagued by the lack of stable supply of the precursor MSCs and their differentiation capacity. These obstacles would be obviated if immortalized hepatocyte-like cells with intact phenotypes could be generated.

Table 1 Fold changes of CYP450 isotypes' expression in three cell types after 72 h of induction with prototypic CYP450 inducers (omeprazole, dexamethasone, rifampicin, artemisinine and ethanol) over the untreated control

P450 isotypes/enzyme inducers	concentration (μM)		mRNA fold chan	e (mean ± SD)	
		HepG2	P-hepatocyte	hMSC	Hep-like cell
CYP1A1					
omeprazole	50	$4.05 \pm 0.38*$	11.13 ± 0.34*	2.09 ± 0.30	2.13 ± 0.15
dexamethasone	25	1.11 ± 0.13	19.68 ± 0.46*	$3.10 \pm 0.33*$	12.86 ± 0.39*
CYP1A2					
omeprazole	50	$3.33 \pm 0.14*$	6.44 ± 0.80	1.67 ± 0.12	2.37 ± 0.13
dexamethasone	25	1.17 ± 0.02	13.62 ± 2.84*	$3.82 \pm 0.96*$	$5.63 \pm 0.65*$
CYP2B6					
rifampicin	40	25.82 ± 1.30*	35.16 ± 2.76**	1.46 ± 0.10	30.70 ± 5.36**
dexamethasone	25	2.58 ± 0.72	41.49 ± 4.58**	3.98 ± 0.71*	24.25 ± 2.30*
CYP2D6					
dexamethasone	25	1.26 ± 0.10	5.70 ± 1.29	2.68 ± 0.43	2.90 ± 0.73
CYP2C9					
rifampicin	40	1.42 ± 0.25	15.25 ± 2.51*	2.03 ± 0.22	7.78 ± 1.82*
CYP2C19					
rifampicin	40	1.87 ± 0.11	29.05 ± 2.02**	2.42 ± 0.61	19.01 ± 2.51*
CYP2C8					
rifampicin	40	9.07 ± 1.03*	24.40 ± 2.48*	$3.03 \pm 0.62*$	12.28 ± 0.81*
CYP3A4					
rifampicin	40	39.43 ± 5.53**	69.50 ± 6.84**	3.64 ± 1.82*	43.29 ± 3.27**
dexamethasone	25	23.18 ± 7.25**	72.27 ± 5.64**	2.87 ± 0.96	84.10 ± 9.25**
artemisinine	50	48.18 ± 6.80**	59.28 ± 8.41**	0.89 ± 0.07	53.54 ± 1.37**
CYP2E1					
ethanol	88	$4.59 \pm 0.53*$	24.23 ± 0.41*	1.46 ± 0.19	10.74 ± 2.10*

hMSC, HepG2, primary hepatocyte and hepatocyte-like cell were induced with prototypic inducer drugs. The CYP450 mRNA level was detected by Real-time PCR. The experiment was performed in triplicate for all compounds. Data was normalized by untreated (non-treated controls) and was analyzed by Non parametric One-tailed Student t test (Mann-Whitney test) * p < 0.05, ** p < 0.01.

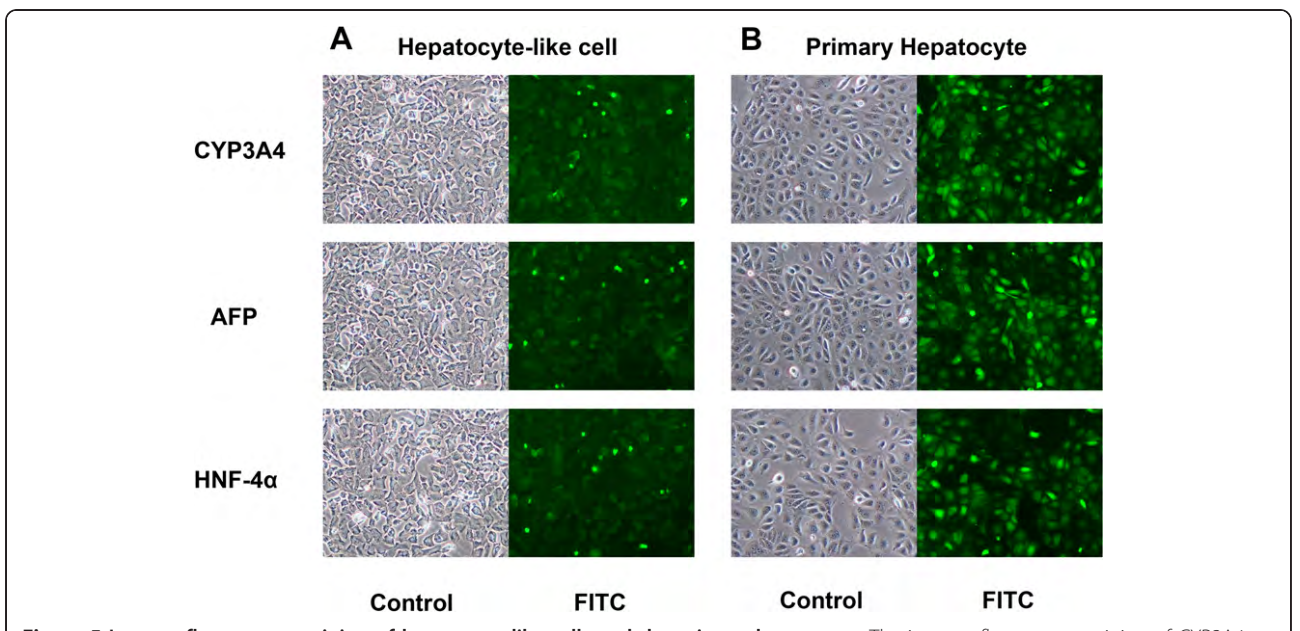


Figure 5 Immunofluorescent staining of hepatocyte-like cells and the primary hepatocyte. The immunofluorescent staining of CYP3A4, α -fetoprotein and HNF-4 α in the cytoplasm of hepatocyte-like cells (A) and the primary hepatocyte (B) were demonstrated with the corresponding phase-contrast pictures over the same fields (10× objective lens). Essentially all hepatocyte-like cells carried all 3 proteins but their staining intensities reached only a half those of the primary hepatocytes.

A classical gene employed for immortalization is the telomerase reverse transcriptase (hTERT) that prevents replicative senescence associated with decreasing telomere length resulting from repeated cell division [43,44]. Lesser known immortalization genes are SV-40 large T antigen (T-Ag) and Bmi-1[25]. Bmi-1 inhibit senescence and extended the life span of normal human cell by suppressing p16^{INK4A} that allows cell entry into division[45]. Moreover, the overexpression of Bmi-1 could inhibit TGF- β signaling[46] that would otherwise induce hepatocyte cell death[47].

MSCs lost their originally high telomerase activity [48] after being seeded as primary cultured cells [49] and eventually lost their stem cell property [50]. We had expected that the addition of a constitutively expressing construct of hTERT (pLOX-TERT-iresTK) to MSCs would solve the senescence [51,52], but a slight postponement of senescence was observed. Only after Bmi-1 (pLOX-CWBmi1)[53] had been co-introduced were the senescence phenotypes extensively delayed. The transduced cells had increasing spindle morphology with at least 80% of the whole population contained both CD90 and CD105. These cells could be maintained for over 1 year while still maintaining their growth in exponential phase. The given constructs have an advantage of the inclusion of *loxP* site that allows the removal from the genomic insertion site.

It is even more exciting when the precursor cells of the hepatocyte-like cells were already immortalized. We modified the hepatogenic differentiation protocol from previous reports [54] by extending the last step of maturation from 2 weeks to 4 weeks in culture medium supplemented with 2% DMSO. Normally, we cannot achieve a complete hepatocyte differentiation. However, after using limiting dilution technique, a stable clone of functional hepatocyte-like cell was established. Our clone of differentiated immortalized cells could propagate in standard culture condition for greater than 6 months with sustainable hepatocyte specific makers and functions.

The confirmed hepatocyte phenotypes that included the expression of albumin, α -fetoprotein cytokeratin 18, HNF-4 α , and tyrosine aminotransferase were up-regulated for 10 - 100 folds that of the undifferentiated MSCs. However, the overall basal gene expressions were 10 - 40% those of the primary hepatocyte. The flow cytometry analysis indicated that at least 80% of the hepatocyte-like cells, in comparison with 90% of HepG2, produced albumin. Likewise, the urea production of our cells was comparable to that of HepG2. Greater proportion of our hepatocyte-like cells (> 95%) carried glycogen than did others[9,30,55,56]. The expression of transcription factors for CYP450 (i.e., CAR, AHR, PXR) as well as that of the phase II enzyme (i.e., UGT1A1)

was observed. The 10 - 50-fold induction of the expression of 8 major CYP450 isotypes (CYP1A1 CYP1A2, CYP2B6, CYP2D6, CYP2C9, CYP2C19, CYP2C8, CYP3A4 and CYP2E1) in response to known enzyme inducers (rifampicin, dexamethasone, omeprazole, phenobarbital and artesunate) was confirmed, although their basal levels were less than those of the primary hepatocyte by 100-1000 folds. Unexpectedly, HepG2 achieved much weaker induction of CYP1A1, CYP2D6, CYP2C9 and CYP2C19 in response to rifampicin, dexamethasone and omeprazole than did hepatocyte-like cells. The immunofluorescent study of CYP3A4 in hepatocyte-like cells after induction indicated that the upregulation of protein level was consistent with the induction of mRNA expression.

Although CYP450 isotypes are presented in most cell types, not all cell types are suitably employed to study the CYP450's response to xenobiotics. To elucidate the suitability of the hepatocyte-like cells for the study of CYP450 isotypes, we have extensively investigated the expressions of all major isotypes plus the enzymatic activity of selected isotypes in response to enzyme inducers. We have demonstrated that the un-modified MSCs contained low basal levels of CYP450 isotypes and elicited only 2 - 5-fold induction to prototypic CYP450 isotype inducers (Table 1). Therefore, the use of MSCs is not considered a viable alternative for CYP450 study. We observed extensively high expressions of most CYP450 isotypes in response to inducers in hepatocytelike cells than those in MSCs or HepG2, although the basal levels of certain CYP450 isotypes were lower than those of primary hepatocytes or HepG2. Changing the precursors of hepatocyte-like cells from MSCs to embryonic stem cells or induced pleuripotential stem cells could not bring up the basal levels of all isotypes [57]. An exception was found in CYP2B6, where the hepatocyte-like cells had comparable expansion to that of the HepG2. The low basal levels of these CYP450 isotypes in hepatocyte-like cells might be attributed to their completely lack of exposure to xenobiotics as opposed to the primary hepatocytes or HepG2. Based on the expansion of CYP450 isotypes' expression in response to inducers, hepatocyte-like cells are considered a more sensitive and informative model.

Conclusion

The continuous hepatocyte-like cell lines have been generated from hTERT plus Bmi-1-immortalized human MSCs. These continuous cell lines contained hepatocyte markers (albumin, AFP, TAT, HNF-4α, G6PD) including all major CYP450 isotypes (CYP1A1, CYP1A2, CYP2C8, CYP2B6, CYP2D6, CYP2C9, CYP2C19, CYP3A4 and CYP2E1). The basal mRNA expression of CYP450 isotypes was low, but readily up-regulated up to

80 folds upon the exposure to enzyme inducers. The high inducibility of CYP450 transcripts would serve as a sensitive model for profiling xenobiotic-induced expression of CYP450.

Methods

The characterization of human mesenchymal stem cells

Human mesenchymal cells (MSCs) were prepared from aspirated bone marrow of consenting normal volunteers (n = 5). This study received an approval from the Ethics Committee on Research Involving Human Subjects at Ramathibodi Hospital, Mahidol University. Written inform consent was obtained from all participants involved in this study. Bone marrow mononuclear cells were separated by IsoPrep (Robbins Scientific, Canada) density gradient centrifugation [58] and seeded at a density of 2×10^6 cells/mL in Minimum Essential Medium (MEM) α Media (Gibco Invitrogen, NY), 10% fetal bovine serum (FBS, Biochrom AG, Germany), 100 units/ mL penicillin, 100 μg/mL streptomycin at 37°C in 5% CO₂. The identification of MSCs was confirmed using FACS analysis. Isolated cells were detached by trypsin, stained for MSC markers (CD105 and CD90) or hematopoietic stem cell markers (CD34, CD45), and analyzed by flow cytometry (FACSCalibur, Becton Dickinson).

Lentivirus production and transduction of target cells

Viral particles were produced using the transient transfection protocol[25]. HEK 293T cells (Clontech, CA) at a density of 2.8×10^6 cells/10-cm tissue culture dish were co-transfected with psPAX2 packaging vector, pMD2.G vesicular stomatitis virus G envelope, and the plasmid encoding either hTERT (pLOX-TERT-iresTK, Addgene plasmid 12245) or Bmi-1 (pLOX-CWBmi1, Addgene plasmid 12240)[53] using calcium phosphate precipitation. The supernatant was harvested and filtered through a 0.45 µm syringe filter. Viral stocks were stored at -70°C. For immortalization, both hTERT and Bmi-1 lentiviruses were diluted in MEM α medium, 10% FBS, 6 μg/mL polybrene at a multiplicity of infection (MOI) of 2, and directly added to the MSCs on sixwell plates (10⁴ cells/well). The MSCs were incubated at 5% CO₂, 37°C for 14 h. After the incubation, medium containing viral particles was removed and replaced with fresh medium.

Cloning of immortalized human mesenchymal stem cell

Three days after the infection, MSCs from 5 donors were trypsinized and counted using a hemacytometer. Single cell suspension was prepared by limiting dilution and transferred onto 24-well culture plate to establish clones from single cells. Each colony was monitored every 2-3 d until confluence. The cells were then trypsinized and seeded on T-25 tissue culture flask. To

establish stable MSC lines, 10 clones per donor were selected based on the fastest cellular proliferation and confirmed for the expression of both hTERT and Bmi-1. Total RNA of MSC was isolated from pooled cells of passages 3-5, converted into cDNA and quantitated using real-time PCR. hTERT and Bmi-1 double positive cells were studied for population doubling level (PDL). The population doubling level was determined using log N/log2, where N is the number of the cells harvested at confluence divided by the number of the initially seeded cells [25].

The induction of MSC hepatogenesis

The MSCs at passages 3-5 or BMI/hTERT-MSCs at a density of 1×10^4 cells/cm² from the fastest dividing clone (n = 3) were taken for differentiation. The MSCs were induced into hepatocyte-like cells using a modified three-step protocol[9]. They were maintained on collagen type IV coated container. The cells were maintained for 2 d in serum-free IMDM (Gibco Invitrogen, NY), 20 ng/mL epidermal growth factor (EGF, Chemicon, CA),10 ng/mL basic fibroblast growth factor (bFGF, Chemicon, CA). Cells were then maintained in IMDM (20 ng/mL HGF, Chemicon, CA), 10 ng/mL bFGF, and 0.61 g/L nicotinamide (Sigma, MO) for 7 d. Cells were further maintained in IMDM, 20 mg/mL oncostatin M (OSM, Chemicon, CA), 1 µM dexamethasone (Sigma, MO), and 50 mg/mL ITS+ (Gibco Invitrogen, NY) for 14 d. The hepatogenesis was assessed by real-time PCR for liver-associated genes. Both human hepatocellular carcinoma cell line (HepG2) and the primary human hepatocyte served as controls. HepG2 was maintained in DMEM/F12 (Gibco Invitrogen, NY), 10% FBS, 100 units/mL penicillin (Sigma, MO), and 100 µg/mL streptomycin (Sigma, MO) at 37°C in 5% CO₂. The primary human hepatocyte was maintained in Williams media E (Gibco Invitrogen, NY), 10% FBS, 100 units/mL penicillin (Sigma, MO), 100 μg/mL streptomycin (Sigma, MO), 4 μg/mL insulin and 1 μM dexamethasone (Sigma, MO) at 37°C in 5% CO₂.

Urea production assay

MSCs, hepatocyte-like cells at passages 0-10 and HepG2 (HB-8065, ATCC, USA) were stimulated with 5 mM NH₄Cl (Sigma, MO) for 48 h. The culture medium was collected and assayed for urea using diacetyl monoxime test[59]. The resulting diazine was measured at 540 nm with the SpectraMax M5 spectrofluorometer (Molecular Devices, CA).

Glycogen Synthesis (Periodic Acid-Schiff, PAS) Assay

Immortalized hepatocyte-like cells at passage 4 were cultured on a chambered slide (Lab-Tek, Nunc, Denmark) for 3d. The slides were fixed in 4% formaldehyde,

permeabilized with 0.1% Triton X-100 for 10 min, incubated with or without diastase for 1 h at 37°C, oxidized in 1% periodic acid (Sigma, MO) for 5 min, rinsed thrice with dH $_2$ O, treated with PAS reagent (Sigma, MO) for 15 min, and rinsed with water for 5 - 10 min. Samples were counterstained with Mayer's hematoxylin for 1 min, rinsed with water, and assessed under light microscope. The resulting gradient of oxidized glycogen would yield a gradient of color starting from pink to strong red.

Analysis of cellular markers using flow cytometry

The cultured cells were stained with fluorochrome-conjugated to primary monoclonal antibodies raised against MSC markers (CD90, CD105); hematopoietic markers (CD34, CD45) (Biosource Invitrogen, CA). For intracellular albumin accumulation, hepatocyte-like cells at passages 2-10 were incubated with FACS Perm (BD Bioscience, CA) and stained with anti-human albumin (Abcam, MA). The goat anti-mouse IgG conjugated to FITC (Santa Cruz Biotechnology, CA) was used as the secondary antibody as necessary. The labeled cells were quantitated using a FACSCalibur flow cytometer (BD Bioscience). The data were analyzed using WinMDI version 2.9.

Immunofluorescence Microscopy

Hepatocyte-like cells and the primary hepatocytes on chambered slide were washed twice with PBS, fixed with 4% paraformaldehyde for 30 min at room temperature followed by 100% ethanol for 10 min. The fixed cells were washed thrice with PBS, blocked with 5% normal serum from the same species as the secondary antibody in 1% BSA/0.2% Triton X-100/PBS for 1 h at room temperature. The cells were incubated with the primary antibody (anti-CYP3A4, anti-HNF4 or anti- α 1-fetoprotein; Abcam, MA) for 1 h at 37°C, washed thrice, incubated with the secondary antibody for 1 h at 37°C, washed thrice, mounted with anti-fade mounting medium on coverslip, and examined under a fluorescent microscope.

The induction of major CYP450 isotypes in hepatocytelike cells using selective enzyme inducers

The modulation of expression levels of CYP450 isotypes was studied after the exposure to the classical inducers [1,22,60,61]. HepG2, MSC or hepatocyte like-cell from passages 3-7 at sub-confluent density were seeded on 6 well-plates for 48 h. These cells were treated for 72 h with the following agents: 40 μM rifampicin, 25 μM dexamethasone, 50 μM omeprazole, 1 mM phenobarbital, 50 μM artesunate, 88 μM ethanol or 0.1% (v/v) DMSO. The cell pellets were washed with 2-3 mL PBS, detached using 0.025% trypsin-EDTA, and neutralized

with 10% FBS in IMDM. The cell pellets from passages 3-7 were pooled and stored at -80°C until analysis for CYP450 gene expression.

Cell isolation, extraction of total mRNA and production of cDNA from primary hepatocyte, hepatocyte-like cell, MSCs and HepG2

The primary human hepatocytes were prepared from discarded surgical specimens using the 2-step collagenase method. The isolated cells were seeded over the collagen type IV-coated container and maintained in the above growth medium for 3 days. Total RNA isolation was performed using RNeasy Mini kit (Qiagen, Germany) according to the manufacturer's instruction. The quality and quantity of the total RNA were determined using a NanoVue Spectrophotometer (GE Healthcare, Buckinghamshire, UK). For cDNA synthesis, 2 µg of total isolated RNA from primary hepatocyte, hepatocyte-like cell, HepG2 and hMSC were converted to cDNA using the ImProm-II reverse transcription system (Promega, WI). Briefly, isolated RNA was incubated with 0.5 μ g oligo (dT)₁₅ primer in a total volume of 5 μL at 70°C for 5 min and chilled on ice-water immediately for at least 5 min. The reverse transcription mix (15 µL of 5X reaction buffer, 25 mM MgCl₂, 2 mM dNTP Mix, 40 U/μL RNasin ribonuclease inhibitor, and 200 U/μL Improm-II[™] RT) was added to the RNA-primer mix to make a total volume of 20 μ L. The mixture was incubated at 25°C for 5 min, and 42°C for another 1 h. The RT reaction was terminated by heating at 70°C for 15 min followed by chilling on ice. The cDNA samples were either used immediately or stored at -70°C. The 1.2 kb kanamycin RNA (1 µg) and non-template control served as positive and negative control system.

Quantitative real-time PCR analysis for cell-specific markers

The employed hepatocyte markers included: ALB (albumin), AFP (α-fetoprotein), CK18 (cytokeratin18), G6PD (glucose-6-phosphate dehydrogenase), HNF-4α (hepatocyte nuclear factor 4α), and TAT (tyrosine amino transferase). The employed CYP450 markers included CYP1A1, CYP1A2, CYP2C8, CYP2B6, CYP2D6, CYP2C9, CYP2C19, CYP3A4 and CYP2E1. The primers for assessing P450s included those recognized aromatic hydrocarbon receptor (AHR), pregnane × receptor (PXR), constitutive aldosterone receptor (CAR). All gene specific primers were designed using Vector NTI version 10 (Invitrogen, Table 2) and ordered from 1st BASE (Singapore). They were amplified using FastStart SYBR® Green Master (Roche diagnostic) and an ABI 7500 Sequence Detector (Applied Biosystems, CA) by following checklist information of RT-qPCR experiment (Additional file 1). Real-time PCR was performed using

Table 2 Primer sets and conditions used in quantitative real-time PCR (qPCR)

Gene	Genbank Accession	Sense primer 5'——— > 3' (Tm°C)	Antisense primer 3'——— > 5' (Tm°C)	Size amplicon (bp)	Annealing temp. (°C)	Putative function
ALB	NM_000477	TGAGAAAACGCCAGTAAGTGAC (60.8)	TGCGAAATCATCCATAACAGC (58.7)	265	60	albumin
AFP	NM_001134	GCTTGGTGGTGGATGAAACA (60.4)	TCCTCTGTTATTTGTGGCTTTTG (59.2)	157	60	lpha-fetoprotein
CK18	X12881	GAGATCGAGGCTCTCAAGGA (62.4)	CAAGCTGGCCTTCAGATTTC (60.4)	357	60	cytokeration 18
G6PD	U01120	GCTGGAGTCCTGTCAGGCATTGC (68.1)	TAGAGCTGAGGCGGAATGGGAG (66.4)	349	60	glucose-6-phosphate dehydrogenase
HNF-4α	AY680696	GCCTACCTCAAAGCCATCAT (60.4)	GACCCTCCCAGCAGCATCTC (66.5)	256	60	hepatocyte nuclear factor 4α
TAT	NM_000353	TGAGCAGTCTGTCCACTGCCT (64.5)	ATGTGAATGAGGAGGATCTGAG (60.8)	338	60	tyrosine aminotransferase
CYP2B6	NM_000767	ATGGGGCACTGAAAAAGACTGA (60.8)	AGAGGCGGGGACACTGAATGAC (66.4)	283	60	Cytochrome P450 2B6
CYP2D6	NM_000106	CTAAGGGAACGACACTCATCAC (62.7)	GTCACCAGGAAAGCAAAGACAC (62.7)	289	60	Cytochrome P450 2D6
CYP2C9	NM_000771	CCTCTGGGGCATTATCCATC (62.4)	ATATTTGCACAGTGAAACATAGGA (57.7)	137	60	Cytochrome P450 2C9
CYP2C19	NM_000769	TTCATGCCTTTCTCAGCAGG (60.4)	ACAGATAGTGAAATTTGGAC (54.3)	277	60	Cytochrome P450 2C19
CYP2C8	NM_000770	ACAACAAGCACCACTCTGAGATATG	GTCTGCCAATTACATGATCAATCTCT	100	60	Cytochrome P450 2C8
CYP3A4	AK298451	GCCTGGTGCTCCTCTATCTA (62.4)	GGCTGTTGACCATCATAAAAGC (60.8)	187	60	Cytochrome P450 3A4
CYP1A1	BC023019	TCCAGAGACAACAGGTAAAACA (58.9)	AGGAAGGGCAGAGGAATGTGAT (62.7)	371	60	Cytochrome P450 1A1
CYP1A2	AF182274	ACCCCAGCTGCCCTACTTG (64.5)	GCGTTGTGTCCCTTGTTGT (62.4)	101	60	Cytochrome P450 1A2
CYP2E1	NM_000773	ACCTGCCCCATGAAGCAACC (64.5)	GAAACAACTCCATGCGAGCC (62.4)	246	60	Cytochrome P450 2E1
PXR	AB307701	GAAGTCGGAGGTCCCCAAA (62.3)	CTCCTGAAAAAGCCCTTGCA (60.4)	100	60	pregnane × receptor
CAR	AB307702	TGATCAGCTGCAAGAGGAGA (60.4)	AGGCCTAGCAACTTCGCACA (62.4)	102	60	constitutive androstane receptor
AhR	BC070080	ACATCACCTACGCCAGTCGC (64.5)	TCTATGCCGCTTGGAAGGAT (60.4)	101	60	aryl hydrocarbon receptor
UGT1A1	BC128414	GGAGCAAAAGGCGCCATGGC (62.5)	GTCCCCTCTGCTGCAGCTGC (64.5)	178	60	uridine diphosphate glucuronyltransferase 1A1
LV-BMI- 1	NM_005180	GCTGAGGGCTATTGAGGCGCA (65.5)	ACCCCAAATCCCCAGGAGCTGT (65.7)	127	60	lentivirus vector BMI-1
hBMI-1	NM_005180	ACCTCCCAGCCCCGCAGAAT (65.9)	AGACGCCGCTGTCAATGGGC (66.4)	280	60	human BMI-1
LV- hTERT	AF018167	CAACCCGGCACTGCCCTCAG (66.9)	GGGGTTCCGCTGCCAAA (68.2)	268	60	lentivirus vector telomerase reverse transcriptase
hTERT	AF018167	CGGAAGAGTGTCTGGAGCAAGT (59.5)	GAACAGTGCCTTCACCCTCGA (61.1)	258	60	human telomerase reverse transcriptase

Sequence of the primers and the conditions used in quantitative real-time PCR (qPCR).

 $5~\mu L$ of $10~\mu g/mL$ cDNA diluted in a $25~\mu L$ reaction mixture containing $0.4~\mu M$ for each primer and $12.5~\mu L$ SybrGreen with the following conditions: $95^{\circ}C$ for 10 min, followed by 40 cycles of amplification at $95^{\circ}C$ for 15 sec, $60^{\circ}C$ for 40 sec, and $72^{\circ}C$ for 40 sec. The fluorescent products were measured at the last step of each cycle. To determine the specificity of amplification, melting curve analysis was applied to all final PCR products, after finishing the thermal cycling. The non-

template negative control (NTC) was performed with each gene-specific primer pair. The number of cycles required for the fluorescent signal to cross the threshold (Ct's) was determined from each primer pair. The obtained Ct's were subtracted with the Ct of the respective house-keeping gene (GAPDH) of the same cells to obtain ΔCt . To enable suitable comparison, the ΔCt 's of the treated cells were subtracted with ΔCt 's of the untreated cells of the same period to obtain $\Delta\Delta Ct$'s.

The relative fold change could be obtained from the expression of $2^{-(\Delta\Delta Ct)}$.

The analysis of CYP450 activity

CYP1A1, CYP1A2, CYP2C9 and CYP3A4 enzyme activities were assayed directly in all cultured cells (immortalized hepatocyte-like cell at passage 3-7, primary human hepatocyte, HepG2 or MSC) attaching to the collagen type IV-coated 6-well plate at a density of 10⁶ cell/well. All cultured cells were divided into three groups. Group 1: cells were cultured in IMDM supplemented with 40 μM rifampicin to induce CYP450 isotypes 3A4 and 2C9. Group 2: cells were cultured in IMDM supplemented with 50 µM omeprazole for inducing CYP1A1 and CYP1A2. Group 3: cells were cultured in IMDM alone as a control. All conditions were incubated for 72 h with daily medium change. Metabolism was assessed based on luciferase activity using the P450-glo 1A1, 1A2, 2C9 and 3A4 assay (V8751, V8771, V8791, V9001; Promega, WI). After 3-d incubation period, cells were incubated with IMDM supplemented with 100 µM Luciferin-CEE, Luciferin-H, Luciferin-ME for 3-4 h or 3 µM Luciferin-IPA for 30-60 min. An aliquot (50 µL) of the medium was transferred to 96-well opaque white luminometer plate (Nunc, Denmark) and luciferin detection reagent was added to each well. After sitting at room temperature for 20 min, luminescence was measured with a SpectraMax M5 spectrofluorometer.

Statistical analysis

Each experiment was performed in triplicate. Data were expressed as mean \pm SD. Data from quantitative RT-qPCR and enzyme activity were evaluated for statistical significance using the Student's unpaired t test (p < 0.05). At least 3-fold induction in mRNA with statistically significant difference was judged as relevant.

Additional material

Additional file 1: Details of quantitative RT-PCR conditions. This file contains the tabulated specific information for qRT-PCR section.

Acknowledgements

This study was funded by research grants from the Thailand Research Fund (TRF) separately awarded to S. Hongeng and A. Wongkajornsilp. K. Sangiamsuntorn is a recipient of Siriraj Graduate Thesis Scholarship. A. Wongkajornsilp is a recipient of Siriraj Chalermprakiat Fund of the Faculty of Medicine Siriraj Hospital, Mahidol University. We would like to thank Professor Amnuay Thithapandha for his help with proof reading.

Author details

¹Department of Pharmacology, Faculty of Medicine Siriraj Hospital, Mahidol University, 2 Prannok Road, Bangkoknoi, Bangkok 10700, Thailand. ²Department of Surgery, Faculty of Medicine Siriraj Hospital, Mahidol University, 2 Prannok Road, Bangkoknoi, Bangkok 10700, Thailand. ³Department of Pediatrics, Faculty of Medicine Ramathibodi Hospital,

Mahidol University, 270 Rama VI Road, Ratchatewi, Bangkok 10400, Thailand. ⁴Department of Pathology, Faculty of Medicine Ramathibodi Hospital, Mahidol University, 270 Rama VI Road, Ratchatewi, Bangkok 10400, Thailand. ⁵Department of Biotechnology, Faculty of Science, Mahidol University, 272 Rama VI Road, Ratchatewi, Bangkok 10400, Thailand.

Authors' contributions

KS performed most of the experiments, designed the protocol, performed the statistical analysis and drafted the manuscript. AW, PA, and SH designed the protocol. SL participated in the preparation of the primary hepatocytes. LN and SB prepared the vectors. AW and SH coordinated the study. SD participated in MSC culture. KK participated in qRT-PCR. All authors have read and approved the final manuscript.

Received: 13 April 2011 Accepted: 30 September 2011 Published: 30 September 2011

References

- Zanger UM, Turpeinen M, Klein K, Schwab M: Functional pharmacogenetics/genomics of human cytochromes P450 involved in drug biotransformation. Anal Bioanal Chem 2008, 392(6):1093-1108.
- Zamek-Gliszczynski MJ, Hoffmaster KA, Nezasa K, Tallman MN, Brouwer KL: Integration of hepatic drug transporters and phase II metabolizing enzymes: mechanisms of hepatic excretion of sulfate, glucuronide, and glutathione metabolites. Eur J Pharm Sci 2006. 27(5):447-486.
- Uno S, Endo K, Ishida Y, Tateno C, Makishima M, Yoshizato K, Nebert DW: CYP1A1 and CYP1A2 expression: comparing 'humanized' mouse lines and wild-type mice; comparing human and mouse hepatoma-derived cell lines. Toxicol Appl Pharmacol 2009, 237(1):119-126.
- Ripp SL, Mills JB, Fahmi OA, Trevena KA, Liras JL, Maurer TS, de Morais SM: Use of immortalized human hepatocytes to predict the magnitude of clinical drug-drug interactions caused by CYP3A4 induction. *Drug Metab Dispos* 2006, 34(10):1742-1748.
- Tao XR, Li WL, Su J, Jin CX, Wang XM, Li JX, Hu JK, Xiang ZH, Lau JT, Hu YP: Clonal mesenchymal stem cells derived from human bone marrow can differentiate into hepatocyte-like cells in injured livers of SCID mice. J Cell Biochem 2009, 108(3):693-704.
- Lange C, Bassler P, Lioznov MV, Bruns H, Kluth D, Zander AR, Fiegel HC: Hepatocytic gene expression in cultured rat mesenchymal stem cells. Transplant Proc 2005, 37(1):276-279.
- Pan RL, Chen Y, Xiang LX, Shao JZ, Dong XJ, Zhang GR: Fetal liverconditioned medium induces hepatic specification from mouse bone marrow mesenchymal stromal cells: a novel strategy for hepatic transdifferentiation. Cytotherapy 2008, 10(7):668-675.
- Shimomura T, Yoshida Y, Sakabe T, Ishii K, Gonda K, Murai R, Takubo K, Tsuchiya H, Hoshikawa Y, Kurimasa A, et al: Hepatic differentiation of human bone marrow-derived UE7T-13 cells: Effects of cytokines and CCN family gene expression. Hepatol Res 2007, 37(12):1068-1079.
- 9. Banas A, Teratani T, Yamamoto Y, Tokuhara M, Takeshita F, Quinn G, Okochi H, Ochiya T: Adipose tissue-derived mesenchymal stem cells as a source of human hepatocytes. *Hepatology* 2007, **46(1)**:219-228.
- Zemel R, Bachmetov L, Ad-El D, Abraham A, Tur-Kaspa R: Expression of liver-specific markers in naive adipose-derived mesenchymal stem cells. Liver Int 2009, 29(9):1326-1337.
- Yamamoto Y, Banas A, Murata S, Ishikawa M, Lim CR, Teratani T, Hatada I, Matsubara K, Kato T, Ochiya T: A comparative analysis of the transcriptome and signal pathways in hepatic differentiation of human adipose mesenchymal stem cells. FEBS J 2008, 275(6):1260-1273.
- Saulnier N, Lattanzi W, Puglisi MA, Pani G, Barba M, Piscaglia AC, Giachelia M, Alfieri S, Neri G, Gasbarrini G, et al: Mesenchymal stromal cells multipotency and plasticity: induction toward the hepatic lineage. Eur Rev Med Pharmacol Sci 2009, 13(Suppl 1):71-78.
- Campard D, Lysy PA, Najimi M, Sokal EM: Native umbilical cord matrix stem cells express hepatic markers and differentiate into hepatocyte-like cells. Gastroenterology 2008, 134(3):833-848.
- Zhao Q, Ren H, Li X, Chen Z, Zhang X, Gong W, Liu Y, Pang T, Han ZC: Differentiation of human umbilical cord mesenchymal stromal cells into low immunogenic hepatocyte-like cells. Cytotherapy 2009, 11(4):414-426.
- Anzalone R, Iacono ML, Corrao S, Magno F, Loria T, Cappello F, Zummo G, Farina F, La Rocca G: New emerging potentials for human Wharton's jelly

- mesenchymal stem cells: immunological features and hepatocyte-like differentiative capacity. Stem Cells Dev 2010, 19(4):423-438.
- Stock P, Bruckner S, Ebensing S, Hempel M, Dollinger MM, Christ B: The generation of hepatocytes from mesenchymal stem cells and engraftment into murine liver. Nat Protoc 2010, 5(4):617-627.
- Cho CH, Parashurama N, Park EY, Suganuma K, Nahmias Y, Park J, Tilles AW, Berthiaume F, Yarmush ML: Homogeneous differentiation of hepatocytelike cells from embryonic stem cells: applications for the treatment of liver failure. FASEB J 2008, 22(3):898-909.
- Piryaei A, Valojerdi MR, Shahsavani M, Baharvand H: Differentiation of Bone Marrow-derived Mesenchymal Stem Cells into Hepatocyte-like Cells on Nanofibers and Their Transplantation into a Carbon Tetrachloride-Induced Liver Fibrosis Model. Stem Cell Rev. 2011. 7(1):103-18.
- Aurich I, Mueller LP, Aurich H, Luetzkendorf J, Tisljar K, Dollinger MM, Schormann W, Walldorf J, Hengstler JG, Fleig WE, et al: Functional integration of hepatocytes derived from human mesenchymal stem cells into mouse livers. Gut 2007, 56(3):405-415.
- Yan Y, Xu W, Qian H, Si Y, Zhu W, Cao H, Zhou H, Mao F: Mesenchymal stem cells from human umbilical cords ameliorate mouse hepatic injury in vivo. Liver Int. 2009. 29(3):356-365.
- Ren H, Zhao Q, Cheng T, Lu S, Chen Z, Meng L, Zhu X, Yang S, Xing W, Xiao Y, et al: No contribution of umbilical cord mesenchymal stromal cells to capillarization and venularization of hepatic sinusoids accompanied by hepatic differentiation in carbon tetrachloride-induced mouse liver fibrosis. Cytotherapy 2010, 12(3):371-383.
- Ek M, Soderdahl T, Kuppers-Munther B, Edsbagge J, Andersson TB, Bjorquist P, Cotgreave I, Jernstrom B, Ingelman-Sundberg M, Johansson I: Expression of drug metabolizing enzymes in hepatocyte-like cells derived from human embryonic stem cells. Biochem Pharmacol 2007, 74(3):496-503.
- Shiojiri N, Sugiyama Y: Immunolocalization of extracellular matrix components and integrins during mouse liver development. Hepatology 2004, 40(2):346-355.
- Le Lay J, Kaestner KH: The Fox genes in the liver: from organogenesis to functional integration. *Physiol Rev* 2010, 90(1):1-22.
- Unger C, Gao S, Cohen M, Jaconi M, Bergstrom R, Holm F, Galan A, Sanchez E, Irion O, Dubuisson JB, et al: Immortalized human skin fibroblast feeder cells support growth and maintenance of both human embryonic and induced pluripotent stem cells. Hum Reprod 2009, 24(10):2567-2581.
- Aninat C, Piton A, Glaise D, Le Charpentier T, Langouet S, Morel F, Guguen-Guillouzo C, Guillouzo A: Expression of cytochromes P450, conjugating enzymes and nuclear receptors in human hepatoma HepaRG cells. *Drug Metab Dispos* 2006, 34(1):75-83.
- Maronpot RR, Yoshizawa K, Nyska A, Harada T, Flake G, Mueller G, Singh B, Ward JM, Botts S: Hepatic Enzyme Induction: Histopathology. *Toxicol Pathol* 2010, 38(5):776-95.
- Sinz M, Wallace G, Sahi J: Current industrial practices in assessing CYP450 enzyme induction: preclinical and clinical. AAPS J 2008, 10(2):391-400.
- Ishii K, Yoshida Y, Akechi Y, Sakabe T, Nishio R, Ikeda R, Terabayashi K, Matsumi Y, Gonda K, Okamoto H, et al: Hepatic differentiation of human bone marrow-derived mesenchymal stem cells by tetracycline-regulated hepatocyte nuclear factor 3beta. Hepatology 2008, 48(2):597-606.
- Zheng YB, Gao ZL, Xie C, Zhu HP, Peng L, Chen JH, Chong YT: Characterization and hepatogenic differentiation of mesenchymal stem cells from human amniotic fluid and human bone marrow: a comparative study. Cell Biol Int 2008, 32(11):1439-1448.
- Burk O, Koch I, Raucy J, Hustert E, Eichelbaum M, Brockmoller J, Zanger UM, Wojnowski L: The induction of cytochrome P450 3A5 (CYP3A5) in the human liver and intestine is mediated by the xenobiotic sensors pregnane x receptor (PXR) and constitutively activated receptor (CAR). J Biol Chem 2004, 279(37):38379-38385.
- Chen ML, Lee KD, Huang HC, Tsai YL, Wu YC, Kuo TM, Hu CP, Chang C: HNF-4alpha determines hepatic differentiation of human mesenchymal stem cells from bone marrow. World J Gastroenterol 2010, 16(40):5092-5103.
- Banas A, Yamamoto Y, Teratani T, Ochiya T: Stem cell plasticity: learning from hepatogenic differentiation strategies. Dev Dyn 2007, 236(12):3228-3241.

- Zhang YN, Lie PC, Wei X: Differentiation of mesenchymal stromal cells derived from umbilical cord Wharton's jelly into hepatocyte-like cells. Cytotherapy 2009. 11(5):548-558.
- Aurich H, Sgodda M, Kaltwasser P, Vetter M, Weise A, Liehr T, Brulport M, Hengstler JG, Dollinger MM, Fleig WE, et al: Hepatocyte differentiation of mesenchymal stem cells from human adipose tissue in vitro promotes hepatic integration in vivo. Gut 2009, 58(4):570-581.
- Hay DC, Zhao D, Ross A, Mandalam R, Lebkowski J, Cui W: Direct differentiation of human embryonic stem cells to hepatocyte-like cells exhibiting functional activities. Cloning Stem Cells 2007, 9(1):51-62.
- 37. Ksiazek K: A comprehensive review on mesenchymal stem cell growth and senescence. Rejuvenation Res 2009, 12(2):105-116.
- Gjerdrum C, Tiron C, Hoiby T, Stefansson I, Haugen H, Sandal T, Collett K, Li S, McCormack E, Gjertsen BT, et al: Axl is an essential epithelial-tomesenchymal transition-induced regulator of breast cancer metastasis and patient survival. Proc Natl Acad Sci USA 2010, 107(3):1124-1129.
- Wagner W, Horn P, Castoldi M, Diehlmann A, Bork S, Saffrich R, Benes V, Blake J, Pfister S, Eckstein V, et al: Replicative senescence of mesenchymal stem cells: a continuous and organized process. PLoS One 2008, 3(5): e2213
- Boker W, Yin Z, Drosse I, Haasters F, Rossmann O, Wierer M, Popov C, Locher M, Mutschler W, Docheva D, et al: Introducing a single-cell-derived human mesenchymal stem cell line expressing hTERT after lentiviral gene transfer. J Cell Mol Med 2008, 12(4):1347-1359.
- Wolbank S, Stadler G, Peterbauer A, Gillich A, Karbiener M, Streubel B, Wieser M, Katinger H, van Griensven M, Redl H, et al: Telomerase immortalized human amnion- and adipose-derived mesenchymal stem cells: maintenance of differentiation and immunomodulatory characteristics. Tissue Eng Part A 2009, 15(7):1843-1854.
- Abdallah BM, Haack-Sorensen M, Burns JS, Elsnab B, Jakob F, Hokland P, Kassem M: Maintenance of differentiation potential of human bone marrow mesenchymal stem cells immortalized by human telomerase reverse transcriptase gene despite [corrected] extensive proliferation. Biochem Biophys Res Commun 2005, 326(3):527-538.
- Masutomi K, Yu EY, Khurts S, Ben-Porath I, Currier JL, Metz GB, Brooks MW, Kaneko S, Murakami S, DeCaprio JA, et al: Telomerase maintains telomere structure in normal human cells. Cell 2003, 114(2):241-253.
- Zhao YM, Li JY, Lan JP, Lai XY, Luo Y, Sun J, Yu J, Zhu YY, Zeng FF, Zhou Q, et al: Cell cycle dependent telomere regulation by telomerase in human bone marrow mesenchymal stem cells. Biochem Biophys Res Commun 2008, 369(4):1114-1119.
- Jagani Z, Wiederschain D, Loo A, He D, Mosher R, Fordjour P, Monahan J, Morrissey M, Yao YM, Lengauer C, et al: The Polycomb group protein Bmi-1 is essential for the growth of multiple myeloma cells. Cancer Res 2010, 70(13):5528-5538.
- Kim RH, Lieberman MB, Lee R, Shin KH, Mehrazarin S, Oh JE, Park NH, Kang MK: Bmi-1 extends the life span of normal human oral keratinocytes by inhibiting the TGF-beta signaling. Exp Cell Res 2010, 316(16):2600-2608.
- Sanchez A, Fabregat I: Growth factor- and cytokine-driven pathways governing liver stemness and differentiation. World J Gastroenterol 2010, 16(41):5148-5161.
- Harrington L: Does the reservoir for self-renewal stem from the ends? Oncogene 2004, 23(43):7283-7289.
- Kolquist KA, Ellisen LW, Counter CM, Meyerson M, Tan LK, Weinberg RA, Haber DA, Gerald WL: Expression of TERT in early premalignant lesions and a subset of cells in normal tissues. Nat Genet 1998, 19(2):182-186.
- Schieker M, Gulkan H, Austrup B, Neth P, Mutschler W: Telomerase activity and telomere length of human mesenchymal stem cells. Changes during osteogenic differentiation. Orthopade 2004, 33(12):1373-1377.
- Simonsen JL, Rosada C, Serakinci N, Justesen J, Stenderup K, Rattan SI, Jensen TG, Kassem M: Telomerase expression extends the proliferative life-span and maintains the osteogenic potential of human bone marrow stromal cells. Nat Biotechnol 2002. 20(6):592-596.
- Jun ES, Lee TH, Cho HH, Suh SY, Jung JS: Expression of telomerase extends longevity and enhances differentiation in human adipose tissue-derived stromal cells. Cell Physiol Biochem 2004, 14(4-6):261-268.
- Salmon P, Oberholzer J, Occhiodoro T, Morel P, Lou J, Trono D: Reversible immortalization of human primary cells by lentivector-mediated transfer of specific genes. Mol Ther 2000, 2(4):404-414.

- Talens-Visconti R, Bonora A, Jover R, Mirabet V, Carbonell F, Castell JV, Gomez-Lechon MJ: Hepatogenic differentiation of human mesenchymal stem cells from adipose tissue in comparison with bone marrow mesenchymal stem cells. World J Gastroenterol 2006, 12(36):5834-5845.
- Ong SY, Dai H, Leong KW: Hepatic differentiation potential of commercially available human mesenchymal stem cells. Tissue Eng 2006, 12(12):3477-3485.
- Moon YJ, Lee MW, Yoon HH, Yang MS, Jang IK, Lee JE, Kim HE, Eom YW, Park JS, Kim HC, et al: Hepatic differentiation of cord blood-derived multipotent progenitor cells (MPCs) in vitro. Cell Biol Int 2008, 32(10):1293-1301.
- Si-Tayeb K, Noto FK, Nagaoka M, Li J, Battle MA, Duris C, North PE, Dalton S, Duncan SA: Highly efficient generation of human hepatocyte-like cells from induced pluripotent stem cells. *Hepatology* 2010, 51(1):297-305.
- Sekiya I, Larson BL, Smith JR, Pochampally R, Cui JG, Prockop DJ: Expansion of human adult stem cells from bone marrow stroma: conditions that maximize the yields of early progenitors and evaluate their quality. Stem Cells 2002, 20(6):530-541.
- Wybenga DR, Di Giorgio J, Pileggi VJ: Manual and automated methods for urea nitrogen measurement in whole serum. Clin Chem 1971, 17(9):891-895.
- Youdim KA, Tyman CA, Jones BC, Hyland R: Induction of cytochrome P450: assessment in an immortalized human hepatocyte cell line (Fa2N4) using a novel higher throughput cocktail assay. *Drug Metab Dispos* 2007. 35(2):275-282.
- Bort R, Signore M, Tremblay K, Martinez Barbera JP, Zaret KS: Hex homeobox gene controls the transition of the endoderm to a pseudostratified, cell emergent epithelium for liver bud development. *Dev Biol* 2006, 290(1):44-56.

doi:10.1186/1472-6750-11-89

Cite this article as: Sa-ngiamsuntorn *et al.*: Upregulation of CYP 450s expression of immortalized hepatocyte-like cells derived from mesenchymal stem cells by enzyme inducers. *BMC Biotechnology* 2011 11:89.

Submit your next manuscript to BioMed Central and take full advantage of:

- Convenient online submission
- Thorough peer review
- No space constraints or color figure charges
- Immediate publication on acceptance
- Inclusion in PubMed, CAS, Scopus and Google Scholar
- Research which is freely available for redistribution

Submit your manuscript at www.biomedcentral.com/submit



APPENDIX II

Manuscript

Subject: Fwd: FW: PLOS ONE Decision: Accept [PONE-D-13-19722R2]

From: Adisak Wongkajornsilp <adisak.won@mahidol.ac.th>

Date: 26/9/2556 17:41

To: Khanit Sa-ngiamsuntorn < khanits@hotmail.com>, Suradej Hongeng

<suradej.hon@mahidol.ac.th>, Sunisa Duangsa-ard <sunisa.dua@mahidol.ac.th>, Kanda

Kasetsinsombat <kanda.kae@mahidol.ac.th>

------ Original Message ------

Subject: FW: PLOS ONE Decision: Accept [PONE-D-13-19722R2]

Date: Thu, 26 Sep 2013 14:40:57 +0700

From: Kittipong Maneechotesuwan <kittipong.man@mahidol.ac.th>

To: Adisak Wongkajornsilp <a disak.won@mahidol.ac.th>

Congratulation

From: em.pone.0.360bd0.0d745187@editorialmanager.com [em.pone.0.360bd0.0d745187@editorialmanager.com] on behalf of PLOS ONE [plosone@plos.org]

Sent: Thursday, September 26, 2013 1:17 PM

To: Kittipong Maneechotesuwan

*Subject: * PLOS ONE Decision: Accept [PONE-D-13-19722R2]

PONE-D-13-19722R2

Sunitinib Indirectly Enhanced Anti-tumor Cytotoxicity of Cytokine-Induced Killer Cells and CD3+CD56+ Subset through the Co-culturing Dendritic Cells

PLOS ONE

Dear Dr. Kittipong,

I am pleased to inform you that your manuscript has been deemed suitable for publication in PLOS ONE.

Your manuscript will now be passed on to our Production staff, who will check your files for correct formatting and completeness. After this review, they may return your manuscript to you so that you can make necessary alterations requested by the Production staff.

Before uploading, you should check the PDF of your manuscript very dosely. THERE IS NO AUTHOR PROOFING. You should therefore consider the corrected files you upload now as equivalent to a production proof. The text you supply at this point will be faithfully represented in your published manuscript exactly as you supply it. This is your last opportunity to correct any errors that are present in your manuscript files.

In addition, now that your manuscript has been accepted, please log into EM at http://www.editorialmanager.com/pone, click the "Update My Information" link at the top of the page, and update your user information to ensure an efficient production and billing process. If you have any questions about billing, please contact authorbilling@plos.org.

If you or your institution will be preparing press materials for this manuscript, you must inform our press team in advance. We no longer routinely supply publication dates to authors; if you need to know your paper's publication date for media purposes, you must coordinate with our press team. Your manuscript will remain under a strict press embargo until the publication date and time. For more information please contact one press plos.org.

Please contact one_production@plos.org if you have any other questions or concerns. Thank you for submitting your work to PLOS ONE.

With kind regards, Seema Singh, Ph.D Academic Editor

Sunitinib Indirectly Enhanced Anti-tumor Cytotoxicity of Cytokine-Induced Killer Cells and CD3⁺CD56⁺ Subset through the Co-culturing Dendritic Cells

Adisak Wongkajornsilp, M.D., Ph.D.¹, Valla Wamanuttajinda, B.Sc.¹, Kanda Kasetsinsombat, M.Sc.¹, Sunisa Duangsa-ard, M.Sc.¹, Khanit Sa-ngiamsuntorn, Ph.D.^{1,4}, Suradej Hongeng, M.D.³, Kittipong Maneechotesuwan, M.D., Ph.D.²

¹Department of Pharmacology and ²Department of Medicine, Faculty of Medicine Siriraj Hospital, Mahidol University, Bangkok 10700, Thailand

³Department of Pediatrics, Faculty of Medicine Ramathibodi Hospital, Mahidol University, Bangkok 10400, Thailand

⁴Department of Biochemistry, Faculty of Pharmacy, Mahidol University, Bangkok 10400, Thailand

Corresponding authors:

Kittipong Maneechotesuwan, M.D., Ph.D.

Department of Medicine

Faculty of Medicine Siriraj Hospital

Mahidol University

Bangkok 10700, Thailand

E-mail: kittipong.man@mahidol.ac.th

Adisak Wongkajornsilp, M.D., Ph.D.

Department of Pharmacology

Faculty of Medicine Siriraj Hospital

Mahidol University

Bangkok 10700, Thailand

E-mail: adisak.won@mahidol.ac.th

Abstract

Cytokine-induced killer (CIK) cells have reached clinical trials for leukemia and solid tumors. Their anti-tumor cytotoxicity had earlier been shown to be intensified after the co-culture with dendritic cells (DCs). We observed markedly enhanced anti-tumor cytotoxicity activity of CIK cells after the co-culture with sunitinib-pretreated DCs over that of untreated DCs. This cytotoxicity was reliant upon DC modulation by sunitinib because the direct exposure of CIK cells to sunitinib had no significant effect. Sunitinib promoted Th1-inducing and pro-inflammatory phenotypes (IL-12, IFN-γ and IL-6) in DCs at the expense of Th2 inducing phenotype (IL-13) and regulatory phenotype (PD-L1, IDO). Sunitinib-treated DCs subsequently induced the upregulation of Th1 phenotypic markers (IFN-γ and T-bet) and the downregulation of the Th2 signature (GATA-3) and the Th17 marker (RORC) on the CD3+CD56+ subset of CIK cells. It concluded that sunitinib-pretreated DCs drove the CD3+CD56+ subset toward Th1 phenotype with increased anti-tumor cytotoxicity.

Funding: This work was supported by research grants from Thailand Research Fund and Mahidol University (to A.W.). A.W. and K.M. are recipients of Chalermphrakiat Grant at the Faculty of Medicine Siriraj Hospital, Mahidol University. K.S. is a recipient of the Postdoctoral Fellowship Grant of Mahidol University. The funders had no role in study design, data collection and analysis, decision to publish, or preparation of the manuscript.

Competing interests: The authors have declared that no competing interests exist.

Introduction

The mechanisms of tumor immune evasion involve several biological molecules including indoleamine 2, 3-dioxygenase (IDO), PD-L1, GATA and interferon (IFN). IDO, a cytosolic protein that catalyzes the rate-limiting step of tryptophan (Trp) metabolism, stimulates immune tolerance in human cancer[1]. IDO generates immunosuppressive dendritic cells (DCs)[2]. Trp metabolites mediate cytotoxic effects on CD8+ tumor-infiltrating lymphocytes and CD4+Th1 cells[3-5]. PD-L1 can have an inhibitory function that primarily acts to inhibit the priming and activation of immune responses and T cell-mediated killing of cancer cells in particular in the tumor beds [6]. The zinc finger DNA binding GATA factors coordinate cellular maturation with proliferation arrest and cell survival[7]. Alteration of GATA factors was shown to be causatively involved in various cancers in human patients[7]. GATA-3 primarily induces Th2 differentiation[8] and therefore causes Th2 immune deviation that leads to the expansion of fibrocytes with immunosuppressive properties observed in patients This may be the mechanism that GATA-3 contributes to tumor with cancer[9]. progression via immune evasion. The above data suggested the requirement of therapeutic overriding of tumor immune evasion by boosting cytotoxic effects of responsible effector cells.

Cytokine-induced killer (CIK) cells have been deployed against a number of solid tumors with *in vitro* and *in vivo* evidences. The major effector of CIK cells is the CD3+CD56+ subset[10,11]. The anti-tumor action of CIK cells could be augmented after being co-cultured with dendritic cells (DCs)[12-15]. The depletion of regulatory T cell (Treg) subset in CIK cells after the co-culture with DCs was proposed as the responsible mechanism[13]. We previously observed similar enhancement of the anti-tumor action of the isolated CD3+CD56+ subset against cholangiocarcinoma[16] and osteosarcoma[17] after being co-cultured with DCs. This observation implied that the activity of CD3+CD56+ subset was not invariably naturally active, but inducible. The *ex vivo* optimization for the anti-tumor activity of the CD3+CD56+ subset as well as the dissection for the involved signal transduction has posed as a challenge for CIK cell-based immunotherapy. We approached this challenge through the treatment of CIK cells, co-cultured DCs with a promising molecule, sunitinib.

Sunitinib, a protein kinase inhibitor (PKI), is conventionally intended for direct treatment of lung cancer and renal cell carcinoma. It indirectly affects the tumors through the host components of immune response[18]. The pharmacological concentrations of sunitinib had no effect toward PI3K and ERK phosphorylation in NK cells and did not exert any toxicity toward peripheral blood mononuclear (PBMCs)[19]. Not all tyrosine kinase inhibitors provide the beneficial effects toward immune cells[18]. Only sunitinib could enhance the maturation and the expansion of DCs. Sorafenib, but not sunitinib, mediated its immunosuppressive effect at pharmacological concentrations through the induction of human NK cell-derived cytotoxic activity, IFN-y release[19], and suppressed mouse DCs and antigen-specific T cells functions[20].

Sunitinib might exert its immunostimulatory activity through the modulation of the ratio of immunostimulatory versus immunoregulatory cells. Recently sunitinib was shown to reverse the immune suppression of tumor microenvironment (TME) by suppressing the development of regulatory T cells (Treg)[21]. Both Treg and myeloid-derived suppressor cells (MDSC) are the major immunosuppressive cellular components in TME[22,23]. The presence of Treg subset compromised the overall anti-tumor activity The fraction of peripheral blood MDSC[25,26] and of CIK cells[16,17,24]. Treg[25,27,28] were dramatically decreased in subjects treated with sunitinib. In contrast, the fraction of DCs was significantly increased after sunitinib treatment and this correlated with tumor regression in patients with renal cell carcinoma[26]. The combination of sunitinib treatment with DC vaccination acted synergistically in suppressing the implanted melanoma in mice[29]. The responders with tumor regression after sunitinib treatment were associated with the reduction in MDSC and Treg in the TME in concomitant with the rising of CD8⁺ T cells. Sunitinib shifted tumorinfiltrating lymphocytes (TILs) in mice from releasing Th2 cytokines (IL-10, TGF-β) to Th1 cytokines (IFN-y). The expression of co-inhibitory molecules (CTLA-4 and PD-1) and Foxp3 in these TILs was also suppressed. This reversal of immunosuppression was proposed to be mediated through the inhibition of c-kit in MDSCs[30]. The MDSC suppressive activity of sunitinib might be counteracted by locally high level of GM-CSF[31]. The immunomodulation might be mediated through anti-VEGFR and NFκB-suppressive actions of sunitinib. The heightened proliferation and antigen-specific T-cell activity of CD8⁺ T cells was attributed to the suppression of STAT3[32]. However, other investigators reported the absence of favorable immunological action of sunitinib. Sunitinib was unable to reverse VEGF / tumor supernatant-induced suppression of DC maturation[33]. Some renal cell carcinoma subjects treated with sunitinib for 4 weeks carried lower Th1/Th2 ratio in peripheral blood[34], as opposed to those found in the earlier studies[27].

Improving the density as well as the activity of CD3⁺CD56⁺ subset, while suppressing those of Treg subset, would be desirable for CIK cell-based immunotherapy. We investigated whether the introduction of sunitinib to the DC-CIK co-culture system could improve anti-tumor effects. We examined the proportion of each subset in CIK cells that represented the quantitative changes in the density of CIK cell subsets. For qualitative change, we measured the alteration in the maturation status or immunological markers of both DCs and CIK cells. In DCs, the markers studied included Th1 promoting genes (IL-12, IFN-γ); Th2 promoting gene (IL-13); Th17 promoting genes (IL-23, IL-6); and Treg promoting genes (PD-L1, IDO, IL-10). In CIK cells, the markers assessed included Th1 genes (IFN-γ, T-bet); Th2 genes (IL-4, GATA-3); Th17 genes (RORC, IL-17, STAT3); and Treg (IDO, IL-10).

Materials and Methods

Ethic Statement

All subjects understood and signed the informed consent form before the participation. The study protocol with the accompanying informed consent form conforms to the ethical guidelines of the 1975 Declaration of Helsinki and was approved by the Institutional Review Board of the Faculty of Medicine Siriraj Hospital, Mahidol University.

Generation of CIK cells and DCs from peripheral blood mononuclear cells

CIK cells and DCs were generated from PBMCs of 6 consented healthy volunteers. PBMCs were isolated from whole blood by Ficoll gradient centrifugation (IsoPrep, Robbins Scientific, Sunnyvale, CA). The cells were allowed to adhere over the 6-well plate at a density of 1.2×10^6 cells/mL/well for 1 h at 37°C in RPMI 1640, 10% FBS, 100 U/mL penicillin, and 100 µg/mL streptomycin. The adherent cells (5.0×10^4 cells/well) were used to generate DCs.

To generate CIK cells, non-adherent PBMCs were resuspended in RPMI 1640 (Invitrogen, Carlsbad, CA), 10% FBS, 25 mM Hepes, 100 U/mL penicillin and 100 μ g/mL streptomycin. Human interferon γ (IFN- γ , 1,000 U/mL (Amoytop Biotech, Xiamen, China) was added and incubated at 37°C, 5% CO₂ for 24 h. After 24-h incubation, 50 ng/mL monoclonal antibody against CD3 (eBioscience, San Diego, CA), and 300 IU/mL IL-2 (Amoytop Biotech) were added. CIK cells were maintained at a density of \leq 6 × 10⁶ cells/mL in RPMI 1640, 10% FBS, 300 IU/mL IL-2, 25 mM Hepes, 2 mM L-glutamine, 100 U/mL penicillin, and 100 μ g/mL streptomycin with medium replacement every 5 days. Cells were harvested on day 14 with apparent viability above 90%.

To generate DCs, the adherent cells were maintained in 2 mL RPMI 1640, 10% FBS, 400 U/mL granulocyte-macrophage colony-stimulating factor (GM-CSF, Amoytop Biotech), 500 U/mL IL-4 (Amoytop Biotech) for 14 d. DC maturation could be achieved by adding 1,000 U/mL tumor necrosis factor α (TNF- α ; Amoytop Biotech) in the final 24 h. Some designated wells were treated with 1 μ M sunitinib (Sigma, St. Louis, MO) for 48 h. The viability of mature DCs was above 95%.

Preparation of CD3⁺CD56⁺ cells

An aliquot of CIK cells (1.0×10^8 cells) on day 14 was purified for CD3⁺CD56⁺ subset using CD3 Microbeads kit and CD56 Microbeads kit (Miltenyi Biotec, Germany) according to the manufacturer instruction. This usually yielded $0.8 - 2.0 \times 10^7$ purified CD3⁺CD56⁺ cells.

Co-culture of CIK cells and DCs

On day 14 after CIK and DCs generation, CIK cells or the purified CD3 $^+$ CD56 $^+$ cells were seeded on DCs of different conditions at the stimulators (DCs): responders (CIK cells)(S:R) ratio of 1: 20. The co-cultured cells were maintained in RPMI 1640, 10% FBS, 25 mM Hepes, 2 mM L-glutamine, 100 U/mL penicillin, and 100 μ g/mL streptomycin, 300 IU/mL IL-2 for 5 days prior to *in vitro* cytotoxicity assay.

Primary cultured cholangiocarcinoma cells isolated from sediments of biliary fluid

A human cholangiocarcinoma cell line prepared from intrahepatic biliary fluid, HubCCA1[16], was propagated in growth medium (DMEM, 15% FBS, 1 mM sodium pyruvate, 1 mg/mL insulin, 0.66 mg/mL transferrin, 0.67 μ g/mL sodium selenite, 0.1 mM non-essential amino acid solution, 2 mM L-glutamine, 50 unit/mL penicillin, and 50 μ g/mL streptomycin) at 37°C with 5% CO₂.

Fluorescence-activated cell sorting (FACS) analysis

Either DCs or CIK cells were washed twice in PBS containing 5% FBS (PBS/FBS) and resuspended in 100 μL PBS/FBS. The cell pellet was incubated with 2 μL of the corresponding primary monoclonal antibodies (1 mg/mL) for 30 min at 25°C, washed twice and resuspended in 200 μL of PBS/FBS. For the staining of intracellular immunogens, cells were fixed and permeabilized prior to the intracellular staining in accordance with the manufacturers. Flow cytometry analysis on 10,000 cells was performed using a FACSCalibur (Becton Dickinson, San Jose, CA). The employed primary mouse monoclonal antibodies raised against human immunogens included anti-FOXP3-Alexa Fluor 488, anti-CD4-PE-Cy5, anti-CD25-PE from Biolegend, anti-IL-10-Alexa Fluor 647, anti-CD3-FITC, anti-CD56-PE, anti-CD80-FITC, anti-CD83-PE, anti-CD86-PE-Cy5, anti-CD40-APC from eBiosceince, anti-RORC-PerCP, anti-IL-17-APC from R&D Systems. Data were analyzed using FlowJo version 10.0.5.

Cytotoxic Assay

Propidium iodide (PI)-based cytotoxic assay was used to estimate the anti-tumor cytotoxic activity of CIK cells. The tumor cells (5×10^3 cells/well) were seeded as target cells on the 96-well plate for 24 h at 37° C, 5% CO₂. The target cells were washed with serum-free RPMI and co-cultured with the effector cells at the designated ratio in 80 µL RPMI/well for 4 h at 37° C, 5% CO₂. For IFN- γ neutralization, 0.02 µg/mL anti-IFN- γ (clone 25718, R&D Systems) was added to the effector cells 2 h prior to the co-culture. PI (20 µL of 10 µg/mL in PBS) was added to and incubated with the cell mixture for additional 30 min. The mixture was measured for fluorescence with an excitation wavelength of 482 nm and an emission wavelength of 630 nm using the SpectraMax M5 microplate reader (Molecular Devices, Sunnyvale, CA). The background wells were those with the corresponding numbers of effector cells, but without target cells. The 100% lysis came from wells containing target in RPMI cells plus 20 µL isopropanol. The 0% lysis came from wells containing only the target cells. The % cytotoxicity was calculated using the following expression:

% cytotoxicity =
$$\frac{Fl_x - Fl_0}{Fl_{100} - Fl_0} \times 100$$

 Fl_0 represents the fluorescence of the well containing the target cells without the exposure to any effector cells. Fl_{100} represents the fluorescence of from the well containing the target cells in RPMI plus 20% isopropanol. Fl_x represents the fluorescence of the well containing the target cells after the exposure to the indicated numbers of effector cells.

RNA preparation and quantitative real-time PCR analysis

Total RNA was extracted from different conditions of CD3⁺CD56⁺ cells, macrophages, iDCs and mDCs. Cells were homogenized in 350 μL of RA1 buffer and 3.5 μL of βmercaptoethanol (illustra™ RNAspin Mini RNA Isolation Kit, GE Healthcare, UK) to isolate total RNA. Reverse transcription was performed with 1 µg of total RNA. Firststrand cDNA synthesis was performed with the ImProm-II Reverse Transcription System (Promega, Madison, WI). The gene-specific primers pairs (Table 1) were designed using Primer Express 3.0 (ABI, Foster City, CA) and ordered from 1st BASE (Singapore). They were amplified using FastStart SYBR® Green Master (Roche Diagnostics, Mannheim, Germany) and StepOnePlus Real-Time PCR system (ABI). Real-time PCR was performed using 1.5 µL of 200 ng/µL cDNA in 15 µL reaction mixture with the following conditions: 95°C for 10 min, followed by 40 cycles of amplification at 95°C for 15 sec, 60°C for 40 sec, and 72°C for 40 sec. The obtained Ct's were subtracted with the Ct of GAPDH of the same condition to obtain Δ Ct. The Δ Ct's of the treated cells were subtracted with Δ Ct's of the untreated cells of the same period to obtain $\Delta\Delta$ Ct's. The fold-changes could be obtained from the expression of **2**-ΔΔCt.

Statistical analysis

The results are shown as mean \pm standard error of the mean (SEM) of triplicate determinants. Data were plotted using GraphPad Prism version 5.03. Two-way ANOVA was used to determine the significance of difference between means of cytotoxic experiments. Student's *t*-test was used for real-time PCR analysis. A *p* value of less than 0.05 was considered significant.

Results

The cytotoxic activity of CIK cells after the priming with sunitinib-treated DCs toward cholangiocarcinoma cell line

Among all investigated conditions of effector cells, the untreated CIK cells provided the lowest cytotoxicity toward the HubCCA-1 (Fig. 1A). The cytotoxicity was improved after the co-culture with mDC. The highest anti-tumor cytotoxic activity came from CIK cells that had been co-cultured with either sunitinib-treated iDCs or sunitinib-treated mDCs. This enhancement could not be obtained from CIK cells co-cultured with sunitinib-treated macrophages. The direct exposure of CIK cells to sunitinib could not

confer any significant improvement in the anti-tumor cytotoxicity over that of the untreated CIK cells until the E:T ratio reached 12:1, and therefore demonstrated little enhancement. Isolated CD3+CD56+ subset contained anti-tumor cytotoxic activity (Fig. 1B). Likewise, the direct exposure of CD3+CD56+ subset to sunitinib could not confer further significant improvement. The co-culture of CD3+CD56+ subset with sunitinib-treated mDCs provided the optimal improvement.

The alteration in the polarization of macrophages, iDCs and mDCs after the exposure to sunitinib

Macrophages, iDCs and mDCs were studied for their polarization using real-time RT-PCR analysis for a number of markers (Table 1). The untreated macrophages contained lower IL-12 expression (Fig. 2A) than those in iDCs and mDCs. After sunitinib treatment, the level of IL-12 expression was enhanced in macrophages and mDCs, but not in iDCs. Both iDCs and mDCs carried higher IFN-y expression than did macrophages. Only in mDCs was the expression of IFN-y (Fig. 2B) significantly increased after sunitinib treatment. The expression level of IL-6 (Fig. 2C) was rising in mDCs after sunitinib treatment, but was reciprocally suppressed in macrophages. The expression of IL-13 in macrophages and iDCs, but not mDCs, was undetectable. The IL-13 expression in mDCs was suppressed after sunitinib treatment (Fig. 2D). The untreated macrophages and iDCs contained higher IL-10 expression (Fig. 2E) than did mDCs. Upon sunitinib treatment, the expression of IL-10 was decreased in macrophages, but not significantly altered in iDCs nor mDCs. Sunitinib treatment suppressed the expression of PD-L1 (Fig. 2F) in mDCs. The IDO expression (Fig. 2G) was suppressed in iDCs and mDCs after sunitinib treatment. Sunitinib enhanced the expression of IL-23 (Fig. 2H) in macrophages and mDCs, but not in iDCs.

The alteration in the maturity of macrophages, iDCs, and mDCs after sunitinib treatment

The flow cytometry analysis of iDCs, and mDCs did not promote their maturation based on the staining of CD80, CD83 and CD86 (Fig. 3A). In contrast, the sunitinib treatment to macrophages resulted in not only less DC maturation markers (CD80, CD83, CD86 and CD40), but also macrophage markers (CD14 and CD40, Fig. 3B). There was no alteration in IL-10, and IDO (Fig. 3C) in both iDCs and mDCs, but there was less IDO in macrophages after sunitinib treatment.

The examination for the alteration of the ratios of CD3⁺CD56⁺, Treg, and Th17 subsets in the whole CIK cell population after the priming with sunitinib-treated DCs

CIK that had been either directly treated with sunitinib, primed with mDCs or primed with sunitinib-pretreated mDCs did not significantly alter the proportions of the

CD3⁺CD56⁺ subset (Fig. 4A), the Th17 subset (Fig. 4B), nor the Treg (CD4⁺CD25⁺Foxp3⁺) subset (Fig. 4C).

The analysis for the polarization of CD3⁺CD56⁺ cells after the priming with either sunitinib-treated mDCs or untreated mDCs

The co-culture of CD3⁺CD56⁺ cells with untreated mDCs raised the expression of IDO, and Th1 markers (IFN-γ and T-bet) (Fig. 5). In contrast, the expression of Th2 markers (GATA-3) and Th17 (RORC, STAT3) markers was reduced. The co-culture of CD3⁺CD56⁺ cells with sunitinib-pretreated mDCs maintained the rising IDO, IFN-γ, T-bet; the lessening of GATA-3 and RORC.

The cytotoxic activity of all treatment conditions of CD3⁺CD56⁺ cells required IFN-γ

The CD3⁺CD56⁺ subset that had been exposed to mDC or sunitinib treated mDCs were examined whether they mediated their anti-tumor cytotoxic action through IFN-γ. The isolated CD3⁺CD56⁺ subset from each condition was pretreated with the neutralizing monoclonal anti-IFN-γ (αIFN-γ) prior to the exposure to the target HubCCA1 target cells. All studied conditions of CD3⁺CD56⁺ subset were susceptible to the suppressive effect of anti-IFN-γ (Fig. 6).

Discussion

To our knowledge, the present finding provided the first notion that the CD3+CD56+ subset of CIK cells was not invariably naturally active. The CD3+CD56+ subset could be polarized toward either Th1 or Th2 phenotype that in turn shapes its anti-tumor activity. The resting CD3+CD56+ subset predominantly expressed Th2 phenotypes, but shifted to Th1 phenotypes upon the exposure to sunitinib-pretreated DCs. The induction of Th1 immune response was first observed in T cells isolated from subjects administered with sunitinib[27]. We investigated further whether the Th1-promoting action of sunitinib was derived directly from CIK cells or indirectly from mDCs. Our data revealed the sequential phenotypic changes in DCs after exposure to sunitinib. Our observation confirmed and expanded the previous report that CD3+CD56+ cells could have their anti-tumor activity expanded after the exposure to mDCs[16] and sunitinib-pretreated mDCs further enhanced this activity. This enhancement could not be simply introduced through the direct exposure of CD3+CD56+ cells to sunitinib.

Modulation of DCs and macrophages by sunitinib

Since the improvement in anti-tumor cytotoxicity of CIK cells resulted mainly from the exposure to sunitinib-pretreated mDCs, we hypothesized that the phenotypic alterations in DCs from sunitinib might be one of the underlying mechanisms. It was possible that sunitinib could induce DC maturation that led to the corresponding enhancement of the anti-tumor cytotoxicity of CIK cells. Using the staining for the DC maturation markers (CD80, CD83 and CD86), apparently there was no significant

change in DC maturation in agreement with an earlier study[33]. The expression of Th1-polarizing cytokines (IL-12, IFN-γ and IL-6) was enhanced, whereas the expression of Th2-polarizing cytokine (IL-13) and the regulatory phenotype (PD-L1, IDO) were suppressed in sunitinib-treated mDCs. The increasing IL-23 expression in sunitinib-treated mDCs should foster the conversion of the nearby Treg toward Th17 cells. The sunitinib-treated monocyte-derived macrophages carried lessen DC maturation markers as well as lessen M1 differentiation markers (CD14 and CD40). The M2 differentiation was also suppressed as evidenced by the lowering IL-10 expression that might favor anti-tumor action. Taken together, sunitinib shifted mDCs toward Th1-polarizing phenotype and away from both Th2-polarizing and regulatory phenotypes.

Sunitinib-pretreated DCs drove CD3⁺CD56⁺ cells toward Th1 polarization

Following the phenotypic change in sunitinib-treated mDCs, we investigated whether there were subsequent alterations in the proportion or the phenotypes of the coculturing CIK subsets. There was no significant alteration in the proportion of any subset with any treatment. As opposed to the earlier study[13], we could not observe the lessening of Treg subset following the co-culture with DCs. The quantitative change was evaluated through the alteration in the proportion of CD3+CD56+ subset within the whole CIK cell population. The CD3⁺CD56⁺ subset proportion was not significantly altered after the exposure to sunitinib-pre-treated mDCs. The functional change was observed through the monitoring for alterations in Th1/Th2/Th17 phenotypes. The polarization toward Th1 differentiation of the CD3⁺CD56⁺ subset was evidenced by the heightening expression of IFN-y and T-bet. differentiation were lessened as evidenced by decreasing GATA3 expression. The alteration in Th1/Th2 phenotypes was in agreement with the observations in DCs. The Th17 differentiation in CD3+CD56+ subset disagreed with the observation in DCs since RORC expression was decreased while STAT3 expression was not significantly altered. This observation was not unexpected, since the Treg subset, not the CD3⁺CD56⁺ subset, was envisaged to undergo Th17 differentiation[35]. heightening antitumor activity in all conditions of CD3⁺CD56⁺ subset relied heavily on IFN-y secretion as this anti-tumor action could be reverse with the neutralizing anti-IFN-y mAb.

Earlier sunitinib study involving mDCs reported the increasing frequency of mDCs in subjects receiving systemic sunitinib treatment[26] with no deleterious effect toward their immunostimulatory function. We have characterized the changes in sunitinib-pretreated mDCs as well as the co-culturing CIK cells regarding to the Th1/Th2/Treg balance. Our *ex vivo* observation implied the immunostimulatory action of sunitinib in addition to the elimination of immunoregulatory cells as reported by others[18,20,21]. Although our studied sunitinib concentration (1 µM) was beyond pharmaceutical concentration, we did not observe any deleterious effect toward mDCs in agreement with the earlier study[20]. The employed concentration was well above the recommended trough plasma concentration (Cmin) at 94 nM[36] and the observed

maximal plasma concentration (Cmax) at 188 nM[37], signified the application of *ex vivo* approach to circumvent systemic adverse reactions[38] in clinical trials. The future direction for CIK cell-based immunotherapy may aim to raise the Th1 phenotype of its effectors in addition to neutralizing the immunosuppressive activity in its Treg subset or in TME.

Acknowledgements

We thank K. Patanapanyasat at the Division of Instruments for Research, Office of Research and Development, Faculty of Medicine, Siriraj, Hospital, Mahidol University for providing flow cytometry facility.

Author Contributions

Conceived and designed the experiments: AW KM SH. Performed the experiments: VW KK SD. Compiled the data: KK SD AW. Analyzed the data: AW, KM, KS. Contributed reagents/materials/analysis tools: AW SH. Wrote the paper: AW KM.

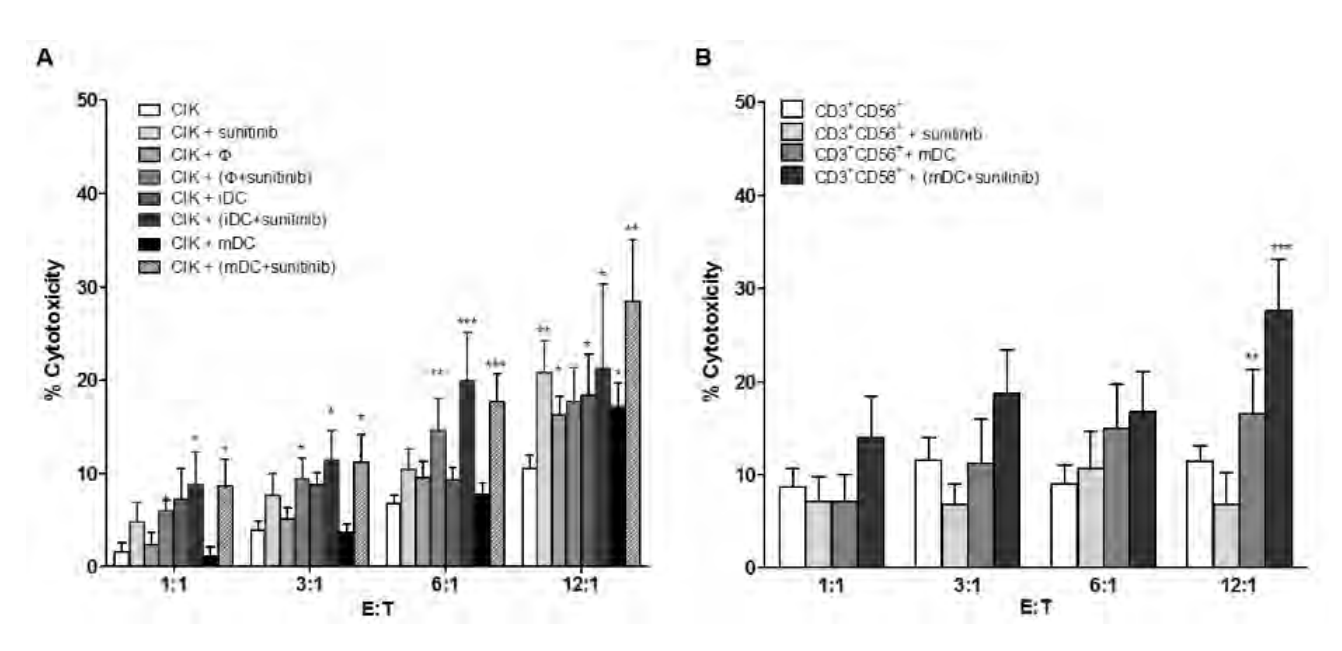
References

- 1. Friberg M, Jennings R, Alsarraj M, Dessureault S, Cantor A, et al. (2002) Indoleamine 2,3-dioxygenase contributes to tumor cell evasion of T cell-mediated rejection. Int J Cancer 101: 151-155.
- Brenk M, Scheler M, Koch S, Neumann J, Takikawa O, et al. (2009) Tryptophan deprivation induces inhibitory receptors ILT3 and ILT4 on dendritic cells favoring the induction of human CD4+CD25+ Foxp3+ T regulatory cells. J Immunol 183: 145-154.
- 3. Frumento G, Piazza T, Di Carlo E, Ferrini S (2006) Targeting tumor-related immunosuppression for cancer immunotherapy. Endocr Metab Immune Disord Drug Targets 6: 233-237.
- 4. Frumento G, Rotondo R, Tonetti M, Damonte G, Benatti U, et al. (2002)

 Tryptophan-derived catabolites are responsible for inhibition of T and natural killer cell proliferation induced by indoleamine 2,3-dioxygenase. J Exp Med 196: 459-468.
- Terness P, Bauer TM, Rose L, Dufter C, Watzlik A, et al. (2002) Inhibition of allogeneic T cell proliferation by indoleamine 2,3-dioxygenase-expressing dendritic cells: mediation of suppression by tryptophan metabolites. J Exp Med 196: 447-457.
- 6. Chen DS, Mellman I (2013) Oncology meets immunology: the cancer-immunity cycle. Immunity 39: 1-10.
- 7. Zheng R, Blobel GA (2010) GATA Transcription Factors and Cancer. Genes Cancer 1: 1178-1188.
- 8. Amsen D, Spilianakis CG, Flavell RA (2009) How are T(H)1 and T(H)2 effector cells made? Curr Opin Immunol 21: 153-160.

- 9. Zhang H, Maric I, Diprima MJ, Khan J, Orentas RJ, et al. (2013) Fibrocytes represent a novel MDSC subset circulating in patients with metastatic cancer. Blood.
- Lu PH, Negrin RS (1994) A novel population of expanded human CD3+CD56+ cells derived from T cells with potent in vivo antitumor activity in mice with severe combined immunodeficiency. J Immunol 153: 1687-1696.
- 11. Schmidt-Wolf GD, Negrin RS, Schmidt-Wolf IG (1997) Activated T cells and cytokine-induced CD3+CD56+ killer cells. Ann Hematol 74: 51-56.
- 12. Marten A, Ziske C, Schottker B, Renoth S, Weineck S, et al. (2001) Interactions between dendritic cells and cytokine-induced killer cells lead to an activation of both populations. J Immunother 24: 502-510.
- 13. Schmidt J, Eisold S, Buchler MW, Marten A (2004) Dendritic cells reduce number and function of CD4+CD25+ cells in cytokine-induced killer cells derived from patients with pancreatic carcinoma. Cancer Immunol Immunother 53: 1018-1026.
- 14. Erhardt M, Schmidt-Wolf IG, Sievers E, Frank S, Strehl J, et al. (2006) Antitumoral capabilities of effector cells after IFN-alpha or CpG-motif treatment of cocultured dendritic cells. Arch Immunol Ther Exp (Warsz) 54: 403-409.
- 15. Li H, Wang C, Yu J, Cao S, Wei F, et al. (2009) Dendritic cell-activated cytokine-induced killer cells enhance the anti-tumor effect of chemotherapy on non-small cell lung cancer in patients after surgery. Cytotherapy 11: 1076-1083.
- 16. Wongkajornsilp A, Somchitprasert T, Butraporn R, Wamanuttajinda V, Kasetsinsombat K, et al. (2009) Human cytokine-induced killer cells specifically infiltrated and retarded the growth of the inoculated human cholangiocarcinoma cells in SCID mice. Cancer Invest 27: 140-148.
- 17. Wongkajornsilp A, Sangsuriyong S, Hongeng S, Waikakul S, Asavamongkolkul A, et al. (2005) Effective osteosarcoma cytolysis using cytokine-induced killer cells pre-inoculated with tumor RNA-pulsed dendritic cells. J Orthop Res 23: 1460-1466.
- 18. Nishioka Y, Aono Y, Sone S (2011) Role of tyrosine kinase inhibitors in tumor immunology. Immunotherapy 3: 107-116.
- 19. Krusch M, Salih J, Schlicke M, Baessler T, Kampa KM, et al. (2009) The kinase inhibitors sunitinib and sorafenib differentially affect NK cell antitumor reactivity in vitro. J Immunol 183: 8286-8294.
- 20. Hipp MM, Hilf N, Walter S, Werth D, Brauer KM, et al. (2008) Sorafenib, but not sunitinib, affects function of dendritic cells and induction of primary immune responses. Blood 111: 5610-5620.
- 21. Ozao-Choy J, Ma G, Kao J, Wang GX, Meseck M, et al. (2009) The novel role of tyrosine kinase inhibitor in the reversal of immune suppression and modulation of tumor microenvironment for immune-based cancer therapies. Cancer Res 69: 2514-2522.
- 22. Lindau D, Gielen P, Kroesen M, Wesseling P, Adema GJ (2013) The immunosuppressive tumour network: myeloid-derived suppressor cells, regulatory T cells and natural killer T cells. Immunology 138: 105-115.
- 23. Morse MA, Hall JR, Plate JM (2009) Countering tumor-induced immunosuppression during immunotherapy for pancreatic cancer. Expert Opin Biol Ther 9: 331-339.
- 24. Li H, Yu JP, Cao S, Wei F, Zhang P, et al. (2007) CD4 +CD25 + regulatory T cells decreased the antitumor activity of cytokine-induced killer (CIK) cells of lung cancer patients. J Clin Immunol 27: 317-326.

- 25. Ko JS, Zea AH, Rini BI, Ireland JL, Elson P, et al. (2009) Sunitinib mediates reversal of myeloid-derived suppressor cell accumulation in renal cell carcinoma patients. Clin Cancer Res 15: 2148-2157.
- 26. van Cruijsen H, van der Veldt AA, Vroling L, Oosterhoff D, Broxterman HJ, et al. (2008) Sunitinib-induced myeloid lineage redistribution in renal cell cancer patients: CD1c+ dendritic cell frequency predicts progression-free survival. Clin Cancer Res 14: 5884-5892.
- 27. Finke JH, Rini B, Ireland J, Rayman P, Richmond A, et al. (2008) Sunitinib reverses type-1 immune suppression and decreases T-regulatory cells in renal cell carcinoma patients. Clin Cancer Res 14: 6674-6682.
- 28. Adotevi O, Pere H, Ravel P, Haicheur N, Badoual C, et al. (2010) A decrease of regulatory T cells correlates with overall survival after sunitinib-based antiangiogenic therapy in metastatic renal cancer patients. J Immunother 33: 991-998.
- 29. Bose A, Taylor JL, Alber S, Watkins SC, Garcia JA, et al. (2011) Sunitinib facilitates the activation and recruitment of therapeutic anti-tumor immunity in concert with specific vaccination. Int J Cancer 129: 2158-2170.
- 30. Kao J, Ko EC, Eisenstein S, Sikora AG, Fu S, et al. (2011) Targeting immune suppressing myeloid-derived suppressor cells in oncology. Crit Rev Oncol Hematol 77: 12-19.
- 31. Ko JS, Rayman P, Ireland J, Swaidani S, Li G, et al. (2010) Direct and differential suppression of myeloid-derived suppressor cell subsets by sunitinib is compartmentally constrained. Cancer Res 70: 3526-3536.
- 32. Kujawski M, Zhang C, Herrmann A, Reckamp K, Scuto A, et al. (2010) Targeting STAT3 in adoptively transferred T cells promotes their in vivo expansion and antitumor effects. Cancer Res 70: 9599-9610.
- 33. Alfaro C, Suarez N, Gonzalez A, Solano S, Erro L, et al. (2009) Influence of bevacizumab, sunitinib and sorafenib as single agents or in combination on the inhibitory effects of VEGF on human dendritic cell differentiation from monocytes. Br J Cancer 100: 1111-1119.
- 34. Kobayashi M, Kubo T, Komatsu K, Fujisaki A, Terauchi F, et al. (2013) Changes in peripheral blood immune cells: their prognostic significance in metastatic renal cell carcinoma patients treated with molecular targeted therapy. Med Oncol 30: 556.
- 35. Barbi J, Pardoll D, Pan F (2013) Metabolic control of the Treg/Th17 axis. Immunol Rev 252: 52-77.
- 36. Mendel DB, Laird AD, Xin X, Louie SG, Christensen JG, et al. (2003) In vivo antitumor activity of SU11248, a novel tyrosine kinase inhibitor targeting vascular endothelial growth factor and platelet-derived growth factor receptors: determination of a pharmacokinetic/pharmacodynamic relationship. Clin Cancer Res 9: 327-337.
- 37. Houk BE, Bello CL, Kang D, Amantea M (2009) A population pharmacokinetic meta-analysis of sunitinib malate (SU11248) and its primary metabolite (SU12662) in healthy volunteers and oncology patients. Clin Cancer Res 15: 2497-2506.
- 38. Heine A, Held SA, Bringmann A, Holderried TA, Brossart P (2011)
 Immunomodulatory effects of anti-angiogenic drugs. Leukemia 25: 899-905.



The cytotoxic activity against HubCCA1 cell line after the priming with sunitinib-pretreated DCs. The CIK cells (A) at 1.0×10⁵ cells/well from each condition were inoculated with the attached HubCCA1 cells (5,000 cells/well) for 4 h before the PI assay. The CIK cell preparations comprised untreated condition, direct sunitinib treatment, macrophage pre-inoculation, sunitinib-treated macrophage pre-inoculation, iDC pre-inoculation, and sunitinib-treated iDC pre-inoculation. The isolated CD3+CD56+ cells (B) were studied in similar fashion. These included untreated CD3+CD56+ cells, direct sunitinib treatment, mDC pre-inoculation, and sunitinib-treated mDC pre-inoculation. * and ** designate data with significant different from those of the untreated CIK cells at the same E:T ratio with p < 0.05 and <0.01 respectively.

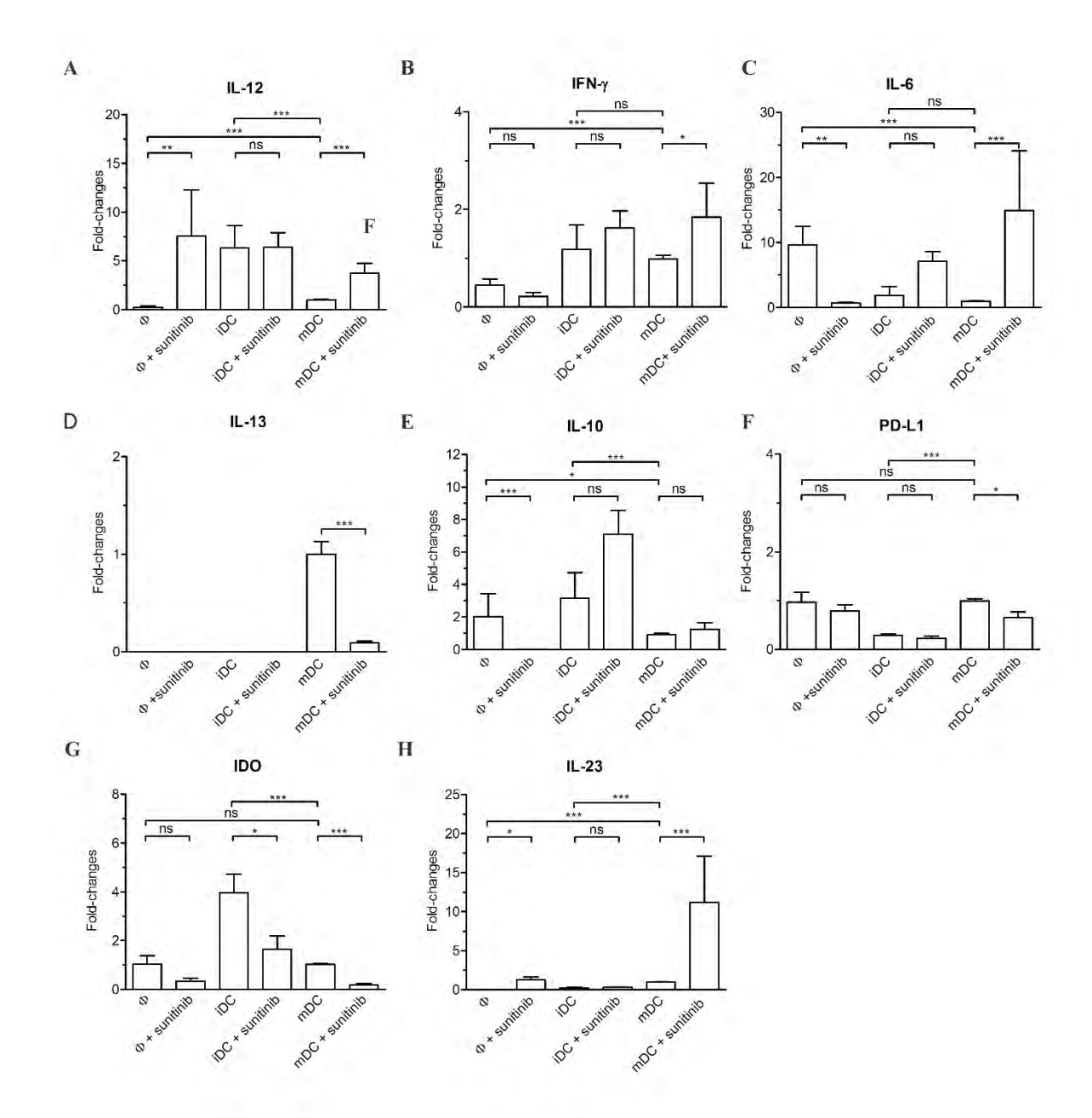
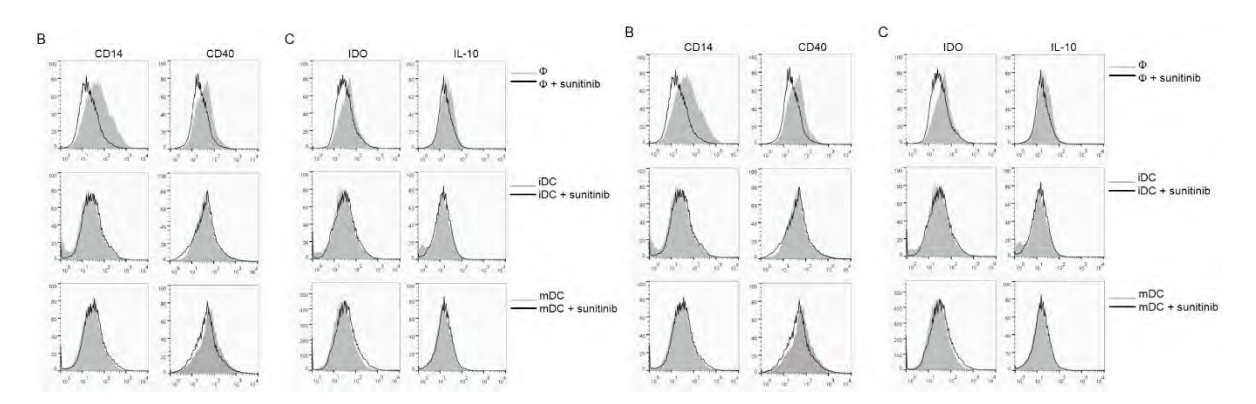


Figure 2. The real-time RT-PCR analysis in macrophages (Φ), iDC and mDC after sunitinib exposure. These cells were evaluated for the expression of IL-12 (A), IFN-γ (B), IL-6 (C), IL-13 (D), IL-10 (E), PD-L1 (F), IDO (G), and IL-23 (H). The expression levels of these genes were normalized with those of their respective untreated mDCs.



The FACS analysis for the maturity of macrophages, iDCs, and mDCs after sunitinib exposure. The markers for the maturity of DCs (A) are CD80, CD83 and CD86. The macrophage markers (B) are CD14 and CD40. The selected immunosuppressive molecules (C) are IDO and IL-10.

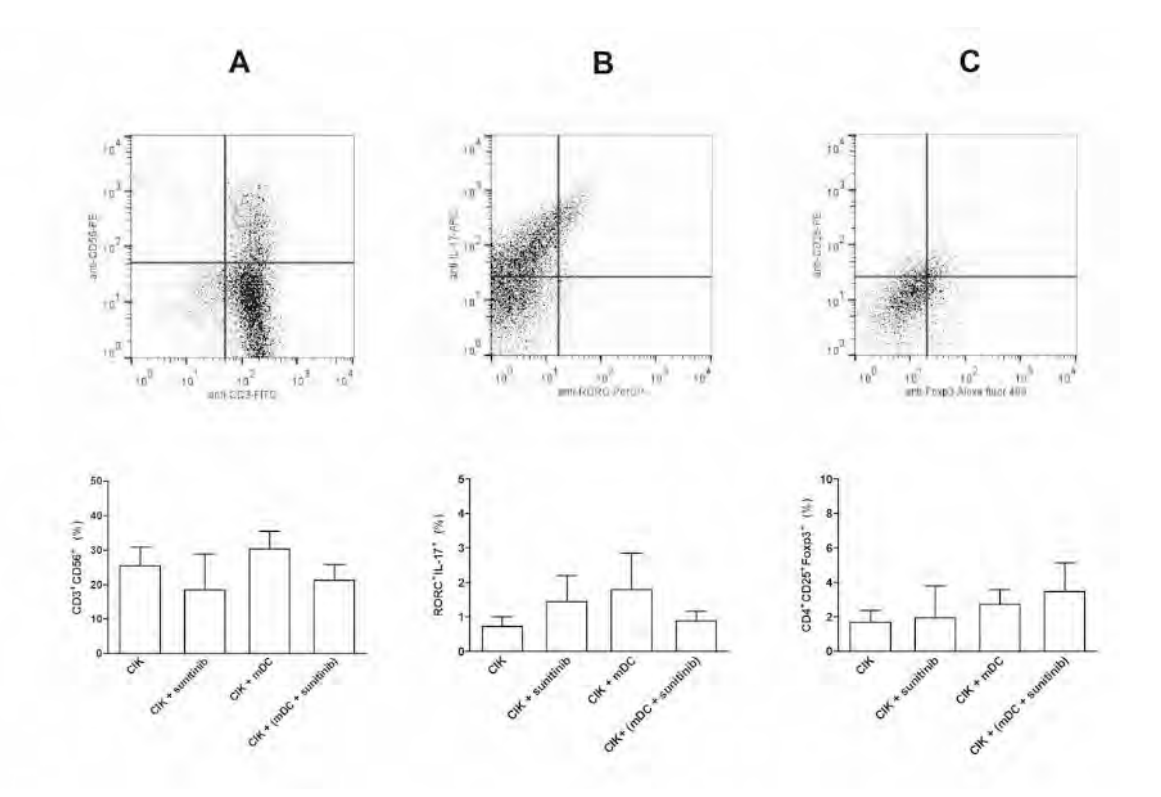


Figure 4. The FACS analysis for the alteration in the proportion of subpopulations in CIK cells. The studied subpopulations included CD3+CD56+(A), Th17 (RORC+IL-17+, B) and Treg (CD4+CD25+Foxp3+, C) subsets. The corresponding dot plot analysis demonstrated the gating of each subset. The CIK cells were either exposed to sunitinib directly, primed with mDCs or primed with sunitinib-pretreated DCs.

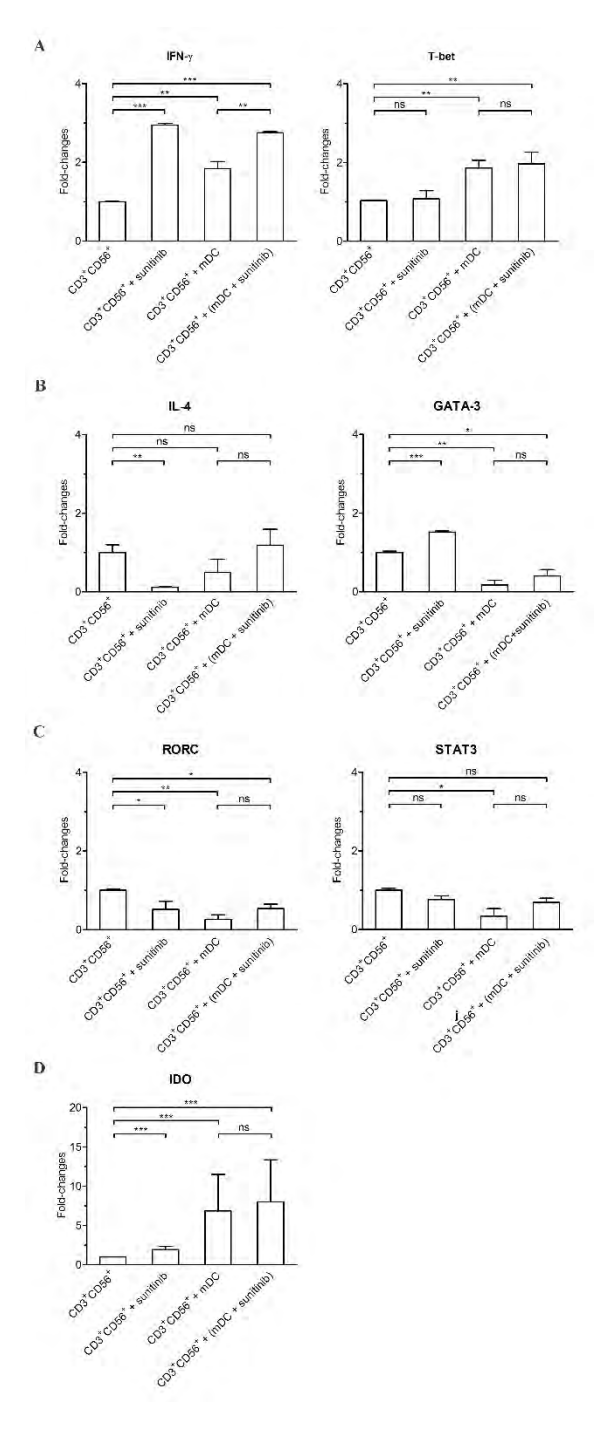


Figure 5. The real-time RT-PCR analysis for the polarization of CD3+CD56+ subset after different treatments. The CD3+CD56+ subset that had been directly exposed to sunitinib or co-cultured with sunitinib-pretreated mDCs were analyzed for the expression of IFN-γ, T-bet, IL-4, GATA-3, RORC, STAT3, and IDO.

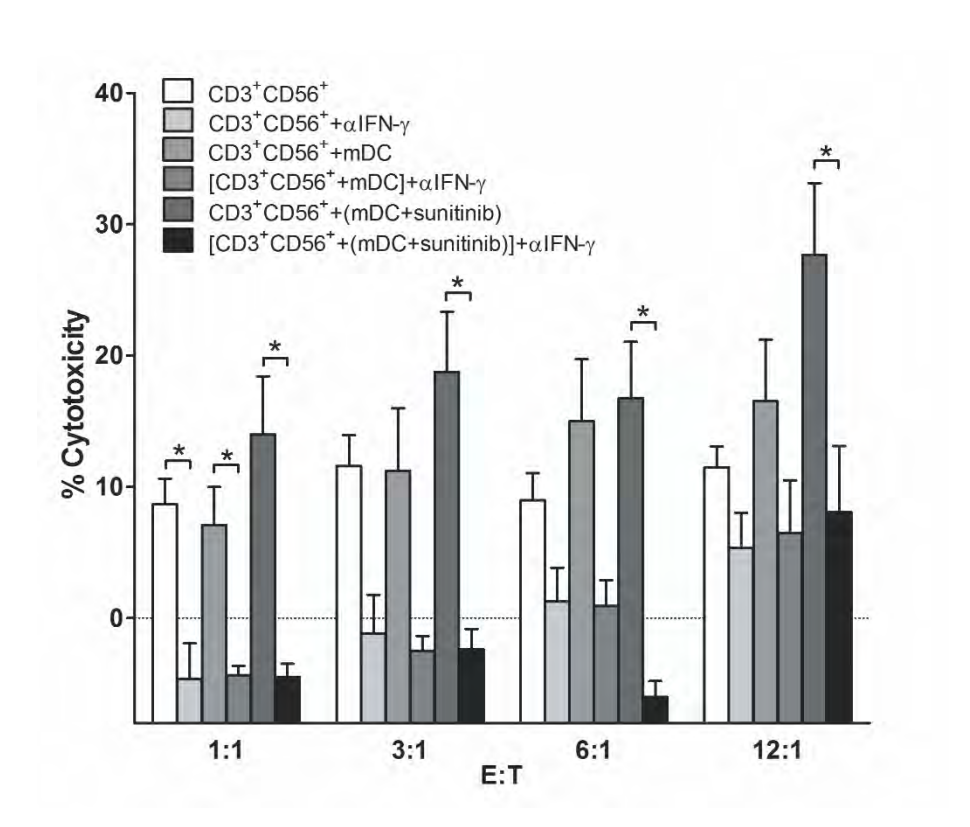


Figure 6. The cytotoxic activity of all conditions of CD3⁺CD56⁺ cells could be neutralized with α IFN- γ treatment. The CD3⁺CD56⁺ cells from each condition were inoculated with the attached HubCCA1 cells (5,000 cells/well) for 4 h before the PI assay. These conditions included the untreated CD3⁺CD56⁺ cells, α IFN- γ treatment to CD3⁺CD56⁺ cells, CD3⁺CD56⁺ cells primed with mDC, α IFN- γ treatment to CD3⁺CD56⁺ cells primed with sunitinib-pretreated mDC, and α IFN- γ treatment to CD3⁺CD56⁺ cells primed with sunitinib-pretreated mDC. * designates conditions that provided statistically difference after α IFN- γ treatment at the same E:T ratio with p < 0.05.

Table 1 The primer pairs for real-time RT-PCR

Genes	Oligonucleotides (5' →3')	Size (bp)	Annealing (°C)
GAPDH	Forward: GAAATCCCATCACCATCTTCC	124	60
	Reverse: AAATGAGCCCCAGCCTTCTC		
PD-L1	Forward: TCAATGCCCCATACAACAAA	120	60
	Reverse: TGCTTGTCCAGATGACTTCG		
IDO	Forward: AGTCCGTGAGTTTGTCCTTTCAA	68	60
	Reverse: TTTCACACAGGCGTCATAAGCT		
GATA-3	Forward: ACTACGGAAACTCGGTCAGG	100	60
	Reverse: CAGGGTAGGGATCCATGAAG		
IFNγ	Forward: GTGTGGAGACCATCAAGGAAGAC	80	60
	Reverse: CAGCTTTTCGAAGTCATCTCGTTT		
IL-4	Forward: AACAGCCTCACAGAGCAGAAGAC	101	60
	Reverse: GCCCTGCAGAAGGTTTCCTT		
IL-6	Forward: GCTGCAGGCACAGAACCA	68	60
	Reverse: ACTCCTTAAAGCTGCGCAGAA		
IL-10	Forward: CTGGGTTGCCAAGCCTTGT	100	60
	Reverse: AGTTCACATGCGCCTTGATG		
IL-12	Forward: GCAAAACCCTGACCATCCAA	100	60
	Reverse: TGAAGCAGCAGGAGCGAAT		
IL-13	Forward: GAGTGTGTTTGTCACCGTTG	253	60
	Reverse: TACTCGTTGGTCGAGAGCTG		
IL-23	Forward: GCTTACAAACTCGGTGAACAACTG	80	60
	Reverse: TCCACTTGCTTTGAGCCTGAT		
RORC	Forward: CCACAGAGACATCACCGAGCC	114	60
	Reverse: GTGGATCCCAGATGACTTGTCC		
STAT3	Forward: ACCAAGCGAGGACTGAGCAT	90	58
	Reverse: TGTGATCTGACACCCTGAATAATTC		
TGF-β	Forward: GCGTGCTAATGGTGGAAACC	100	60
	Reverse: GCTTCTCGGAGCTCTGATGTGT		
T-bet	Forward: AGGATTCCGGGAGAACTTTGA	123	60
	Reverse: TACTGGTTGGGTAGGAGAGAGAGTA		